INVESTIGATION ON NUCLEIC ACID INTERACTION WITH VARIOUS CATIONIC LIGANDS FOR GENE DELIVERY APPLICATIONS

A Thesis
Submitted for the degree of

Doctor of Philosophy

By
Hema Kumari Alajangi

DEPARTMENT OF APPLIED CHEMISTRY
DELHI TECHNOLOGICAL UNIVERSITY
SHAHBAD-DAULATPUR, MAIN BAWANA ROAD, DELHI 110042, INDIA

April 2017

DEDICATED
TO
MY PARENTS

Delhi Technological University

(Formally Delhi College of Engineering)

Department of Applied Chemistry

Shahbad-Daulatpur, Bawana Road, Delhi – 110042, India

DECLARATION

This is to certify that the work presented in this thesis entitled **"INVESTIGATION ON NUCLEIC ACID INTERACTION WITH VARIOUS CATIONIC LIGANDS FOR GENE DELIVERY APPLICATIONS"** is original and has been carried out by me for the degree of ***Doctor of Philosophy*** under the supervision of ***Dr. Deenan Santhiya, Assistant professor****, Department of Applied Chemistry.*

This thesis is a contribution of my original research work. Wherever research contributions of others are involved, every effort has been made to clearly indicate the same. To the best of my knowledge, this research work has not been submitted in part or full for the award of any degree or diploma of **Delhi Technological University** or any other university/Institution.

Hema Kumari Alajangi
Candidate

Delhi Technological University

(Formally Delhi College of Engineering)

Department of Applied Chemistry

Shahbad-Daulatpur, Bawana Road, Delhi – 110042, India

CERTIFICATE

This is to certify that the Ph.D. thesis entitled **"INVESTIGATION ON NUCLEIC ACID INTERACTION WITH VARIOUS CATIONIC LIGANDS FOR GENE DELIVERY APPLICATIONS"** submitted to the Delhi Technological University, Delhi – 110042, in fulfilment of the requirements for the award of the degree of ***Doctor of Philosophy*** by the candidate ***Mrs. Hema Kumari Alajangi*** under the supervision of ***Dr. Deenan Santhiya, Assistant professor***, *Department of Applied Chemistry*. It is further certified that the work embodied in this thesis has neither partially nor fully submitted to any other university or institution for the award of any degree or diploma.

Dr. Deenan Santhiya
Assistant professor
Supervisor

Dr. Archna Rani
Head of the Department
Applied Chemistry

CONTENTS

ACKNOWLEDGEMENT

This thesis is the culmination of my journey of Ph.D which was just like climbing high peak step by step accompanied with encouragement, hardship, trust, and frustration. When I found myself at top experiencing the feeling of fulfillment, I realized though only my name appears on the cover of this thesis, a great many people including my family members, well-wishers, my friends, colleagues and various institutions have contributed to accomplish this huge task.

I am extremely privileged to have worked with Dr. Deenan Santhiya as my advisor. The topic for my research itself was a suggestion given by her and for that as well I am grateful as it introduced me to this stupendous interdisciplinary area of nano-biotechnology. She provides freedom and poses faith in her students that lead not only to academic growth but helps develop many leadership qualities for future. She lets the students discover things for themselves. Working with her is a privilege for a student who wants to pursue research as a career as her vision and perspectives are encouraging. Although, my Ph.D years were adventurous, but her consistent support and guidance made everything possible.

I express my gratitude to my supervisor for making some insightful comments and useful suggestions during the course of my work. I thank her for being patient with my impatience and for putting up with my shortcomings. A special interest taken by her in moulding this thesis has meant a great deal to me.

It is a great privilege to be surrounded by people who were very meticulous and provided their invaluable guidance and facilities. The credit for such support goes to Dr. Souvik Maiti. I thank Dr. Souvik Maiti for providing me the opportunity to work at CSIR-IGIB and instilling interest in biophysics while I was inclined to wet lab work and also I thank Dr. Munia Ganguli for providing me the opportunity to work in her lab for further cell culture techniques.

I thank DST for JRF fellowship, which took care of most financial needs.

Thanks are due to Prof. P. B. Sharma, the past vice-chancellor and Prof. Yogesh Singh, the present vice-chancellor, Delhi Technological University, for providing all the facilities to carry out this investigation.

My thanks are also due to Dr. Santosh Kumar for Biophysical experimental analysis, Ms. Poornema Natarajan, Mr. Daniel and Ms. Manika Vij research students from the CSIR-IGIB, Delhi, for the assistance rendered in conducting my research work and also for their help, friendly gesture and co-operation.

My seniors Dr. Tani Agarwal, Dr. Teena goel, Dr. Santosh Kumar, Dr. Gopal Gunanathan Jayraj, Dr. Satya Pandey, Dr. Debojit Bose and Mr. Soundhar Ramasamy were a source of wise counsel and provided a host of favours during my research work at CSIR-IGIB.

My friend Ms. Prajakta Bajad provided a host of favours during my stay at CSIR-IGIB: I wish to express a very special thanks to her.

Acknowledgements are rendered to my lab mates Ms. Nidhi Gupta, Mrs. Meenakshi Gautam and other supporting staff members of the Applied Chemistry and Polymer Technology Department for providing their assistance.

I have been blessed with many wonderful teachers during my life and in some way each of them had an influence on my success.

I have been guided, morally supported by husband Mr. Baapu who was always there by me and rendered a helping hand with affection and love in innumerable ways. He was always a source of inspiration. He was always around at times I thought that it is impossible to continue, he had helped me to keep things in perspective. I greatly value his contribution and deeply appreciate his belief in me. I appreciate my toddler, my little cute prince Jai for abiding my ignorance and the patience he showed during my thesis writing. Words would never say how grateful I am to both of them. I consider myself the luckiest in the world to have such a lovely and caring family, standing beside me with their love and unconditional support.

My Amma and Nanna, who always encouraged me to reach this level, they were indeed a source of inspiration and they deserve the ultimate accolades for their selfless support, encouragement and patience.

My heart felt regard goes to my father in law, brother in law for their love and moral support. I thank the Almighty for giving me the strength and patience to work through all these years so that today I can stand proudly with my head held high.

Hema Kumari Alajangi

SYNOPSIS

1. Introduction

A new paradigm in medicine called gene therapy involves altering of genes entailed in disease by delivering therapeutic gene (nucleic acid based drugs). Delivering such therapeutic gene to the specific target site is an irresistible challenge to drug delivery scientists. However, the polyanionic nature of DNA limits the cellular membrane interactions. Hence, successful therapeutic DNA based gene delivery highly relies on the efficient extracellular and intracellular delivery of DNA molecules for empowering target interaction.[1-5] Various Carrier molecules have been designed specifically to enter cells & deposit therapeutic genes. Vectors can be viral or non-viral.

Viral vectors are one of the successful gene delivery systems available, such as retrovirus, adenovirus (types 2 and 5), adeno-associated virus, herpes virus, pox virus, human foamy virus (HFV), and lentivirus. The genomes of the viral vector have been modified by deleting some areas of their genomic sequences so that their replication becomes deranged and it makes them more safe, but these viral systems has accompanied with some problems, such as their marked immunogenicity that causes induction of inflammatory system leading to degeneration of transducted tissue; and toxin production, including mortality, the insertional mutagenesis; and their limitation in transgenic capacity size. These limitations could be overcome by using synthetic non-viral gene carrier systems. [6]

Non-viral vectors are being used in improving potential therapeutic effect of DNA because they are safe and non-immunogenic as compared to viral vectors. Even though lower transfection efficiency of non-viral vectors are proven compared to viral-mediated gene transfection, the observed shortcomings could be overcome by appropriate structural designing of carriers like cationic polymers or lipids. For example, non-viral vectors can easily be targeted to a target tissue or cell by coupling of cell- or tissue-specific targeting moieties on the carrier. Additionally, by controlling

the size of DNA-cationic vector complex the bio-distribution, cellular internalization and intracellular trafficking of the micro- or nanoparticle can be influenced. Most importantly, the success of the non-viral gene therapy is dependent on the various extra- and intracellular barriers that affect the efficiency of all gene delivery systems, including cellular uptake, endosomal escape, nuclear uptake and gene expression.[7-9]

Poly cationic vector such as poly (amidoamine) (PAMAM) dendrimer is one of the versatile non-viral based gene delivery systems for efficient targeted delivery of DNA amongst numerous other cationic vectors.[10-12] In particular, PAMAM dendrimer is shown as a potential vehicle especially through several routes of administration, including oral, ocular, parenteral and transdermal.[10,13,14] The uniqueness of these dendrimers are that they are monodisperse, hyperbranched and of controlled size and molecular weight, possessing number of terminal groups with the increasing generation number.[15] More interestingly, PAMAM-DNA complexes have been found to be highly soluble and stable in almost all the physiological conditions and also observed to be resistant to nuclease digestion by Bielinska *et al.*[16] These distinctive characteristics of PAMAM dendrimer coupled with their architecture has attracted attention of several research groups and their applications in biology and medicine have been explored.[10,17-19]Additionally, various research groups also commenced to determine dendrimer toxicity and immunogenicity and reported that cytotoxicity increases with increase in generation number i.e. smaller the generation of PAMAM dendrimer less the chances of cytotoxicity.[20,21]In spite of high cost and high cytotoxicity, there exist enormous successful targeted transfection reports using unmodified and modified dendrimers of higher generations.[11,21-23] It is pertinent to mention that even though PAMAM dendrimer-based gene transfection reagents such as Superfect and Priofect are already commercially available, these products are based on toxic high generation dendrimers and also not cost effective.[24]

In spite of numerous attempts made for efficient gene transfection using surface

engineered lower generation dendrimers,[25-27] there are also a few remarkable recent highlights on the possibility of using unmodified lower generation dendrimer in skin penetration[28] as well as in the rapidly growing area of dendrimer mediated RNAi therapeytics[29]. Therefore , there is a necessity to focus on the systematic control of the physicochemical properties of less toxic and cost effective low-generation dendrimers for successful gene transfection. A careful review on literature reveals that only a few researchers used unmodified lower generation PAMAM dendrimer for gene transfection. One decade ago, Braun *et al.*[30] beautifully demonstrated a structure–function relationship between the biophysical properties of dendrimer/pDNA complexes (Plasmid DNA pMB 290(4.9 kbp)) of various generation and the corresponding *invitro* transfection efficiencies into CHO-K1 cells. Based on the experiments it was observed thatG4 at 1–10 charge ratio and G7 at 2–10 charge ratios showed remarkable biological activity among dendrimers of generation G2, G4, G7 and G9. It is noteworthy that Haensler and Szoka[31] investigated transfection of a series of PAMAM dendrimer generation from G1 to G10 into CV1 cells and reported that charge ratio and diameter of the dendrimer are the key factors for the transfection. More interestingly, Tajarobi[32] observed highest *in vitro* transfection of PAMAM dendrimer generation G4 across Madin Darby Canine Kidney cells followed by G1 or G0, G3, G2. It is also noteworthy that low generation, G2 and G3, poly(propylenimine) dendrimers have been evaluated successfully for the potential cellular delivery of antisense oligonucleotides (ODNs) targeting the epidermal growth factor receptor (EGFR) in A431 epidermoid carcinoma cells.[33] Based on various interesting review articles on dendrimers in gene transfection[11,13,22] it has been seen that there is a lack of systematic analysis on gene transfection studies with the unmodified PAMAM dendrimer especially from the generation G1to G3. Hence, considering the importance of low generation PAMAM dendrimers especially G1 to G3 as effective, economic and non-toxic gene carriers the following major objectives are drawn for the investigation on nucleic acid interaction.

2. Major Objectives

- To explore low generation PAMAM dendrimer short oligonucleic acid packing interactions as nano-complexes for gene silencing applications by FRET technique.
- To investigate kinetic parameters that characterize the formation of dendriplexes with 14 mer oligonucleotide, and how such parameters vary with the architecture of the dendrimer.
- To explore the possibility of usage of the lower generation PAMAM dendrimers based dendriplexes using therapeutic pDNA for *In vitro* gene therapeutic studies through the human skin cells.

3. CONCLUSION

Objective one concludes, the highest FRET occurring in the aggregates of second generation polymer molecules revealed that the effective oligonucleotide packing in the dendriplex depends on the dendrimer architecture. Additionally, the observed decrease in the FRET intensities in the DFT–G2 as well as the DFT–G3 system confirms that there exists a critical dendrimer to oligonucleotide charge ratio for effective dendrimer packing into the dendriplex.

Objective two concludes the architecture of the PAMAM dendrimer was found to have a significant impact on the kinetics of the dendriplex formation. Among the first three generations of PAMAM dendrimers, G2 and G3 exhibited significantly faster binding kinetics compared to the G1 dendrimers.

Conclusion of the objective three reveals that the successful demonstration of pDNA transfection using G2 and G3 into HaCaT cells with negligible toxicity indicated a versatile platform for cell-specific nucleic acid therapeutics for skin disorder. Finally, the observed serum stability of G2 as well as G3 based dendriplexes in CHO-K1 cells promises for in vivo gene delivery applications without extrinsic serum inhibition.

4. References

1. W. F. Anderson, Human gene therapy, *Science* 1992, 256, 808-813.
2. R. C. Mulligan, The basic science of gene therapy, *Science* 1993, 260, 926-932.
3. H. A Magid,. Gene therapy for cancer: present status and future perspective, *Mol. Cell. Ther*. 2014, 2*,* 27-46.
4. C. E. Thomas, A. Ehrhardt and M. A. Kay, Progress and problems with the use of viral vectors for gene therapy, *Nat. Rev. Genet.* 2003; 4, 346-358.
5. G. U. Dachs, D G. J. Dougherty, I. J. Stratford, D. J Chaplin, Targeting gene therapy to cancer: a review, *Oncol. Res.* 1997*,* 9, 313-325.
6. H. Yin, R. L. Kanasty, A. A. Eltoukhy, A. J. Vegas, J. R. Dorkin and D. G. Anderson, Non-viral vectors for gene-based therapy, *Nat. Rev. Genet.* 2014, 15, 541–555.
7. C. W. Pouton and L. W. Seymour, Key issues in non-viral gene delivery, *Adv. Drug Deliv. Rev.*1998, 34, 3–19.
8. M. S. Al-Dosari and X. Gao, Nonviral gene delivery: principle, limitations, and recent progress, *Am. Assoc. Pharm. Sci. J.* 2009, 11, 671-681.
9. S. Svenson and D. A. Tomalia, Dendrimers in biomedical applications – reflections on the field, *Adv. Drug Deliv. Rev*. 2005, 57, 2106–2129.
10. C. Dufes, I. F. Uchegbu and A.G. Schatzlein, Dendrimers in gene delivery, *Adv. Drug Deliv. Rev.*2005, 57, 2177–2202.
11. Y. Gao, G. Gao, Y. He, T. Liu and R. Qi, Recent advances of dendrimers in delivery of genes anddrugs. *Mini Rev. Med. Chem.* 2008, 8, 889–900.
12. Q. Xu, C.H. Wang and D. W. Pack, Polymeric Carriers for Gene Delivery: Chitosan and poly(amidoamine) dendrimers. *Curr. Pharm. Des.* 2010, 16*,* 2350–2368.
13. Y. Cheng, Z. Xu, M. Ma and T. Xu, Dendrimers as drug carriers: Applications in different routes of drug administration, *J. Pharm. Sci.* 2008, 97, 123–143.

14. R. Esfand and D. A. Tomalia, Poly(amidoamine) (PAMAM) dendrimers: From biomimicry to drug delivery and biomedical applications, *Drug Discov. Today* 2001, 6, 427–436.

15. A. U. Bielinska, J. F. Kukowska-Latallo and J. R.Baker, Jr. The interaction of plasmid DNA with polyamidoaminedendrimers: mechanism of complex formation and analysis of alterations induced in nuclease sensitivity and transcriptional activity of the complexed DNA, *Biochim. Biophys. Acta.* 1997, 1353, 180–190.

16. H. Arima , K. Motoyama and T. Higashi, Potential use of poly (amidoamine) dendrimer conjugates with cyclodextrins as novel carriers for siRNA, *Pharmaceuticals* 2012, 5, 61-78.

17. S. Biswas, and V. P. Torchilin, Dendrimers for siRNA Delivery*, Pharmaceuticals* 2013, 6, 161-183.

18. D. G. Shcharbin, B. Klajnert and M. Bryszewska, Dendrimers in gene transfection. *Biochem. (Moscow)* 2009, 74, 1070-1079.

19. J. F. Kukowska-Latallo, A. U.Bielinska, J. Johnson, R. Spindler, D. A. Tomalia and J. R. Baker, Jr. Efficient transfer of genetic material into mammalian cells using Starburst polyamidoaminedendrimers, *Proc. Natl. Acad. Sci. U. S. A.* 1996, 3, 4897−4902.

20. Y. Cheng, L. Zhao, Y. Li and T. Xu, Design of biocompatible dendrimers for cancer diagnosis and therapy: current status and future perspectives. *Chem. Soc. Rev.* 2011, 40, 2673−2703.

21. J. D. Eichman, A. U. Bielinska, J. F. Kukowska-Latallo and J. R. Baker, Jr. The use of PAMAM dendrimers in the efficient transfer of genetic material into cells. *Pharm. Sci. Technol. Today* 2000, 3, 232–245.

22. A. Naik, Y. N. Kalia and R. H. Guy, Transdermal drug delivery: overcoming skin's barrier function, *Pharm. Sci. Technol. Today* 2000, 9, 318–326.

23. K. L. Killops, L. M. Campos and C. J. Hawker, Robust, efficient, and orthogonal synthesis of dendrimers via thiolene "click" chemistry, *J. Am. Chem. Soc.* 2008, 15, 5062-5064.

24. J. Yang, Q. Zhang, H. Chang and Y Cheng, Surface-Engineered Dendrimers in Gene Delivery, *Chem. Rev.* 2015, *115,* 5274−5300.

25. H. Liu, H. Wang, W. Yang, and Y. Cheng, Disulfide cross-linked low generation dendrimers with high gene transfection efficacy, low cytotoxicity, and low cost, *J. Am. Chem. Soc*. 2012, *134*, 17680−17687.

26. M. Wang, H. Liu, L. Li and Y. Cheng, A fluorinated dendrimer achieves excellent gene transfection efficacy at extremely low nitrogen to phosphorus ratios, *Nat. Com*. 2014, DOI: 10.1038/ncomms405.

27. J. Yang, Q. Zhang, H. Chang and Y Cheng. Surface-Engineered Dendrimers in Gene Delivery. *Chem. Rev.* 2015, *115,* 5274−5300.

28. V. Vamsi, K. Venuganti and O. Perumal, P. Poly (amidoamine) dendrimers as skin penetration enhancers: Influence of charge, generation,and concentration, *J. Pharm. Sci.* 2009, 98, 2345–2356.

29. P. Kesharwani, S. Banerjee, U. Gupta, M. C. I. M. Amin, S. Padhye, F. H. Sarkar and A. K. Iyer, PAMAM dendrimers as promising nanocarriers for RNAi therapeutics *Mater. Today* 2015, 18, 565–572.

30. C. S. Braun, J. A. Vetro, D. A. Tomalia, G. S. Koe, J. G. Koe and C. R. Middaugh, Structure/Function Relationships of Polyamidoamine/DNA Dendrimers as Gene Delivery Vehicles, *J. pharm. Sci.* 2005, 94, 423-436.

31. J. Haensler and F. C. Szoka, Jr. Polyamidoamine cascade polymers mediate efficient transfection of cells in culture, *Bioconjugate Chem*. 1993, 4, 372–379.

32. F. Tajarobi, M. El-Sayed, B. D.Rege, J. E. Polli and H. Ghandehari, Transport of poly (amidoamine) dendrimers across Madin-Darby canine kidney cells, *Int J. Pharm.* 2001, 215, 263–267.

LIST OF FIGURES

LIST OF TABLES

CHAPTER 1
INTRODUCTION

1.1 Overview of Gene Therapy

Gene therapy is the process of introducing therapeutic genetic material into the target cells of the nucleus in the body[(1)]. Gene therapeutic studies are mostly aimed to treat both the genetic and infectious diseases. More importantly, the substantial therapeutic prospects of gene therapy are appreciable due to its significant possibility for the treatment of inborn and ominous diseases induced by genetic deficiencies and abnormalities[(2)]. Gene therapy involves the addition / transfer of recombinant genetic material into the body, which may take place either directly or indirectly through somatic or germline cells. The human gene therapy remains a challenge and several techniques need further development. The approaches of gene therapy include somatic gene therapy and germline gene therapy.

1.2 Approaches of Gene Therapy:

1.2.1 Somatic gene therapy

In somatic gene therapy, the genetic material is transferred indirectly into the somatic (bone marrow, skin, blood) cells of a patient.

1.2.2 Germline gene therapy

In germline gene therapy, the genetic material is introduced by the modidfication of germ cells (sperms or eggs) which further integrate into the patient genome. So that functional gene change due to therapy is heritable and also extends its function on to subsequent generations.

1.3 Types of gene therapy

1.3.1 *Ex-vivo* gene therapy

This technique involves the indirect transfer of genes (first cultured in the laboratory and then reintroduced into patient) into the target site of the patient. It is noteworthy that this technique avoids the risk of adverse immunological responses after transplantation. The genetic disorders related to bone marrow transplantations would be treated by this method.

1.3.2 *In-vivo* gene therapy

The direct transfer of genes into the target site in the tissue of the patient is called in-vivo gene therapy.

1.4 Mechanism of Gene Delivery

A successful gene therapy relies on efficient transfer of nucleic acid molecules which can act as a therapeutic agent into the cells by the gene delivery vectors (Figure 1). There are several barriers need to be crossed in order to achieve successful gene delivery. The barriers involved in the mechanism of gene delivery are as follows:

The first step in the mechanism of gene delivery is the **Interaction** of nucleic acid with vector which leads to complexation of nucleic acid by strong compaction. After interaction, the **cellular uptake** of nucleic acid takes place by **endocytosis.** At which internalization of the nucleic acid complex into the cell takes place by binding to the extracellular membranes like Plasma membrane or receptors.

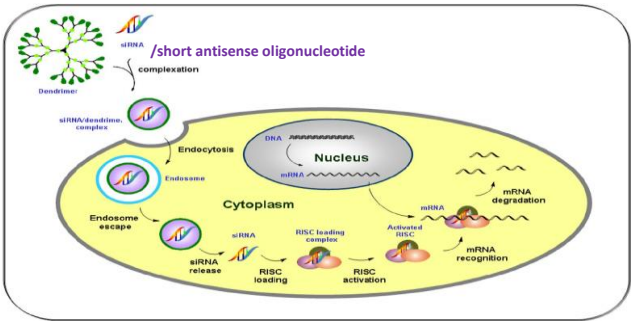

Figure 1.1 The mechanism of dendrimer mediated siRNA delivery and gene silencing. Modified from: Liu X, et al, BiotechnolAdv (2013) [3]

After endocytosis, the nucleic acid complex must escape from **Intracellular trafficking or endosomal escape.** Because the internalized molecules tend to be trapped in intracellular vesicles and eventually fuse with endosomes/lysosomes where they are degraded. Therefore, the problem of gene delivery involves not only the cellular uptake of genes but also their intracellular availability at the target sites in the nucleus. Finally, the therapeutic agent is to be delivered into the target site, nucleus which is known **as nuclear delivery**. Or the other way, the so-released nucleic acid molecules from the intracellular vesicles then move into the RNA interference (RNAi) machinery to execute their corresponding RNAi function. RNA interference (RNAi) is the recent discovery in the field of gene silencing process in which Dicer facilitates the activation of the RNA-induced silencing complex (RISC). RISC has four different functional subunits in catalytic component argonaute, in which one functional subunit called an endonuclease capable of degrading messenger RNA (mRNA). So that expression of gene can be controlled[3]. Despite the fact that there are several obstacles confine the exploitation of gene therapy, which is an attractive field of research will certainly ameliorate the future of medicine[4].

1.5 Vectors/ carriers

As is long-familier, the direct diffusion of nucleic acids through plasma membrane is difficult due to their size and their physicochemical properties, versatile carrier molecules have been designed specifically to enter into the cells and deposit therapeutic genetic materials into the respective target sites. Vectors can be viral or non-viral.

1.5.1 Viral vectors

The initial gene therapy clinical trials were began using viral vectors (Figure 1.2) to introduce copies of the adenosine deaminase (ADA) gene into T-lymphocyte cells from a patient with ADA deficiency by *ex-vivo* gene therapy [5,6]. Widely used viral carriers for gene delivery purposes are namely retrovirus, lentivirus, Adenovirus, Adeno-associated virus, Herpes simplex virus. Most gene

therapeutic trials have used viral vectors, with the prominent involvement of retroviral vectors. But the proper selection of a viral vector is made based on the type of therapy being performed due to their individual properties, advantages, and disadvantages for use in gene therapy. The random desegregation of viral genome into the host genes of special concern may disrupt endogenous genes, which can further leads to increased cancer risk.

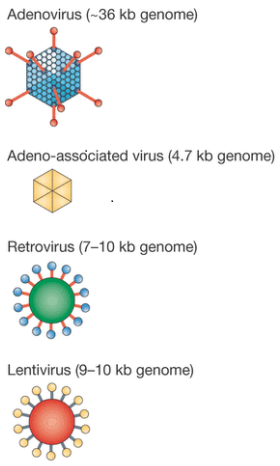

Figure 1.2 Gene-transfer viral vectors that are used to treat hereditary disorders (Modified from O'Connor, T.P. & Crystal, R.G. *Nat. Rev. Genet.* 7, 261–276 (2006))[7]

The major disadvantages of viral vectors found during clinical delivery as follows,

1. Raise of immune responses with subsequent expression of viral proteins kill the target cells which involves to production of therapeutic gene product.
2. Production of an innate humoral immune response due to certain previous exposure of the naturally occurring viruses.
3. Random integration of some viral vectors into the host chromosome occurs and cause activation of proto- oncogenes ensure cancer formation.
4. Clearance of viral vectors delivered systemically by complement activation can occur.
5. Viral vectors can be inactivated upon readministration by the humoral immune response and
6. Potential for recombination of the viral vector with DNA sequences in the host chromosome that generates a replication-competent infectious virus also exists.

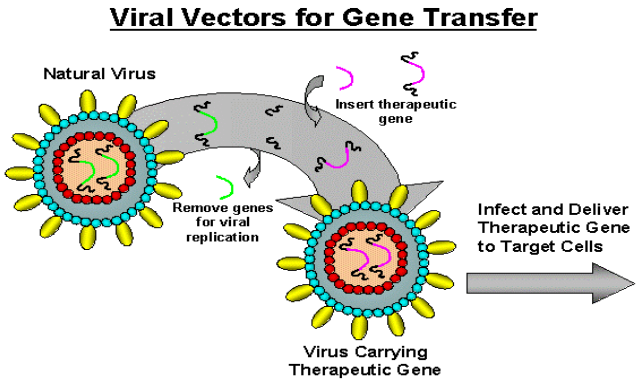

Figure 1.3 Viral Vectors for Gene transfer (from www.gnencure.com)[8]

The summary of main advantages and disadvantages of viral vectors is shown in the following Table I. Hence, due to their safety concerns and immunogenicity viral vectors are least preferred.

Table I: Some of the major types of viral vector used in gene therapy with DNA incorporation type and summary of main advantages and disadvantages [11].

Viral vector	Type	Advantage	Disadvantages
Retrovirus	Integrates with host chromatin	Effective over long periods Efficient transfection *ex vivo* Low immune response in host	Small, max 8kb insert size Inefficient transfection *in vivo* Relies on target cell mitosis Safety concerns
Lentivirus	Integrated with host chromatin	Transfects proliferation and non-proliferating hosts and haemo stem cells New generations are self-inactivation for safety	Need active transport into Small, max 8kb insert size Technologically challenging Safety concerns , immunodeficiency origins
Adeno Associated Virus	Either	Very good length of expression especially *in vivo* Efficient transfection *in vivo* Low immune response in host	Safety problems wing to potential insertional mutagenesis Small, max 4.5kb insert size High immune response Technologically challenging
Adenovirus	Extra chromosomal DNA	Highly efficient transfection *in vivo* and *ex vivo* Transfects proliferating and non-proliferating hosts	Repeat treatments ineffective due to strong immune response Small, max 7.5kb insert size Technologically challenging Short expression duration
Herpes simplex virus	Extra chromosomal DNA	Very good length of expression especially *in vivo* Safe for use in immunocompromised patients Large insert size up to 30kb Effective on many cell types	Difficult to produce in large quantities

Other disadvantages of viral vectors include the inability to administer certain viral vectors more than once, the high costs for producing large amounts of high-titer viral stocks for clinical uses, and can carry very limited size of the nucleic acid that can be compacted and used for viral gene therapy. Attempts are being made to defeat the immune responses produced by viral vectors such as gutted adenoviral vectors or encapsulation of viral vectors in liposomes [9, 10]. Nevertheless, complete voiding of all immune responses to viral vectors may be impossible.

1.5.2 Non-viral vectors

Several efforts have been made to overcome the disadvantages of viral gene delivery and introduced non-viral gene delivery methods by using non-viral gene carrier molecules. Non-viral vectors or synthetic vehicles have potential to answer the many limitations occurred by viral vectors. Among the gene delivery vectors used for gene transfer, non-viral vectors are safer, less immunogenic and can carry larger DNA molecule than the viral vectors. Use of cationic polymers in therapeutic gene delivery is advantageous over viral gene delivery as non-immunogenic, non-cancerous and easy to produce.

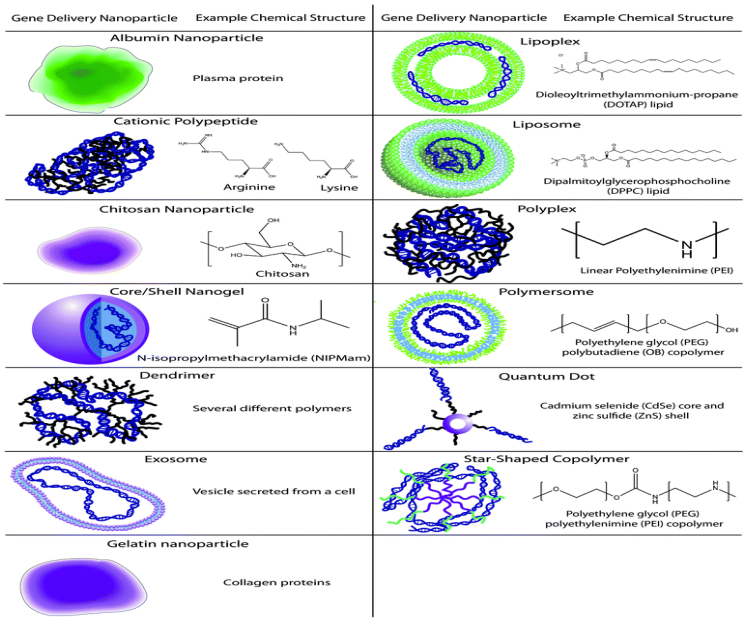

Figure 1.4 Various synthetic non –viral vectors used for gene delivery[12].

However, the cytotoxicity is still an obstacle in the non-viral gene delivery applications. For overcoming the problem, many new cationic compounds have been developed. Cationic polymers are the alternative class of non-viral vectors like poly(l-lysine) (PLL), polyethylenimine (PEI), poly[(2-dimethylamino) ethyl methacrylate] (pDMAEMA), carbohydrate-based polymers such as chitosan and β-cyclodextrin-containing polycations, polyamidoamine (PAMAM) dendrimers and degradable poly(β-aminoester) polymers are having significant importance in gene delivery as a very good transfecting agent and negligible immunogenicity[(12)].

(a) Polyamidoamine (PAMAM) dendrimers

The word dendrimer means tree/ neuron like dendritic patterns may be found in biological systems. The outer shell of the dendrimers are made up of hydrophilic moieties and soluble in aqueous media and inner shell is made up to hydrophobic core. The PAMAM dendrimers can be synthesized by two methods like convergent and divergent synthesis. The divergent synthesis of PAMAM dendrimers involves the ethyleneamine functional core unit produced by Michael addition reaction. This results in the formation of two new branches per amine group with ester-terminated dendrimer, which is called 'half-generation' dendrimer. Subsequent amidation of the methyl ester with ethylene diamine gives a 'full- generation (G)' amine-terminated dendrimer.

The successive repetition of Michael addition and amidation reaction gives the next-higher 'generation' dendrimer with increase in the molecular weight, number of amine terminated functional groups and size [(15, 16)]. The convergent synthesis of PAMAM dendrimers involves the orthogonal protecting groups that eventually become the surface of the dendrimer and proceeds inward which are not present in divergent approach of PAMAM dendrimer synthesis.

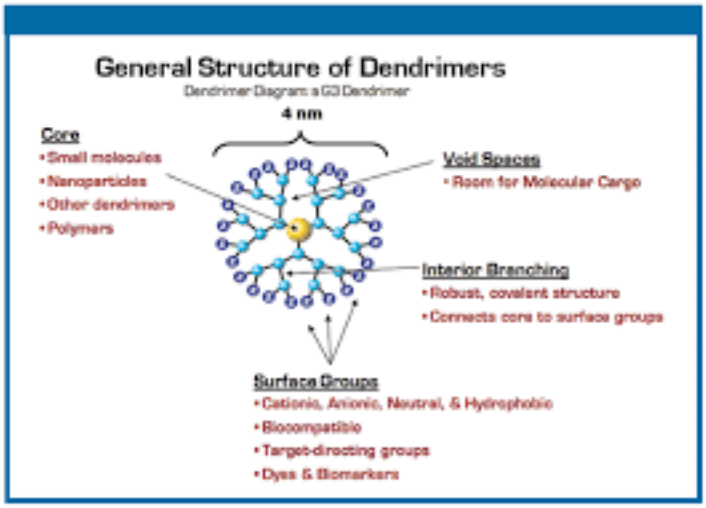

Figure 1.5 Schematic illustration of a G3 dendrimer. (Figure 1.5 is courtesy of Dendritic Nanotechnologies)[13]

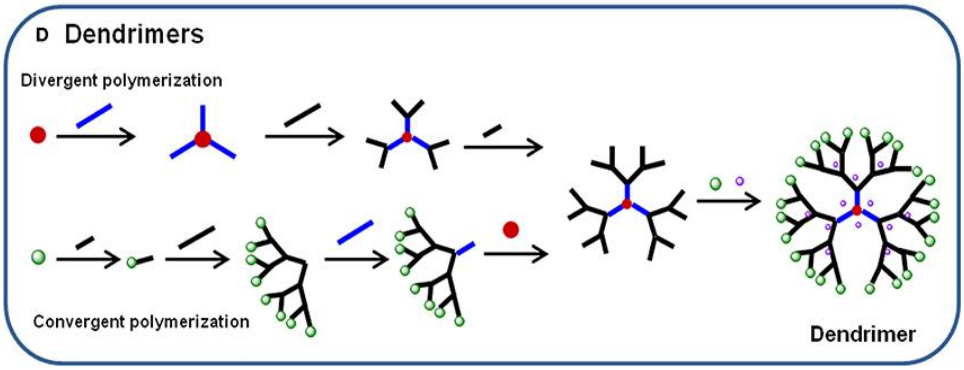

Figure 1.6 The schematic representation of PAMAM dendrimer synthesis [14].

Since the pioneering studies on dendrimer synthesis by Tomalia *et al*, subsequent investigations also are probing the specific physicochemical properties of dendrimers. Significant potential applications for dendrimers are now approaching, whilst there are many strange factors still persists. Dendrimers are macromolecules have uniform size, mono-dispersed, biocompatibility, low cytotoxicity, stability, modifiable surface functionality in addition to inner core surfaces. The other characteristics of dendrimers like high water solubility make them attractive non-viral polymeric vehicles for gene delivery and pharmaceutical applications of future medicine. In fact, most of the recent gene delivery studies are focused on the features of dendrimer-based devices for *in vivo* as non-viral therapeutic gene delivery ligand [16].

PAMAM dendrimers have polycationic charged macromolecules which can bind the polyanionic nucleic acid (DNA, short interfering RNA (siRNA), miRNA, antisense oligonucleotides) by strong compaction and can carry the therapeutic gene into the nucleus of the cell. Since the most important aspects of cationic polymers for gene delivery are transfection efficiency and cytotoxicity [17-20], PAMAM dendrimers have been majorly aimed to develop cationic polymer based gene delivery is to improve transfection efficiency and also to lower cytotoxicity *in-vivo*. But the problem of cytotoxicity with PAMAM dendrimers of higher generations (highly branched) still persists. The literature shows that the transfection efficiency of therapeutic gene increases with increasing size or generation of the dendrimer along with the cytotoxicity. The PAMAM dendrimers of first three generations (1-3) are said to be lower generation ones whereas higher generation starts fourth generation onwards through eleventh generation (i.e. 4-11). The size of the dendrimer determines the increase in functional groups present on the surface. For example, the fourth generation PAMAM dendrimer has 64 functional surface amine groups which is constituently high and may lead to toxicity. The more the increase of functional terminal amino groups more the toxicity. The literature shows that efficiency of transfection decreases with decrease in generation of the dendrimer along with the toxicity. In recent years, researchers have also developed functional modification of PAMAM dendrimers to further increase the transfection efficiency and to minimize the toxicity.

In general, higher generation (highly branched G4-G10) PAMAM dendrimers are majorly focused for *in-vitro* therapeutic gene expressions which are predicted to possess 64 to 4096 surface functional amino groups [21, 22]. High generation PAMAM dendrimers are found to have facilitated more efficient gene delivery than low generation PAMAM dendrimers through transfection. For instance, PAMAM dendrimers of generation six have shown higher transfection efficiency than generation ten in which G10 exhibit no significant transfection[23]. Russell et al shown that PAMAM dendrimer G2 exhibited low transfection efficiency than higher

generation PAMAM dendrimers of G4, G7 and G9[24]. In spite of the above literature, major shortcoming of the higher generation PAMAM dendrimers associated with high cytotoxicity which limits their use in both *in-vitro* and *in-vivo*. The cytotoxicity is said to be generation dependent i.e. with increasing generation toxicity increases. Higher generation dendrimers of G5 and G7 exhibited increasing cytotoxicity than low generation PAMAM dendrimer G3[21] and Haensler and Szoka have been shown that higher generation (≥ 4th generation) PAMAM dendrimers exhibit more than threefold cytotoxicity than low generation PAMAM dendrimers like PAMAM G2 and G3[25]. Several attempts has been done on surface modification of PAMAM dendrimers to circumvent the cytotoxicity of higher generations whereas, modification of functional surface amino groups reduced the number of active binding sites thereby effectiveness of ligands decreases in therapeutic gene complexation[26, 27].

The few highlights of lower generation dendrimers are proven over high generation dendrimers here while access of enzymatic degradation after the therapeutic gene delivery; as dendrimers of low generation numbers might be degraded fastly than higher generation number due to its intermediate topology, high conformational flexibility and hydrophilicity. Due to limited conformational flexibility, high degree of branching and severe steric effect of higher generation dendrimers with impenetrable outer surface in a close shield might degrade very slowly than lower generation number. In recent years, the profound surface functionalizations of dendrimers with some functional unit changes or modifications have been approached for the better structural relationship, cellular uptake, targeting and biocompatibility of dendrimers. For instance, Schluter*et al*. concluded that surface functionalization of PAMAM dendrimers highly influcences on toxicity[28]. Baker. Jr. and coworkers also used the PAMAM dendrimers for functionalization with methotrexate (an anticancer drug), FITC and folic acid for cancer therapy[29]. The surface functionalization with PEGylation of PAMAM dendrimers[30, 31] and poly (l-lysine)[32] or triazinedendrimers[33] showed a drastic effect on hydrophilicity, thereby which prevented the binding/assembling of

drug or gene, cellular internalization[34], targeting tissues and also persistence of drug into the blood. Therefore, these factors affect the kinetic release of therapeutic genes directly in *in-vitro* and *in-vivo* studies [35].

The route of administration is an important determinant for the success of nanoparticle-based gene silencing therapeutics. The application of polyplexes for extracellular and intracellular delivery of synthetic antisense oligonucleotide and therapeutic gene molecules by various routes of administration and therapeutic effects in preclinical disease models facilitate site specific gene delivery. But the consideration will be given to intracellular barriers for site specific target interaction and possible nanoparticle-mediated therapeutic effects.

1.6. The Aim and Outline of This Thesis

1.6.1 Thesis Objectives

Following are the major objectives of the thesis:

- To explore low generation PAMAM dendrimer short oligonucleic acid packing interactions as nano-complexes for gene silencing applications by Förster Resonance Energy Transfer (FRET) technique.
- To investigate kinetic parameters that characterize the formation of lower generation based dendriplexes with 14mer oligonucleotide, and also to show the variation of the kinetic parameters vary with the architecture of the dendrimer and ionic strength.
- To explore the possibility of usage of the lower generation PAMAM dendrimers based dendriplexes using therapeutic pDNA for *In vitro* gene therapeutic studies through the human skin cells.

1.6.2 Outline of the Thesis

Chapter one if this thesis discusses general introduction of gene therapy in which the overview and approaches of gene therapy have been discussed along with the types

of therapeutic gene delivery systems like ***in-vivo*** and ***ex-vivo*** gene therapy. Furtherly, the barriers involved in the gene delivery also talked about. Carrier molecules like viral and non-viral vectors to enter and deposit the therapeutic materials into the site specific target discussed too. The importance of PAMAM dendrimers was discussed as one of the best gene carrier for successful gene delivery. Finally, the outline and main objectives of this thesis have been highlighted well.

In chapter two, the details of various materials, cell lines used, the various characterization and experimental procedures followed are described. A few selected experimental methodologies are briefed as follows:

- **Gel retardation**- The condensation of DNA by cationic polymers can be measured by a reduction of the mobility of DNA on agarose that leads to the retention of DNA in the wells. This assay can be performed using ethidium bromide to detect DNA and may be analysed on the photo-imaging kit to quantify how much DNA is retained in the wells at different charge ratios.
- **FRET (Forster Resonance Energy Transfer)**- FRET is a widely used technique for the quantification of molecular dynamics in phenomena like protein-protein interaction, protein-DNA interactions and protein conformational changes. In order to monitor complex formation between two molecules, one of the molecules is labeled with a donor fluorophore and the other with an acceptor fluorophore. When the donor and acceptor are in close proximity (1-10 nm) due to complex formation, the predominantly observed emission is that of the acceptor because of intermolecular FRET from donor to acceptor, whereas, in the absence of complex formation, FRET from donor to acceptor cannot occur, and donor emission predominates.
- **EtBr exclusion assay**- The concentration of ethidium bromide used in this assay is an important parameter that can affect the condensation of DNA. If too much ethidium bromide is used it will cause stabilisation and neutralisation of the DNA structure and inhibit its condensation with cationic polymers. For this reason, and to keep the assay as physiologically

relevant as possible, the concentration of ethidium bromide used was as low as possible (400 ng/ml) given the limits of detection of the Kontron fluorimeter. This concentration of ethidium bromide was used in all fluorimetric assays to standardise the technique and allow comparison of the ability of different polymers to condense DNA.

- **Circular DichorismMeasurement**- Circulardichroism (CD) spectroscopy measures differences in the absorption of left-handed polarized light versus right-handed polarized light which arise due to structural asymmetry. The absence of regular structure results in zero CD intensity, while an ordered structure results in a spectrum which can contain both positive and negative signals.

- **Stopped flow fluorescence kinetics-** A stopped flow instrument is a rapid mixing device used to study the chemical kinetics of a reaction in solution. After two or more solutions containing the reagents are mixed, they are studied by whatever experimental methods are deemed suitable. Different forms of spectroscopy and scattering of radiation are common methods used. The dead time is the time between the end of mixing the two solutions and the beginning of observation of the kinetics of the reaction. The usual dead time of a stopped flow apparatus is 1-2 milliseconds but some new devices have been developed that have dead times of 0.3-0.6 ms.

- **AFM imaging**- Atomic force microscopy (AFM) or scanning force microscopy (SFM) is a very high-resolution type of scanning probe microscopy, with demonstrated resolution on the order of fractions of a nanometer, more than 1000 times better than the optical diffraction limit. The AFM consists of a cantilever with a sharp tip (probe) at its end that is used to scan the specimen surface. The cantilever is typically silicon or silicon nitride with a tip radius of curvature on the order of nanometers. When the tip is brought into proximity of a sample surface, forces between the tip and the sample lead to a deflection of the cantilever according to Hooke's law.

- **Transfection-** Transfection is the process of inserting genetic material, such as DNA and double stranded RNA, into mammalian cells. The insertion of DNA enables the expression, or production, of proteins using the cells own machinery, whereas insertion of RNA into a cell is used to down-regulate the production of a specific protein by stopping translation. While the site of action for transfected RNA is the cytoplasm, DNA must be transported to the nucleus for effective transfection. There, the DNA can be transiently expressed for a short period of time, or become incorporated into the genomic DNA, where the change is passed on from cell to cell as it divides.

Discussions in chapter three involves the study of synthetic 14-mer oligonucleotide interactions with poly (amidoamine) (PAMAM) dendrimers of generations one, two and three (G1, G2 and G3) using fluorescence and Förster resonance energy transfer (FRET) methods. FRET is a widely used technique that quantifies molecular dynamics in protein–protein interactions, protein–DNA interactions and protein conformational changes. In this investigation we seek to explore dendrimer–short oligonucleic acid packing interactions as nano-complexes for gene silencing applications using the FRET technique. The required fluorometric experiments were carried out as follows: a synthetic oligonucleotide with 14 base pairs was tagged at 5' end with fluorescein (strand I) as well as with tetramethylrhodamine (TAMRA) (strand II) and fluorometric titrations were performed with a PAMAM dendrimer of the first three generations. Similarly, fluorometric titrations were also carried out for oligonucleotides 5'-tagged with either fluorescein or TAMRA. The oligonucleotide–dendrimer interactions were also investigated by ethidium bromide exclusion and gel electrophoresis studies for the first three generations.

As a major focus of the chapter three, the importance of short oligonucleotide packing in dendriplex-mediated gene delivery, a direct insight into the 14-mer oligonucleotide and dendrimer interactions using fluorescence and FRET techniques is considered. Fluorometric titrations of various fluorophore-tagged oligonucleotides with the first three PAMAM dendrimer generations showed a decrease in the

fluorescence intensity with two break points, namely $Z1_{\pm}$ and $Z2_{\pm}$, for each titration. The first break point for each dendrimer was identical to the neutralization point observed by basic biophysical studies for the corresponding dendrimer generations. Additionally, FRET studies on dual tagged oligonucleotide (DFT) molecules revealed a third break point at the charge ratio ($Z3_{\pm}$) where there was the highest fluorescence energy transfer from the donor to the acceptor fluorophores. Altogether, dendriplex formation was considered to take place via three steps with an increase in the dendrimer concentration, where initially there was monomeric complexation at the neutralization point ($Z1_{\pm}$) followed by loosely held molecular aggregation of the dendrimer ($Z2_{\pm}$). In the final step, dendrimer molecular aggregates were held tightly together for the closest possible packing of the oligonucleotide molecules onto their surface. The effective molecular packing is identified by the highest FRET intensity for the dendrimer of generation 2 at a charge ratio of 0.34 ($Z_{\pm}$).

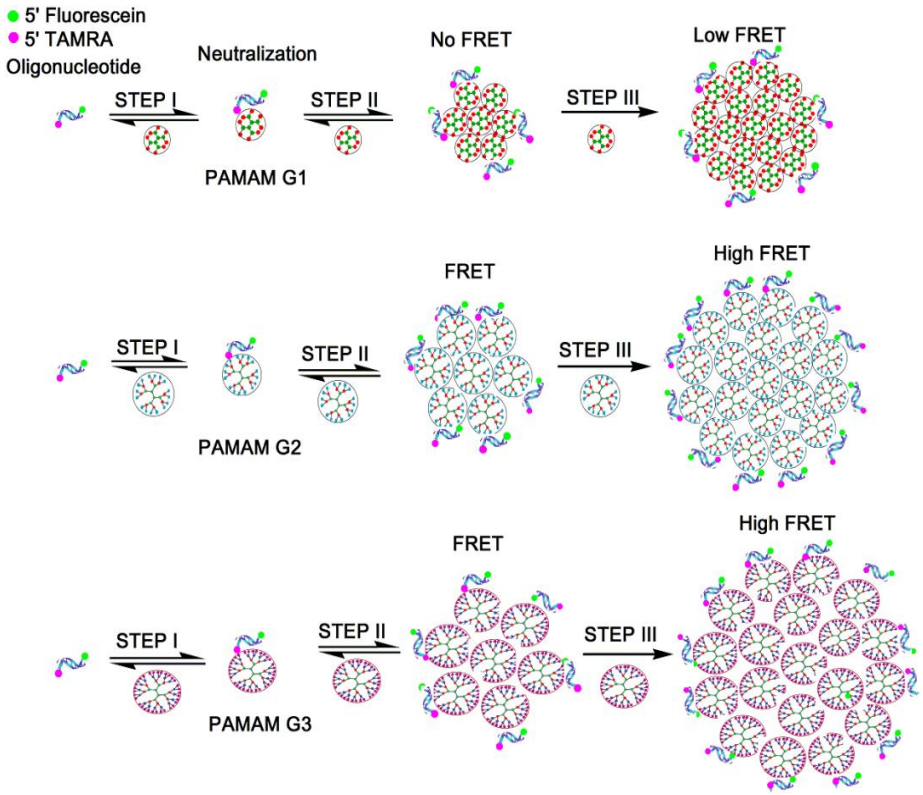

Figure 1.7 Schematic representations of the PAMAM dendrimer and oligonucleotide interactions for G1, G2 and G3.

The discussions in fourth chapter involves binding kinetics of the low generation PAMAM dendrimer (G1, G2 and G3) due to interaction with 14mer DNA oligonucleotides is well discussed by using the stopped-flow spectrofluorometry. Besides the effect of dendrimer architecture, we have looked into the dendrimer-to-DNA charge ratio and ionic strength. Based on these findings it was observed that the dendrimer binding on DNA took place in three consecutive steps, for which the corresponding first, second and third relative rate constants (k_1, $k_2$and k_3) were determined. The first step corresponds to interaction of single oligonucleotide molecule with the dendrimer molecule whereas the second step refers to miceller aggregation of the dendrimer in the vicinity of the 14-mer oligonucleotide and further arrangement of the oligonucleotide molecules on the surface of the dendrimer aggregates takes place in step 3. Interestingly, the architecture of the dendrimer was found to have a significant impact on the kinetics of the dendriplex formation. Among the first three generations of PAMAM dendrimers, G2 and G3 exhibited significantly faster binding kinetics compared to the G1 dendrimers.

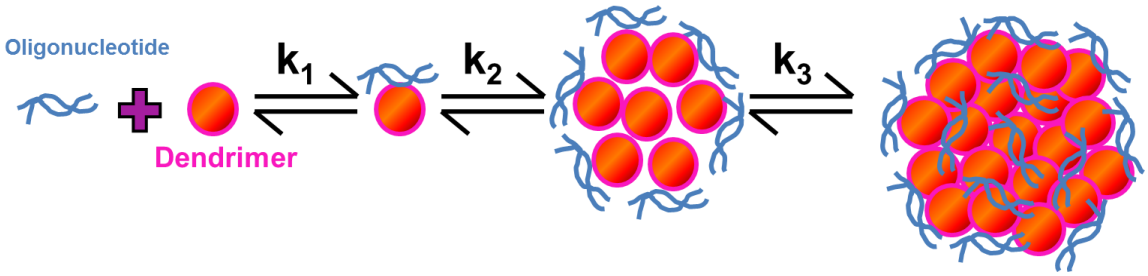

Figure 1.8 Schematic representation of the proposed lower generation PAMAM dendrimer binding mechanism and DNA compaction. The different components are not at scale.

Chapter five involves the study by considering together lower cytotoxicity and skin penetrability of lower generation PAMAM dendrimers, we have explored pDNA condensation using PAMAM dendrimers of first three generations G1, G2 and G3 by agarose gel as well as ethidium bromide (EtBr) condensation assays and subsequent DNA release is observed by EtBr release assay. Further, in order to understand dendrimer binding on DNA, stopped-flow fluorescence experiments are performed. *In vitro* DNA uptake and endosomal escape are demonstrated in CHO-K1 cells using

flow cytometry and confocal microscopy. Additionally, transfection efficiency of pDNA into the nucleus is also observed by luciferase assay in CHO-K1 cells in the presence as well as in the absence of endosomotropic agents like bafilomycin A1 and chloroquine. Cytotoxicity of these lower generation dendrimers is determined by MTT assay in CHO-K1 cells. Further, these observations are extended in human skin cell line, HaCaT as an application for gene delivery to check whether the low generation PAMAM dendrimers can deliver DNA into the human skin cells and the corresponding cytotoxicity is also tested. In addition to these, in order to explore the possibility of usage of the lower generation based dendriplexes in future for *in vivo* gene therapeutic studies, serum stability assays are carried out by exposing the dendriplexes to different concentrations of fetal bovine serum.

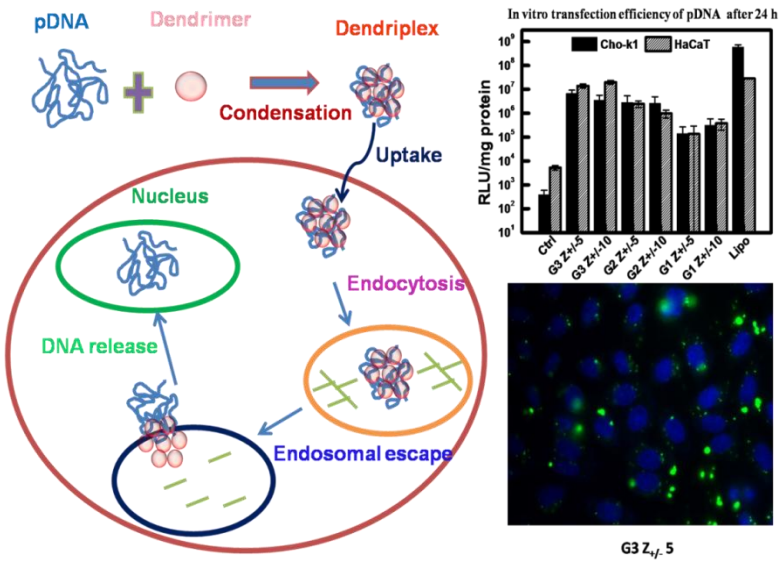

Figure 1.9 Schematic representation for the formation and internalization of PAMAM dendrimer and pDNA for G1, G2 and G3 and its applications.

In this study, we have first carried out a systematic biophysical analysis to analyze their ability for plasmid DNA (pDNA) condensation and subsequent release by ethidium bromide assay to optimize dendrimer to DNA charge ratio for effective pDNA condensation and release. Interestingly, stopped flow fluorescence spectroscopic analysis on pDNAdendrimer binding kinetics revealed the efficiency of generations G2 and G3 in pDNA condensation in comparison with G1 through four steps. Importantly, it validates aggregation and association of the dendrimer in the

vicinity of pDNA. Based on these understanding, successful in vitro cellular uptake of dendriplexes followed by their transfection into CHO-K1 cells was demonstrated at the charge ratio $Z_{\pm}$ 5 and 10. The interesting observations of gene transfection with CHO-K1 cells were extended to HaCaT cell line and efficient pDNA transfections were evidenced with negligible cytotoxicity. In addition to this, the stability of the dendriplexes at the charge ratio $Z_{\pm}$ 5 for G3 and $Z_{\pm}$10 for G2 was found even upto 50 % serum concentration suggesting possible future applicability in *Invivo*. Overall, the current approach promises the use of lower generation dendrimers for pDNA delivery to the skin using only electrostatic nanocomplex formation without any covalent linkage.

References

1. Anderson WF. Human gene therapy. *Nature*. (**1998)**; 392, 25–30.
2. Lain Jin, XinZeng, Ming Liu, Yan Deng, and Nongyue He. Current Progress in Gene Delivery Technology Based on Chemical Methods and Nano-carriers. *Theranostics*. (**2014),** 4(3), 240-255.
3. Liu X, et al. Structurally flexible triethanolamine-core poly(amidoamine) dendrimers as effective nanovectors to deliver RNAi-based therapeutics. *BiotechnolAdv.* **(2014)**, 32, 844–852.
4. Sneha Lingam. Mechanism of Transfer in Gene Therapy 7/30/07 Cluster 7. *Gene Therapy.*
5. Blaese RM, Culver KW, Miller AD, Carter CS, Fleisher T, Clerici M, Shearer G, Chang L, Chiang Y. T lymphocyte- directed gene therapy for ADA-SCID: Initial trial results after 4 years. *Science. (***1995),** 270, 475–480.
6. Muul LM, Tuschong LM, Soenen SL, Jagadeesh GJ, Ramsey WJ, Long Z, Carter CS, Garabedian EK, Alleyne M, Brown M, Bernstein W, Schurman SH, Fleisher TA, Leitman SF, Dunbar CE, Blaese RM, Candotti F, Tolstoshev P, Greenblatt JJ, Rosenberg SA, Klein H, Berger M, Mullen CA, Ramsey WJ, Muul L, Morgan RA, Anderson WF. Persistence and expression of the adenosine deaminase gene for twelve years and immune reaction to gene transfer components: Long-term results of the first clinical gene therapy trial. *Blood*. Nov 27, (**2002)**.

7. Timothy P. O'Connor and Ronald G. Crystal. Genetic medicines: treatment strategies for hereditary disorders. *Nature Reviews Genetics*. (**2006)**, VOLUME 7, 261-276.
8. Genecure.com Technology. Retrieved from: http://www.genecure.com/ technology.html.
9. Yotnda P, Chen D-H, Chiu W, Piedra PA, Davis A, Templeton NS, Brenner MK. Bilamellar cationic liposomes protect adeno- vectors from preexisting humoral immune responses. *MolTher. (***2002)**, 5, 233–241.
10. D Stone, A David, F Bolognani, P R Lowenstein and M G Castro. Viral vectors for gene delivery and gene therapy within the endocrine system. *Journal of Endocrinology.* (**2000**), 164, 103–118.
11. Edwards, M. T. Gene Therapy: Current Treatment Options and Likely Near-Term Developments. *Inquiries Journal/Student Pulse*. (**2014**). 6(09). Retrieved from: http://www.inquiriesjournal.com/a?id=914.
12. Rachel M. Levine, Carolyn M. Scott and EfrosiniKokkoli. Peptide functionalized nanoparticles for nonviral gene delivery. *Soft Matter.* (**2013)**, 9, 985–1004.
13. Hannah H. Choi and Gaurav T. Tolia. The Role of Dendrimers in Topical Drug Delivery. *Pharmaceutical Technology.* (**2008**), Volume 32, Issue 11. Retrieved from: http://www.pharmtech.com/role-dendrimers-topical-drug-delivery.
14. Hao Yin, Rosemary L. Kanasty, Ahmed A. Eltoukhy, Arturo J. Vegas, J. Robert Dorkin and Daniel G. Anderson. Non-viral vectors for gene-based therapy. *Nature Reviews Genetics.* (**2014)**, 15, 541-555.
15. Tomalia, D. A.; Baker, H.; Dewald, J.; Hall, M.; Kallos, G.; Martin, S.; Roeck, J.; Ryder, J.; Smith, P. A new class of polymers: Starburst-dendritic Macromolecules. *Polym J*. (**1985)**, 17, 117–132.
16. Donald A. Tomalia, Jean M. J. Fre ´Chet. Discovery of Dendrimers and Dendritic Polymers: A Brief Historical Perspective. *Journal of Polymer Science: Part A: Polymer Chemistry.* (**2002**), Vol. 40, 2719–2728**.**

17. Anil K Patri, István J Majoros and James R Baker Jr. Dendritic polymer macromolecular carriers for drug delivery. *Current Opinion in Chemical Biology.* (**2002)**, 6, 466–471.

18. L. Vincent, J. Varet, J.Y. Pille, H. Bompais, P. Opolon, A. Maksimenko, C. Malvy, M. Mirshahi, H. Lu, J.P. Vannier, C. Soria, H. Li. Efficacy of dendrimer-mediated angiostatin and TIMP-2 gene delivery on inhibition of tumor growth and angiogenesis: in vitro and in vivo studies. *Int. J. Cancer.* (**2003**), 105, 419–429.

19. A.U. Bielinska, A. Yen, H.L. Wu, K.M. Zahos, R. Sun, N.D. Weiner, J.R. Baker, B.J. Roessler. Application of membrane-based dendrimer/DNA complexes for solid phase transfection in vitro and in vivo. *Biomaterials.* (**2000**), 21, 877–887.

20. A.M. Funhoff, C.F. van Nostrum, G.A. Koning, N.M.E. SchuurmansNieuwenbroek, D.J.A. Crommelin, W.E. Hennink. Endosomal escape of polymeric gene delivery complexes is not always enhanced by polymers buffering at low pH. *Biomacromolecules.* (**2004**), 5, 32–39.

21. A.M. Funhoff, C.F. van Nostrum, A.P.C.A. Janssen, M.H.A.M. Fens, D.J. A. Crommelin, W.E. Hennink. Polymer side-chain degradation as a tool to control the destabilization of polyplexes. *Pharm. Res*. (**2004**), 21, 170–176.

22. Roberts JC, BhalgatMK, Zera RT. Preliminary biological evaluation of polyamidoamine (PAMAM) Starburst(TM) dendrimers. *J. Biomed. Mater. Res.* (**1996)**, 30, 53–65.

23. Malik N, Wiwattanapatapee R, Klopsch R, Lorenz K, Frey H, Weener JW, Meijer EW, PaulusW, Duncan R. Dendrimers: Relationship between structure and biocompatibility in vitro, and preliminary studies on the biodistribution of I-125-labelled polyamidoamine dendrimers in vivo. *J. Controlled Release*. (**2000),** 65, 133–148.

24. Kukowska LatalloJF, Bielinska AU, Johnson J, Spindler R, Tomalia DA, Baker JR. Efficient transfer of genetic material into mammalian cells using Starburst polyamidoamine dendrimers. *Proc. Natl. Acad. Sci. U. S. A*. (**1996)**; 93, 4897–4902.

25. Braun CS, VetroJA, TomaliaDA, KoeGS, KoeJG, Middaugh CR. Structure/function relationships of polyamidoamine/DNA dendrimers as gene delivery vehicles. *J. Pharm. Sci.* (**2005)**, 94, 423–436.

26. Haensler J, SzokaJr FC. Polyamidoamine cascade polymers mediate efficient transfection of cells in culture. *Bioconjugate Chem.* (**1993)**, 4, 372–379.

27. Krishna TR, Jain S, Tatu US, Jayaraman N. Synthesis and biological evaluation of 3-amino-propan-1-ol based poly (ether imine) dendrimers. *Tetrahedron*. (**2005)**, 61, 4281–4288.

28. Boyd BJ. Past and future evolution in colloidal drug delivery systems. *Expert Opinion on Drug Delivery*. (**2008),** 5, 69–85.

29. Sabine Fuchs, TimoKapp, Henning Otto, TorstenSchˆneberg, Peter Franke, Ronald Gust, and A. Dieter Schl¸ter. A Surface-Modified Dendrimer Set for Potential Application as Drug Delivery Vehicles: Synthesis, In Vitro Toxicity, and Intracellular Localization. *Chem. Eur. J.* (**2004)**, 10, 1167- 1192.

30. Istva´n J. Majoros, Thommey P. Thomas, Chandan B. Mehta, and James R. Baker Jr. Poly(amidoamine) Dendrimer-Based Multifunctional Engineered Nanodevice for Cancer Therapy. *J. Med. Chem*. (**2005)**, 48, 5892-5899.

31. Transepithelial transport of PEGylated anionic poly(amidoamine) dendrimers: Implications for oral drug delivery. *J.Control. Release*. (**2009)**, 138, 19, 78-85.

32. Lisa M. Kaminskas, Brian D. Kelly, Victoria M. McLeod, Ben J. Boyd, Guy Y. Krippner, Elizabeth D. Williams, and Christopher J. H. Porter. Pharmacokinetics and Tumor Disposition of PEGylated, Methotrexate Conjugated Poly-L-lysine Dendrimers. *Molecular Pharmaceutics*. (**2009),** VOL. 6, NO. 4, 1190–1204.

33. Yoonkyung Kim, Athena M. Klutz and Kenneth A. Jacobson. Systematic Investigation of Polyamidoamine Dendrimers Surface-Modified with Poly(ethylene glycol) for Drug Delivery Applications: Synthesis, Characterization, and Evaluation of Cytotoxicity. *Bioconjugate Chemistry.* (**2008)**, *19* (8), 1660–1672.

34. Alona P. Umali , Hannah L. Crampton , and Eric E. Simanek. Triazine Dendrimers with Orthogonally Protected Amines on the Periphery. Masking Amines with Dde and BOC Groups Provides an Alternative to Carrying Protected Alcohols and Disulfides through an Iterative Synthesis. *Journal of Organic Chemistry*. (**2007)**, 72, 9866-9874.

35. Angkana Saovapakhiran, Antony D'Emanuele, David Attwood, and Jeffrey Penny. Surface Modification of PAMAM Dendrimers Modulates the Mechanism of Cellular Internalization. *Bioconjugate Chemistry*. (**2009)**, 20, 693–701.

CHAPTER 2
EXPERIMENTAL MATERIALS AND METHODS

In this chapter, the details of the different reagents, cell culture medium and cell lines used, the biophysical characterization techniques adopted and the experimental procedures followed for various investigations have been described.

2.1 Materials and Reagents

2.1.1 0.1 M Phosphate buffer (PB)

(a) **0.2 M Monobasic stock:** 6.95 g sodium phosphate monobasic was added into 250 mL autoclaved milli-Q water.

(b) **0.2 M Dibasic stock:** 5.365 g sodium phosphate dibasic heptahydrate was mixed into the 100 mL of autoclaved milli-Q water.

(c) **0.1 M Buffer:** To prepare buffer, the following quantities of each stock solutions were mixed as shown below, followed by the addition of autoclaved milli-Q water to bring upto 600 mL.

Monobasic	Dibasic	pH
205.5 mL	94.5 mL	6.5

2.1.2 DNA Duplex stock preparation

14mer DNA short oligonucleotides were used for all the biophysical studies with the following sequences:

(a) **Unlabelled duplex (D_0) DNA oligonucleotide preparation:** the equimolar amount of stand I and strand II were mixed and subjected to heat at 95 °C for 10 minute.

Strand I (5'-GATGTTCACTCCAG-3') (SBS-Genetech)

Strand II (5'-CTGGAGTGAACATC-3') (SBS-Genetech)

(b) **Duplex labelled with 5'-fluorescein (D_F) preparation:** Equimolar quantity of 5'-fluorescein labelled stand I was mixed with unlabelled strand II and heated at 95 °C for 10 minute.

Strand I (Fluorescein 5'-GATGTTCACTCCAG-3') (SBS-Genetech)

Strand II (5'-CTGGAGTGAACATC-3') (SBS-Genetech)

(c) **Duplex labelled with 5'-TAMRA (D_T) preparation:** To the unlabelled strand I Equimolar amount of stand II tagged with 5'-TAMRA was mixed and heated at 95 °C for 10 minute.

Strand I (5'-GATGTTCACTCCAG-3') (SBS-Genetech)

Strand II (TAMRA 5'-CTGGAGTGAACATC-3') (SBS-Genetech)

(d) **Duplex tagged with 5'-fluorescein as well as 5'-TAMRA (D_{FT}) preparation:** Equimolar amount of 5'-fluorescein labelled stand I with stand II tagged with 5'-TAMRA were added together and heat at 95°C for 10 minute.

strand I (Fluorescein 5'-GATGTTCACTCCAG-3') (SBS-Genetech)

strand II (TAMRA 5'-CTGGAGTGAACATC-3') (SBS-Genetech)

2.1.3 Plasmid DNA (pDNA)

(a) **pEGFP-C1 plasmid**

(b) **pMIR plasmid**

2.2 Biophysical and Biochemical characterization techniques:

The nucleic acids (short oligonucleotide and pDNA) used in this investigations for the interaction of various lower generation PAMAM (polyamidoamine) dendrimers were characterized by various biophysical and biochemical techniques such as gel electrophoresis studies, UV-Visible spectroscopy, Circular Dichroism, fluorescence spectroscopy and stopped flow fluorescence spectroscopy are illustrated as below:

2.2.1 Gel electrophoresis studies [1-4]

Gel electrophoresis is used to separate and analyze DNA, RNA and proteins by their size and charge using the electric field. Here, The electrophoretic mobilities of PAMAM dendrimer of generations 1, 2 & 3 and untagged oligonucleotide (14 mer) complexes at various charge ratios $Z_{\pm}$ were determined by using 15% native-PAGE in a buffer consisting of 45 mM Tris-borate and 1 mM EDTA at pH 8.0. In these studies, in order to prepare oligonucleotide-dendrimer complex of required chargeratio, 1 μM concentration of oligonucleotide (equivalent to 26 μM phosphate unit) was mixed with various concentrations of the desired dendrimer generations (1, 2 & 3) solution and incubated for 30 min. Polyacrylamide gels were run at 120 V for 4 h at 4 °C. Further, the corresponding dendriplex bands were visualized under UV illumination after staining the gels with ethidium bromide for 30 min at room temperature.

(a) 15% native-PAGE

The following table shows the composition for preparing the 10 ml of 15% stacking gel.

TABLE II. Composition of 15 % native-PAGE gel for 30 ml

Acylamide percentage	15% native-PAGE
Acrylamide/Bis-acrylamide(40%/0.8% w/v)	5ml
0.375M Tris-HCl(pH=8.8)	4.89ml
*10% (w/v) ammonium persulfate (AP)	100µl
*TEMED	10µl

* Prepared and added right before each use.

- **Acrylaminde and N,N'-methylene bisacrylamide** *(Loba Chemicals, Mumbai, India)* A stock solution containing 29% (w/v) acrylamide and 1% w/v N,N'-methylene bisacrylamide was prepared in autoclaved milli-Qwater and stored in a brown bottle at 4°C.

- **Running gel buffer** 1.5M tris was dissolved in autoclaved milli-Q water and pH of the solution was adjusted to 8.8 with HCl.
- **TEMED (N,N,N'-N'-tetramethylethylene-diamine)** (SRL Chemicals, Mumbai, India) TEMED accelerates the polymerisation of acrylamide and bisacrylamide by catalysing the formation of free radicals from ammonium-persulphate.
- **Ammonium persulphate(AP)**(Aldrich Chemicals, USA) Ammonium persulphate provides the free radicals that drive polymerisation of acrylamide and bisacrylamide. 10% (w/v) of this solution was prepared freshly before use.

(b) Preparation of gel

1. Required amounts of Acrylamide/Bis-acrylamide (30%/0.8% w/v) in separating gel buffer into a 10 ml falcon tube was added along with the specific volumes of AP and TEMED and gently swirled the falconto ensure a propermixing. The gel solution was pipetted into the gap between the glass plates of gel casting (Filled around 80%). The rest space was filled with water (isopropanol alternatively) and the comb was inserted. For a complete gelation, the glass plate was allowed to stand for 20-30min
2. The samples were mixed with gel loading 6X dye.
3. The sample mixture was loaded, the voltage was set to 120 V and the gel was allowed to run for 40 minutes to run at 4° C.
4. Finally the gel was stained with ethidium bromide.

(c) Gel staining

The investigation of nucleic acid-PAMAM dendrimer interaction was done by staining the gel in the running buffer containing ethidium bromide and kept on the rotator shaker for 20 minutes to make sure the sufficient staining of the gel. After staining the gel, observed in the gel documentation and taken the picture for permanent records.

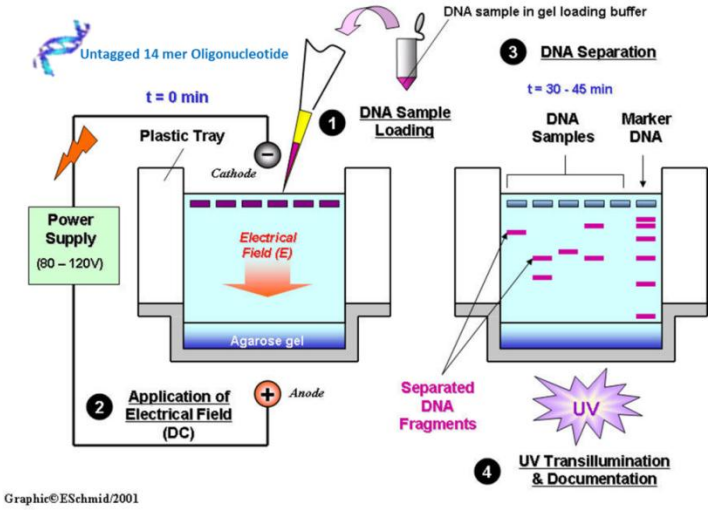

Figure 2.1 Principle of the agarose gel electrophoresis technique (modified from https://goo.gl/images/Xo35Pn)[(4)].

2.2.2 Agarose gel

Similarly, agarose gel electrophoresis studies have been performed to study the pDNA interactions with PAMAM (polyamidoamine) dendrimers of first three generations as mentioned clearly in chapter 5.

2.2.3 UV melting studies [(5-9)]

The association-dissociation characteristics of DNA could be assessed by melting or thermal melting curve analysis by using UV spectroscopy technique. The thermal denaturation of double stranded DNA is progressive and the concerted melting of the whole structure occurs at a well defined temperature, corresponding to the mid-point of a smooth transition. This temperature is known as the **melting temperature**. Figure 2.2 shows a typical UV melting curve (UV absorption as a function of temperature)[(5)].UV-melting experiments were performed using Cary 100 UV-visible spectrophotometer with temperature controller to study the various duplexes. Melting experiments were carried out by heating 1 μM concentration of unlabelled (D_0) duplex, the duplex tagged with 5′-fluorescein (D_F), the duplex labelled with 5′-TAMRA (D_T) and the duplex tagged with 5′-fluorescein as well as 5′-TAMRA (D_{FT}) from 20 to 95°C at a scanning rate of 1.0 °C/min in a 1000 µL cuvette. The melting profiles of the oligonucleotides were recorded by monitoring the absorbance of the

complexes at 260 nm as a function of temperature. Transition temperatures were calculated from the melting curves and revealed that their T_m values were in the rage of 33 to 37 °C (data not shown).

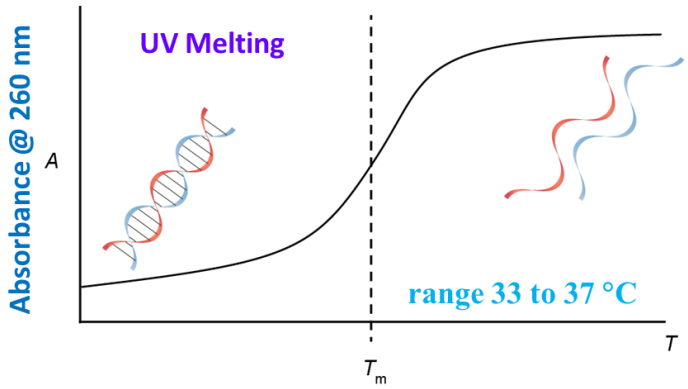

Figure 2.2 A typical UV melting curve. UV absorption as a function of temperature[5]

2.2.4 Circular Dichroism (CD) Spectroscopy [10-17]

CD measures the difference in absorption between left and right handed circularly polarized light in chiral molecules. CD spectroscopy is an established biophysical method to examine the secondary structure (figure 2.4) (e.g. α-helices, betasheets, turns etc.) of peptides, proteins and nucleic acids which have distinguishable CD bands.

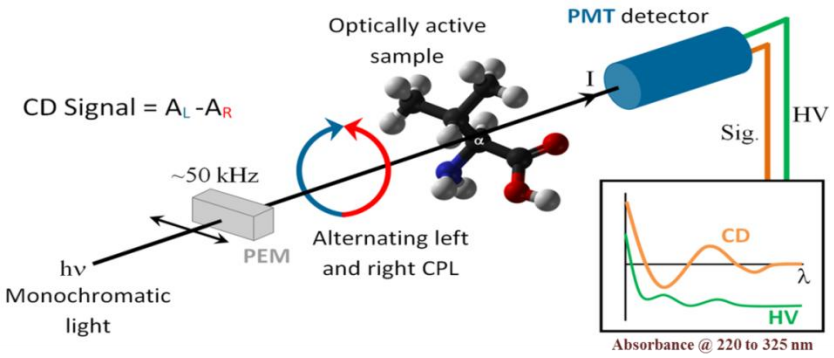

Figure. 2.3 Principle behind Circular Dichroism (CD) Spectroscopy[12](Modified from reference 12)

The principle behind CD spectroscopy technique is that the monochromatised light is passed through a Photo Elastic Modulator (PEM) which converts the linear polarised light into alternating left and right handed polarised light. The two polarizations are differently absorbed, and the difference in absorption is detected with a Photo Multiplier Tube (PMT).

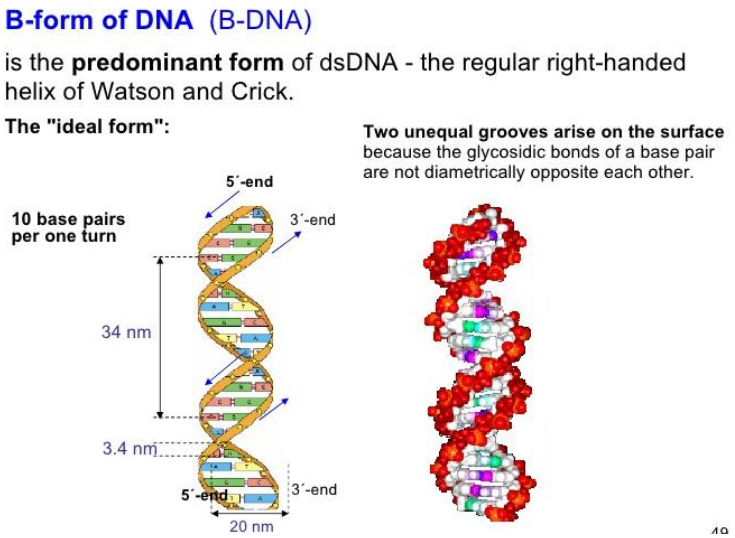

Figure 2.4 Secondary structure of B-form DNA[17].

2.2.5 Fluorescence Spectroscopy [18-20]

Fluorescence spectroscopy is primarily concerned with electronic and vibrational states. Generally, the species being examined hasinitial ground electronic state level (a low energy state) of interest, and an excited electronic state of higher energy. Within each of these electronic states are various vibrational states[18].

In fluorescence spectroscopy, the species is first excited, by absorbing a photon, from its ground electronic state to one of the various vibrational states in the excited electronic state. Collisions with other molecules cause the excited molecule to lose vibrational energy until it reaches the lowest vibrational state of the excited electronic state. This process is often visualized with a Jablonski diagram shown in figure 2.5.

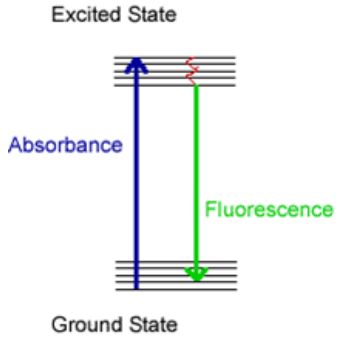

Figure 2.5 Principle of fluorescence spectroscopy [19]

In these studies, ethidium bromide, a planar aromatic dye is used as a fluorescence spectroscopic probe to determine relative affinities of PAMAM dendrimer of various generations (G1, G2 and G3) for the oligonucleotide. EB is well known to show a striking increase in fluorescence efficiency by intercalating between the base pairs of double helix DNA. The competition between the EB and the cationic co-solutes can be followed by determining quenching in fluorescence intensity of DNA-EB complex shown in figure 2.6.

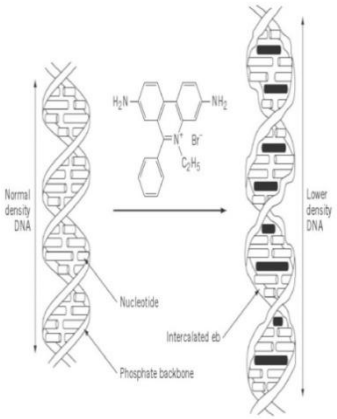

Figure.2.6 Intercalation of ethidium bromide with in the base pairs of double helix DNA[20].

2.2.6. Forster Resonance Energy Transfer (FRET)[21-23]

FRET is a widely used technique for the quantification of molecular dynamics in phenomena like protein-protein interaction, protein-DNA interactions and protein conformational changes. In order to monitor complex formation between two molecules, one of the strand of DNA is labeled with a donor fluorophore and the other with an acceptor fluorophore. When the donor and acceptor are in close proximity (1-10 nm) due to complex formation, the predominantly observed emission is that of the acceptor because of **intermolecular FRET** from donor to acceptor, whereas, in the absence of complex formation, FRET from donor to acceptor cannot occur, and donor emission predominates. Jablonski diagram of FRET has been shown in figure 2.7[23].

2.2.7 Stopped flow spectrofluorometry[24, 25]:

Stopped flow instrument is a rapid mixing device used to study the chemical kinetics of a reaction in solution. After two or more solutions containing the reagents are mixed, they are studied by whatever experimental methods are deemed suitable. Different forms of spectroscopy and scattering of radiation are common methods used. The dead time is the time between the end of mixing the two solutions and the beginning of observation of the kinetics of the reaction. The usual dead time of a stopped flow apparatus is 1-2 milliseconds but some new devices have been developed that have dead times of 0.3-0.6 ms.

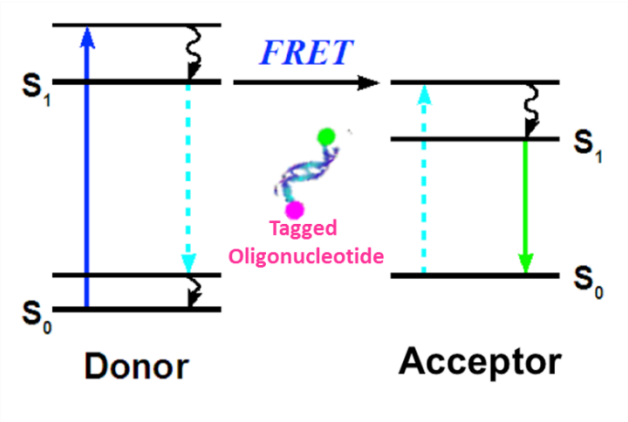

Figure 2.7 Jablonski diagram of FRET. Modified from wikipedia[23].

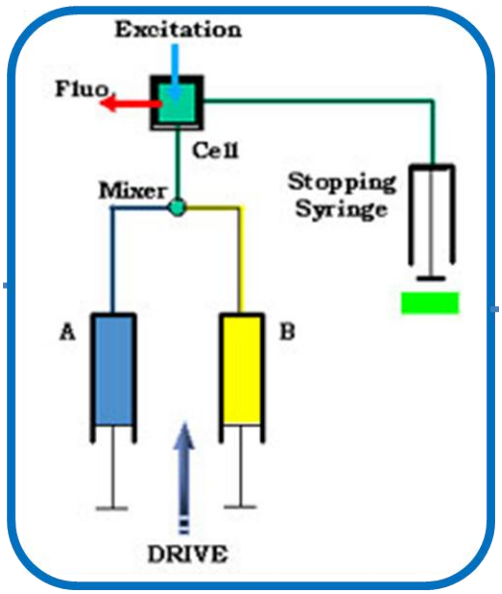

Figure 2.8 The schematic method of typical Stopped Flow spectrofluorometry device[25].

2.3 *In-vitro* cell culture techniques

2.3.1 Cell Lines used[26-31]

(a) Chinese hamster ovary (CHO.K1) cell line

Cell Line Origin. The origin of the cell line is from Chinese Hamster ovary. A subclone of the parental CHO cell line, which was derived from the ovary of an adult Chinese hamster. Cells require proline due to the absence of the gene for proline synthesis, the block in the biosynthetic chain lies in the step converting glutamic acid to glutamine gamma serialdehyde. They undergo morphological changes in response to cholera toxin.

Culture Medium used Ham's F12+ 2mM Glutamine+ 10% Foetal Bovine Serum FBS / FCS.

(b) Human skin cell line (HaCaT):

HaCaT is a spontaneously transformed aneuploid immortal keratinocyte cell line from adult human skin, widely used in scientific research. HaCaT cells are utilized for their high capacity to differentiate and proliferate in vitro.

Organism Type Human immortalized keratinocytes

Tissues Keratinocyte

Culture MediaDMEM media with 10% FCS and 1% Pencillin/Streptomycin.

Cell doubling time is approximately 24 hours (to calculate dilutions for splitting cells)

Splitting of HaCaT Cells.

1. Media was removed from flask followed by the addition of 10ml PBS to rinse cells then remove;
2. 2-3ml trypsin was added and left until all cells had rounded up and begun to detach (for ~10min) in $37^{o}C/5\%$ CO_2 incubator;
3. Flask was banged to dislodge cells (If cells are not sliding down flask easily then placed flask back in incubator for a further 1-2min and tried again);
4. 10ml DMEM/10% FBS media was added to flask and pipetted up and down to remove clumps and resuspend cells;

5. Resuspended cells were transferred to a 15ml Falcon tube and centrifuged @ 1,500 rpm for 5min with a balance;
6. Supernatant was poured off and the pellet was resuspended in approximately 10 ml of fresh media
7. Required amount was transferred (this will depend on how long one wish to grow them for) into a new flask and added fresh media so final volume in the flask was maintained between 20 and 25 mL.
8. Finally a cell count was performed on cell suspension and adjusted to required cell concentration with fresh media to perform assay or experiment.

2.3.2 *In-Vitro* cell Transfection [32, 33]:

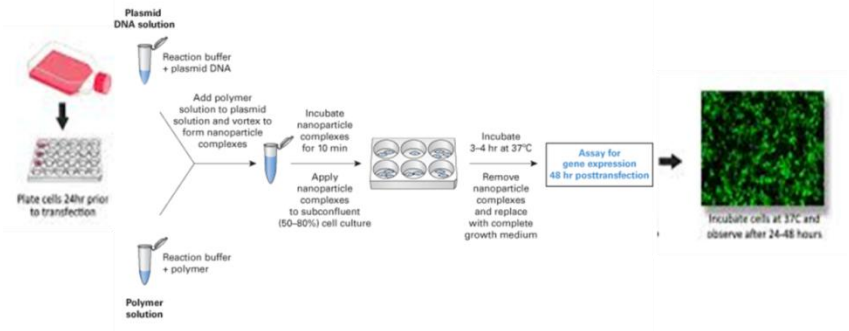

Figure 2.9 Schematic representation of in-vitro transfection procedure[33].

The introduction or transfer of foreign DNA/ gene into nucleus of eukaryotic cells is defined as transfection. And the introduced foreign DNA into the cells is called as transfectant. The method of transfection have been developed by F. L. GRAHAM and A. J. VAN DER EB in 1973 introduced viral DNA using calcium phosphate[]. The transfer of nucleic acids into cells is one of the most valuable and frequently used tools of gene therapeutic studies. Transfection methods are used for wide range of applications, including gene function studies, gene expression, biochemical gene mapping, mutational analysis and production of recombinant proteins.

The transfection techniques which are commonly used today can be majorly classified into three groups

1. Methods that make use of genetically engineered viruses

2. Chemical methods or methods that rely on carrier molecules
3. Physical methods or methods which deliver nucleic acids directly to the cytoplasm.

Not all transfection methods can be applied to all types of cells or experimental methods, and there is wide variation with respect to the attained transfection efficiency, viability, level of gene expression etc. Determination of the best transfection method for a specific application depends on several factors like cell type (primary cells or cell line), cellular context (in vitro, in vivo, ex vivo), capability of transgene, general safety like immunogenitcity, desired transfection efficiency, cost, time etc.

References

1. MuhittinYılmaz, CemOzic and İlhamiGok (2012). Principles of Nucleic Acid Separation by Agarose Gel Electrophoresis, Gel Electrophoresis - Principles and Basics, Dr. SamehMagdeldin (Ed.), ISBN: 978-953-51- 0458-2, InTech, Available from:http://www.intechopen.com/books/gel-electrophoresis-principles-andbasics/principles-of-nucleic-acid-separation-by-agarose-gel-electrophoresis
2. Smith, S. B., Aldridge, P. K., Callis, J. B. Observation of individual DNA molecules undergoing gel electrophoresis. *Science*. **(1989),** 243**,** 203-206.
3. Aaji, C., Borst, P. The gel electrophoresis of DNA. *Biochim. Biophys. Acta*. **(1972)**, 269**,** 192-200.
4. Gel electrophoresis. Available from:http://classroom.sdmesa.edu/BioWebS; page no.2.
5. Prof. Tom Brown and Dr Tom Brown (Jr). DNA duplex stability. Available from: http://www.atdbio.com/content/53/DNA-duplex-stability.
6. Ansevin, A.T.; Vizard, D.L.; Brown, B.W.; McConathy, J. High-resolution thermal denaturation of DNA. I. Theoretical and practical considerations for the resolution of thermal subtransitions. *Biopolymers*. **(1976),** 15 (1), 153–74.

7. Nucleic Acid Thermal Stability Analysis (Tm Analysis), SHIMADZU: Analytical and Measuring Instruments. Available from: http://www.shimadzu.com/ an/uv/support/uv/ap/ nucleic.html
8. Ririe, K.M.; Rasmussen, R.P.; Wittwer, C.T. Product differentiation by analysis of DNA melting curves during the polymerase chain reaction. *Anal. Biochem* **(1997)**, 245 (2), 154–60.
9. Wienken CJ, Baaske P, Duhr S, Braun D. Thermophoretic melting curves quantify the conformation and stability of RNA and DNA. *Nucleic Acids Research*. **(2011),** 39 (8), e52.
10. Walter A.Baase and W.Curtis Johnson,Jr. Circular dichroism and DNA secondary structure. *Nucleic Acids Research.* **(1979)**, Vol.4 no.2, 797-814.
11. JaroslavKypr, Iva Kejnovska, Daniel Renc iuk and Michaela Vorlı´c kova. Circular dichroism and conformational polymorphism of DNA. *Nucleic Acids Research.* **(2009)**, Vol. 37, No. 6, 1713–1725.
12. Physical Biochemistry: Principles and Applications, David Sheehan, John Wiley & Sons, **(2000)**.
13. Biophysical Chemistry, Part II: Techniques for the study of biological structure and function, Charles R. Cantor and Paul R. Schimmel, W.H. Freeman & Co., **(1980)**.
14. JASCO J-810 spectropolarimeter operating Manual.
15. Nichola C Garbett, Patricia A Ragazzon& Jonathan B Chaires, Circular dichroism to determine binding mode and affinity of ligand–DNA interactions, *Nature Protocols*. **(2007),** VOL.2 NO.12, 3166-3172.
16. ISA, CENTRE FOR STORAGE RING FACILITIES, AARHUS. Available from: http://www.isa.au.dk/news/Rosetta-Nov2014.asp.
17. Polysaccharides Heteroglycosides Nucleosides, nucleotides, nucleic acids Medical Chemistry (**2007**) (J.S.) Lecture 10.
18. Akul Mehta, Animation for the Principle of Fluorescence and UV-Visible Absorbance. Analytical Chemistry, Animations, Notes | March 20, **(2013)**. Avalable from: http://pharmaxchange.info/press/2013/03/animation-for-the-principle-of-fluorescence-and-uv-visible-absorbance/

19. Fluorescence Spectroscopy, Background. Available from: https://www.kutztown.edu/academics/colleges-and-departments/liberal-artsand-sciences/departments/physical-sciences/chemistry-and biochemistry/instrumentation/fluorescence-spectroscopy.htm
20. M.J. Waring. Complex formation between ethidium bromide and nucleic acids. *J Mol Biol.* (**1965**), 13(1), 269-282.
21. Förster, Theodor, ZwischenmolekulareEnergiewanderung und Fluoreszenz. Intermolecular energy migration and fluorescence. **(1948),** 437, 55–75.
22. Helms, Volkhard. Fluorescence Resonance Energy Transfer. *Principles of Computational Cell Biology*. Weinheim: Wiley-VCH. p. 202 **(2008)**. ISBN 978-3-527-31555-0.
23. Forster resonance energy transfer. Available from: https://en.wikipedia.org/wiki/F%C3%B6rster_resonance_energy_transfer.
24. Dick Fielding, Stopped-Flow Spectroscopy, Applied Photophysics, tutorials.Retrieved from: http://www.photophysics.com/tutorials/stopped-flow-spectroscopy.
25. SFA-20 Stopped Flow Device, Horiba Scientific accessories.
26. Cell culture guidelines, retrieved from: abcam.com/technical.
27. CHO Cell Line General Information and Resources. Retrieved from: http://www.chocelltransfection.com/cellcultureinformationandprotocol/
28. CHOK1 (ATCC CCL61).
29. Ham's F-12K (Kaighn's) Medium,ThermoFisher scientific.
30. XiongDingding; Lee Gil-Hwan; Badorff Cornel; Dorner Andrea; Lee Sang; Wolf Paul; Knowlton Kirk U;Dystrophin deficiency markedly increases enterovirus-induced cardiomyopathy: a genetic predisposition to viral heart disease. *Nat. Med*. **(2002)**, 8, 872-877.
31. CLS Cell Lines Service GmbH - Dr. Eckener-Straße 8 - 69214 Eppelheim– Germany.
32. JoVE Science Education Database. Basic Methods in Cellular and Molecular Biology. *An Introduction to Transfection*. JoVE, Cambridge, MA, doi: 10.3791/5068 **(2017)**.
33. DNA-In® Transfection Reagent. Retrieved from: https://www.mti-globalstem.com/DNA-In%20Transfection.

CHAPTER 3

FLUORESCENCE AND FÖRSTER RESONANCE ENERGY TRANSFER INVESTIGATIONS ON DNA OLIGONUCLEOTIDE AND PAMAM DENDRIMER PACKING INTERACTIONS IN DENDRIPLEXES

3.1 Introduction

In recent years, therapeutic gene silencing has attracted a numerous researchers for treating a variety of diseases including viral infections, cancers, myopathies and neurodegenerative diseases by regulating genes due to its potency, selectivity and versatility. Interestingly, gene silencing activity is currently being researched by delivering short synthetic oligonucleotides, such as antisenses, siRNAs and miRNA to control the expression of a specific target gene by inhibiting the corresponding mRNA function without influencing genomic DNA.[1-6] Such an attractive therapeutic strategy is expected to overcome several critical hurdles including off-target effects, toxicity due to saturation of the endogenous RNAi functions, limited duration of silencing, and ineffective targeted delivery before its widespread clinical adoption.[5] In order to overcome these clinical hurdles in gene silencing activity, the use of 21-23 base-pared siRNA is considered to be one of the most promising tool due to its high potency and minimum off-target interaction.[7] However, the successful delivery of siRNA molecule with high efficiency still faces challenges for *in vivo* delivery due to its low resistance against enzymatic degradation, limited translocation across the cell membrane and a substantial liver clearance.[8] Apart from these, due to the relatively small size of these oligonucleotides, the requirement for vectors designed for their *in vitro* or *in vivo* delivery is observed to be more stringent than the delivery of long DNA.[9]

However, a numerous non-viral cationic molecules such as liposomes and cationic polymers including poly(L-lysine), poly(amidoamine) (PAMAM) dendrimers,

poly(alkylcyanoacrylate) nanoparticles and poly(ethylene imine) are observed to be successful for the siRNA delivery into the target cells.[10-14] These cationic carriers are well known to interact electrostatically with the anionic nucleic acid molecules by forming nano-sized siRNA-polymer complexes which can protect nucleic acids from non-specific interactions and enzymatic degradation in the systemic circulation.[15] Among the other cationic vectors, dendrimers are considered to be interesting polymeric gene carriers in non-viral gene therapy due to their synthetically tunable molecular structure, size, surface charge as well as functionality. More importantly, highly definable mono-dispersed population is observed in dendrimers due to their uniform size and distribution of surface charge for efficient delivery of *therapeutic* genes. Furthermore, these cationic macromolecular vectors without as well as with varied core/branching structures are shown to form stable complexes with nucleic acids by protecting them from nucleases and are used extensively for the *in vitro* delivery of plasmid DNA as well as antisense oligonucleotides and siRNA in various cell lines.[16-19] For example, PAMAM-DNA, poly(ethyleneglycol)-modified PAMAM-DNA, PAMAM-PEG-PAMAM-DNA, PPI-DNA and PEI-DNA interactions reveal ~~a~~ numerous formulations for dendrimer-DNA polyplexes [18,19] and a few reports also indicating usefulness of functionalized PAMAM dendrimers as *in vivo* gene delivery vehicles into kidney [20] and brain [21] tissue of mice. Even though PAMAM dendrimers of higher generations especially above 4 are shown to be better gene carriers in spite of their cytotoxicity [18, 19] recently there are few interesting studies highlighting the importance of lower generation dendrimers. For example, the lower generation dendrimers G2 and G4 are shown as potential POPC (palmitoyloleoylphosphatidylcholine) model bio-membrane transfection mediators.[22] Interestingly, siRNA/G1 PAMAM dendriplex is found to decrease both p42-MAPK mRNA and protein levels and could potentiate the antitumoral activity of anticancer drugs [23] and the lower PAMAM dendrimer generation 2 is proved to be superior to those of G4 in skin penetration.[24]

Most of these dendrimer studies also reveal that there is a need of controlled and triggered nucleic acid delivery from the carrier complex by analyzing structure-property relationships of dendrimer-oligonucletide delivery systems for successful gene and gene silencing therapies. For example, Nordén and co-workers [(25)] demonstrated how the condensation degree of plasmid DNA-poly(amidoamine) dendrimer of generation 5 complex affects enzyme accessibility and gene expression. Interestingly here, a high-density dendriplex was identified to turn off gene expression, whereas uncondensed DNA behavior was observed in the case of low-density dendriplex. Using fluorescence lifetimes and time-resolved spectra, Yliperttula *et al* [(26)] showed easy release of DNA from DNA-poly (ethylenimine) (PEI) complex to the right intracellular site was possible due to their different binding energies. In contrast, because of only one DNA conformation exists in the poly (L-lysine) (PLL) based polyplexes, DNA disintegration was found to be difficult.

Unlike plasmid DNA, rigid rod-structured therapeutic short oligonucleotides (antisenses, siRNAs, and miRNA) do not compact efficiently when complexed with a vector and leads to incomplete encapsulation and the formation of undesirably large complexes.[(27,28)] Consequently, the usual cationic polymers proven effective for gene delivery are not necessarily optimal for these short nucleic acids.[(29)] Although, recent literature highlights well about siRNA binding capacity of dendrimers indirectly through techniques like dynamic light scattering (DLS), nanoparticle tracking analysis (NTA), atomic force microscopy (AFM), Transmission electron microscopy (TEM), poly(acrylamide) gel electrophoresis, and ethidium bromide displacement assay,[(30,31,32)] most direct insights into dendrimer and short oligonucleotide packing interaction in the dendriplexes are scare and still need to be explored with more advanced tools. With this consideration, present study involves synthetic 14mer oligonucleotide interaction with Poly (amidoamine) (PAMAM) dendrimers of generations one, two and three (G1, G2 and G3) using fluorescence and Förster resonance energy transfer (FRET) methods. FRET is widely used technique to quantify molecular dynamics in protein-protein interaction, protein-DNA interactions

and protein conformational changes. Using FRET technique, three steps in oligonucleotide-CTAB interactions were investigated by us [33] using labelled oligonucleotide strands with a donor fluorophore and the other with an acceptor fluorophore. Here, the effective accommodation of oligonucleotide around the micellar aggregation of surfactant molecule is interestingly revealed by predominant fluorescence emission of the acceptor molecule due to intermolecular FRET from donor to acceptor. In this investigation we seek to explore dendrimer-short oligonucleic acid packing interactions as nano-complexes for gene silencing applications by FRET technique. Required fluorometric experiments were carried out as follows: synthetic oligonucleotide of 14 base pair was tagged at 5′ with fluorescein (strand I) as well as with tetramethylrhodamine (TAMRA) (strand II) and fluorometric titrations were performed with PAMAM dendrimer of first three generations. Similarly, fluorometric titrations were also carried out for oligonucleotides 5′-tagged with either fluorescein or TAMRA. The oligonucleotide-dendrimer interaction was also investigated by ethidium bromide exclusion and gel electrophoresis studies for first three generations.

3.2 Materials and Methods

3.2.1 Materials. PAMAM (starburst) dendrimer of generation one, two and three (G1, G2 & G3) of highest purity (>99%) were obtained from Sigma-Aldrich. Chemical structure of one of the representative PAMAM dendrimer, G1, is shown in Figure 3.1 along with a schematic representation of the first three dendrimer generations. These dendrimers can be named appropriately following the short hand nomenclature introduced by Tomalia *et al*.[34] Accordingly, the nomenclature for the three PAMAM dendrimers will be as follows - (i) G1: [Core: ethylenediamine]; (4→2); *dendri*-{poly(amidoamine)-(NH_2)8}; (G=1) dendrimer (ii) G2: [Core: ethylenediamine]; (4→2); *dendri*-{poly(amidoamine)-(NH_2)16}; (G=2) dendrimer (ii) G3: [Core: ethylenediamine]; (4→2); *dendri*-{poly(amidoamine)-(NH_2)32}; (G=3) dendrimer. Unlabeled 14mer DNA oligonucleotide of strand I (5′-GATGTTCACTCCAG-3′) and

strand II (5'-CTGGAGTGAACATC-3') were procured from SBS-Genetech. In addition to these, fluorescein tagged with 5' end of the 14mer strand I oligonucleotide (5'-GATGTTCACTCCAG-3') and its complementary strand II oligonucleotide (5'-CTGGAGTGAACATC-3') tagged with tetramethylrhodamine (TAMRA) at the 5' end were also supplied by SBS-Genetech. As per the manufacturer the GC content of the oligonucleotide was reported to be 50%. The concentration of unlabeled oligonucleotide was calculated by extrapolation of tabulated values of the monomer bases at 25 °C [35, 36] whereas, concentrations of labelled strands were determined based on optical density (OD) values provided by the manufacturer.

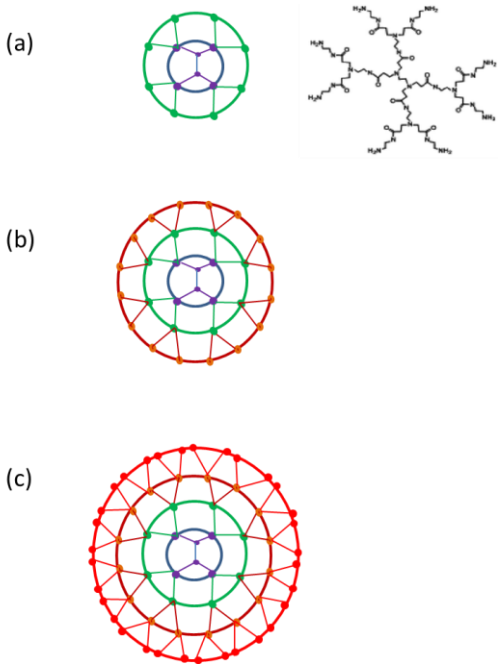

Figure 3.1 Chemical structure of poly (amidoamine) (PAMAM) dendrimer of Generation 1 (G1) and Schematic representation of first three PAMAM dendrimer generations (a) G1, (b) G2 and (c) G3. Color Code: Purple: Core; Green: Generation 1; Brown: Generation 2; Red: Generation 3.

3.2.2 Preparation of various duplexes with different combinations of oligonucleotides

In order to obtain untagged (D_0) duplex, equimolar concentrations of both the unlabeled oligonucleotide strands were mixed and the mixture was heated to 95°C for 10 minutes and cooled to room temperature for 4-6 h. Similarly, labeled duplexes

were also prepared. To prepare 5′-fluorescein labeled duplex (D_F), 5′-fluorescein tagged strand I was mixed with untagged strand II. 5′-TAMRA tagged duplex (D_T) was made by mixing unlabeled strand I and 5′ -TAMRA tagged strand II. Dual tagged oligonucleotide (D_{FT}) was obtained by mixing 5′ fluorescein tagged strand I and 5′-TAMRA labeled strand II. All experiments were done in 10 mM sodium phosphate buffer, pH 7.0. Here 1 μM 14mer oligonucleotide is equivalent to a 26 μM (as 14mer single strand oligonucleotides contain 13 phosphate groups) phosphate unit. Stock solutions of PAMAM dendrimer of 1, 2 and 3 generations were prepared by dissolving the required amount of dendrimer of desired generation in a known volume of phosphate buffer solution (18.2 mg/10 mL) and the corresponding concentrations were determined gravimetrically. In the entire text, in order to study the PAMAM dendrimer to DNA interaction, the resulting DNA-Dendrimer complex has been quantified by charge ratio ($Z_{\pm}$) which expresses the ratio (N/P) of concentration of cationic charges on dendrimer (N) to DNA phosphate groups (P). All the other reagents used were of AR grade purity. Milli-Q water was used for all the experiments.

3.2.3 Gel Electrophoresis Studies

The electrophoretic mobilities of PAMAM dendrimer of generations 1, 2 & 3 and untagged oligonucleotide (14 mer) complexes at various charge ratios $Z_{(\pm)}$ were determined by using 15% native-PAGE. Gel electrophoresis experiments were carried out in a buffer consisting of 45 mM Tris-borate and 1 mM EDTA at pH 8.0. In these studies, in order to prepare oligonucleotide-dendrimer complex of required charge ratio, 1 μM concentration of oligonucleotide (equivalent to 26 μM phosphate unit) was mixed with various concentrations of the desired dendrimer generations (1, 2 & 3) solution and incubated for 30 min. Polyacrylamide gels were run at 120 V for 4 h at 4 °C using the oligonucleotide-dendrimer complexes of various charge ratios.

Further, the corresponding dendriplex bands were visualized under UV illumination after staining the gels with ethidium bromide for 30 min at room temperature.

3.2.4 UV-melting studies

UV-melting experiments were performed using Cary 100 concentration UV-visible spectrophotometer with temperature controller on various duplexes. Melting experiments were carried out by heating 1 μM concentration of unlabelled (D_0), tagged with 5′-fluorescein (D_F), labelled with 5′-TAMRA (D_T) and tagged with 5′-fluorescein as well as 5′-TAMRA (D_{FT}) from 20 to 95°C at a scanning rate of 1.0 °C/min in a 1000 µL cuvette. The melting profiles of the oligonucleotides were recorded by monitoring the absorbance of the complexes at 260 nm as a function of temperature. Transition temperatures (T_m) were calculated from the melting curves and revealed that their T_m values were in the range of 33 to 37 °C (data not shown).

3.2.5 Circular Dichroism studies

CD spectra of the untagged oligonucleotide (D_0) were recorded using a Jasco spectropolarimeter (model 715) equipped with a peltier thermostat controlled cell holder at 20 °C and a cuvette with a path length of 1 cm. The CD spectra of untagged duplex were recorded between 220 and 325 nm in the absence and presence of the desired dendrimer generations of 1, 2 & 3 in 10 mM sodium phosphate buffer, pH 7.0. Various amounts (maximum of 30 μL) of the polymer stock solutions (mostly 5 mM dendrimer generations of 1, 2 & 3) were added to 5 μM oligonucleotide solutions. The complexes were incubated for 10 min before each CD measurement. The titration of the dendrimer was terminated, when significant change was not observed in the corresponding CD signal. Once again, the dilution of oligonucleotide was maintained within 10%.

3.2.6 Ethidium bromide exclusion studies

In order to understand dendrimer based short oligonucleotide delivery system, ethidium bromide (EB) exclusion studies were carried out as follows: Fluorescence spectra of oligonucleotide-EB complexes were recorded in the absence and presence

of the desired generation of PAMAM dendrimer from 500 to 700 nm, at an excitation wavelength (λ_{ex}) of 480 nm using a spectrofluorometer (JobinYvon FluoroMax 3) with a peltier thermostat. A 14 µM concentration of EB was mixed with a 1 µM concentration of oligonucleotide solutions (1EB:1base pair) in 10 mM sodium phosphate buffer at pH 7.0 and equilibrated for 10 min at 20 °C. For these experiments, a stock EB solution was prepared by dissolving 1.97 mg of EB in 1000 μL of water, and the corresponding stock concentration was determined using a Cary 100 concentration UV-visible spectrophotometer assuming molar extinction coefficient 5600 L mol^{-1} cm^{-1} at 480 nm.[37] 300 µL of this oligonucleotide-EB mixture was taken in a fluorescence cuvette, and increasing amounts of the cationic polymer of the required concentration were added into the mixture. After each addition of the polymer, the content of the fluorescence cuvette was incubated for 10 min before recording each spectrum. The concentrations of dendrimer stock solutions were prepared in such a way that the maximum dilution of oligonucleotide-EB complex was maintained well within 10% due to the dendrimer addition. The dilution factors considered for the calculation were of final charge ratios. The percentage of EB release from the DNA upon the interaction with the cationic polymers was calculated according to: $\mathbf{(I_0\text{-}I)/(I_0\text{-}I_{EB})\times 100}$, where I_0 and I_{EB} are the fluorescence intensities of free and oligonucleotide-bound EB, and I is the fluorescence intensity in the presence of different amounts of dendrimer.

3.2.7 Fluorescence and FRET Studies

The fluorescence spectra of dual labeled oligonucleotide (D_{FT}) were recorded by following our earlier procedure:[33] Initially, fluorescence spectra of a 1 μM concentration of fluorescein tagged strand I were recorded from 500 to 700 nm, at an excitation wavelength (λ_{ex}) of 490 nm and at temperature 15 °C using a spectrofluorometer (JobinYvonFluoroMax 3) with a Peltier thermostat. Then the strand I was mixed with the required amount of TAMRA tagged strand II to maintain equimolar concentration as 1 μM in 300 μL. The corresponding duplex was prepared in the fluorescence cuvette by heat-cool treatment using a Peltier thermostat, and

the spectrum was recorded. The required amount of desired generation of PAMAM dendrimer was added to the duplex. After each addition, the resulting oligonucleotide-dendrimer complexes were equilibrated for 10 min before recording of each fluorescence spectrum. The addition of the cationic polymer was terminated when the corresponding maximum intensity (I_{max}) of the fluorescence signal for the dual labeled duplex became saturated. Similarly, fluorescence spectra of oligonucleotides containing fluorescein labeled strand I and unlabeled strand II (D_F) as well as untagged strand I and TAMRA tagged strand II (D_T) were recorded both in the absence and in the presence of dendrimer at an excitation wavelength (λ_{ex}) of 490 and 520 nm respectively at 15 °C. In all the experiments, the stock concentration of dendrimer generations – 1, 2 & 3 solutions was chosen such that the maximum dilution of oligonucleotide- dendrimer complex was maintained well within 10% due to the addition of the cationic polymer. The polymer as well as oligonucleotide concentrations were calculated by including the dilution factors, which were also maintained within 10% of the initial volume (300 μL).

3.3 Results and Discussion

3.3.1 Gel electrophoresis studies

The interaction between therapeutic nucleic acid and cationic vector can be visualized by gel electrophoresis for the development of non-viral gene delivery system. Due to the association of positively charged cationic vector with the negatively charged nucleic acid, there exists partial or complete neutralization of the negative charges of the nucleic acid. The migration of such partially or completely neutralised DNA is either slow down or completely hindered through the gel.[38] Gel electrophoresis studies were carried out on the 14mer before and after interaction with PAMAM dendrimer of three generations G1, G2 and G3 and the results are displayed in Figure 3.2. First and second wells of all the three PAGEs correspond to the migration of 10 bp molecular weight marker and free DNA respectively. Whereas, subsequent wells of the PAGE represent the migration of oligonucleotide-dendrimer complexes at increasing PAMAM dendrimer to the 14mer

oligonucleotide charge ratio (from $Z_{\pm}$ = 0.3 to $Z_{\pm}$ = 2.7). In Figure 3.2a, migration of oligonucleotide is seen upto dendrimer G1 to oligonucleotide charge ratio 0.3. It is pertinent to mention that smearing and reduction in the intensity of the band corresponding to the DNA-G1 complex at charge ratio 0.3 is observed compared to free DNA ($Z_{\pm}$ = 0). Further, DNA migration is completely not visible from the charge ratio 0.6 to 2.7 ($Z_{\pm}$). The observation in the case of Figure 3.2a suggests interactions between the 14 mer DNA and the corresponding dendrimer are highly cooperative. There exists a coexistence of both partially as well as completely neutralised oligonucleotide in the case of G1upto $Z_{\pm}$ = 0.3 and thereafter it becomes completely saturated. In the presence of dendrimer of generation 2 (Figure. 3.2b), a very short DNA smearing is observed up to the charge ratio $Z_{\pm}$ = 0.6 indicating the existence of partially neutralised oligonucleotide in trace amounts. Interestingly, DNA migration is retarded completely for oligonucleotide-G2 as well as oligonucleotide-G3 systems from the charge ratio $Z_{\pm}$ = 1.2 to 2.7 (Figure. 3.2b) and $Z_{\pm}$ = 0.3 to 2.7 (Figure. 3.2c) respectively and the corresponding wells of the gel are found to contain perturbed DNA-dendrimer complex for generation two (from $Z_{\pm}$ = 0.6 to 2.7) and three (from $Z_{\pm}$ = 0.3 to 2.7).

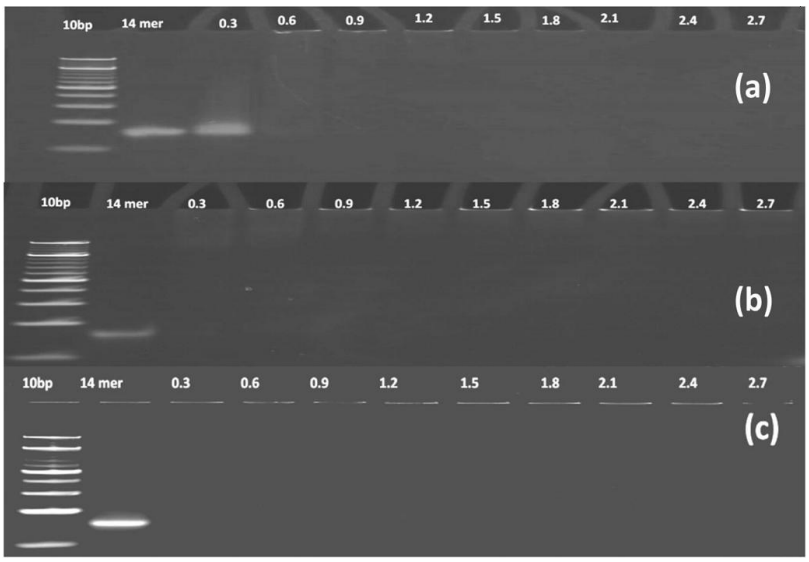

Figure 3.2 Gel electrophoresis assay. 15% non-denaturing PAGE was run with complexes of PAMAM dendrimer (a) G1 (b) G2 and (c) G3 at various PAMAM dendrimer to oligonucleotide charge ratios (as mentioned on the corresponding lanes). The gel was run in buffer consisting of 45 mM Tris-borate and 1 mM EDTA at pH 8.0, at 120 V for 60 min at 4°C. The gels were visualized under UV illumination after staining with ethidium bromide at room temperature.

Such disappearance of the DNA band at lower charge ratios ($Z_{\pm}$ = 0.3) is suggestive of effective neutralization of the 14mer with dendrimer of generation two (G2) and three (G3) compare to G1 due to the increase in positive surface charge density of the PAMAM dendrimer with increase in generation. In the presence of G2 and G3, prominently visible retarded DNA at the wells indicates the accessibility of the stain inside the polyplex, which may also reveal inability of the shortest oligonucleotide to undergo compaction.

3.3.2 CD Measurements

Based on CD measurements, minute conformational changes in the double helix of 14mer oligonucleotide can be followed due to the possible binding interactions with PAMAM dendrimer of various generations. The CD spectra of 5 µM concentration of oligonucleotide and its complexes with PAMAM dendrimer of generation one (G1) at various charge ratios are depicted in Figure. 3.3a. From the figure, the observed positive peak at 274 nm and negative peak at 240 nm for the free 14 mer oligonucleotide confirms its typical B form signature of double helical DNA and is in good agreement with the literature.[39] Interestingly, the intensity of positive as well as negative CD signals decrease gradually upon successive increase in polymer-oligonucleotide charge ratio, but not disappeared. The appearance of CD signals even at the highest polymer to oligonucleotide charge ratio indicates the existence of the oligonucleotide in B form. The observed incomplete encapsulation of 14mer oligonucleotide by the dendrimer is also evidenced by many researchers especially in the case of rigid rod-structured therapeutic short oligonucleotides in the vicinity of cationic vectors [28-30]. The reduction in amplitude of both the CD signals at 274 and 240 nm are in good agreement with the literature[39] and attributed to the electrostatic attraction of the 14mer oligonucleotide on the dendrimer of generation one. Additionally, there was no major shifting observed in the 14mer CD signals after interaction with the dendrimer. Similarly, in the presence of PAMAM dendrimer of generation two (G2) (Figure. 3.3b) and three (G3) (Figure. 3.3c), the intensity of positive as well as negative peaks of CD spectrum decreases with increase in polymer

concentration. In comparison, extend of reduction in the intensity of CD signals increase with charge ratio. Such increase in the reduction clearly indicates stronger electrostatic interaction of DNA with increase in the positive surface charge density of dendrimer. As observed with dendrimer generation one, the CD signals are not collapsed in the presence of the polymer generation two and three, even at the increase in the generation of dendrimer for similar dendrimer to oligonucleotide highest charge ratio used. Figure 3.3d summarises the changes observed to CD signals at 274 nm in the presence of dendrimers G1, G2 and G3 at various charge ratios normalised at 1. A saturation in CD signals was observed at charge ratios 0.30, 0.18 and 0.12 for the polymer generation one, two and three respectively. Based on the observations of CD signal saturation, it can be concluded that only a lesser amount of the dendrimer is sufficient to neutralise the 14mer with increase in dendrimer generation due to the increase in its positive charge density with generation. The reported CD saturation results are in good agreement with gel electrophoresis studies (Figure. 3.2) in which disappearance of DNA bands are observed after the charge ratio ($Z_{\pm}$) 0.3 for G1 and 0 for G2 and G3.

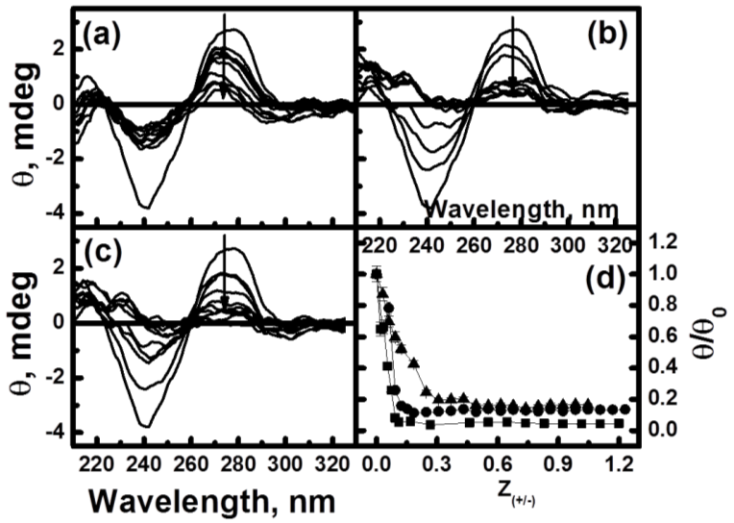

Figure 3.3 CD spectra of oligonucleotides in the presence of varying amounts of PAMAM dendrimers of (a) generation 1 (G1), (b) generation 2 (G2), (c) generation 3 (G3), and (d) θ/θ_0 vs $Z_{(\pm)}$ plot for PAMAM dendrimers of various generations G1 (▲), G2 (●) and G3 (■) in 10 mM sodium phosphate buffer (pH 7.0). The oligonucleotide concentration was 5 µM in 10 mM sodium phosphate buffer.

3.3.3 Ethidium bromide exclusion studies

In these studies, ethidium bromide, a planar aromatic dye is used as a fluorescence spectroscopic probe to determine relative affinities of PAMAM dendrimer of various generations (G1, G2 and G3) for the oligonucleotide. EB is well known to show a striking increase in fluorescence efficiency by intercalating between the base pairs of double helix DNA and is used extensively to probe DNA-cationic vector interactions in the development of non-viral gene delivery systems. The competition between the EB and the cationic co-solutes can be followed by determining quenching in fluorescence intensity of DNA-EB complex.[40,41] Figures 3.4a-3.4c at the left panel portray fluorescence emission spectra of free EB solution, oligonucleotide intercalated with EB and oligonucleotide-PAMAM dendrimer complex of generation one (G1), two (G2) and three (G3) respectively. Traces 1 and 2 in each figure represent the spectra due to the free and bound EB with the 14 mer. The observed fluorescence quenching of DNA-EB complex with increase in dendrimer concentration is represented by the down arrow. For all the three dendrimer generations, a reduction in fluorescence intensity with increase in the concentration of dendrimer was observed initially followed by a small negligible fluorescence decrease at higher concentration. The amount of EB that was efficiently released from the DNA molecule by the addition of cationic dendrimer was clearly different for various dendrimer generations used. The percentage EB released from the oligonucleotide with respect to dendrimer-DNA charge ratio (Figure not shown) has also been carried out. For dendrimer generation one, EB release was initially gradual upto the charge ratio ($Z_{\pm}$) 0.3, thereafter became very slow and finally 90% of EB was released from the oligonucleotide at the highest charge ratio studied ($Z_{\pm}$ = 1). Similar EB release behaviour was also observed for PAMAM dendrimer of generation two and three. Interestingly, the break between gradual as well as slow release of EB from the 14mer was also seen at $Z_{\pm}$ = 0.2 and $Z_{\pm}$= 0.1 for G2 and G3 respectively. Both the dendrimer generations two and three were able to release 90% as well as almost 100% EB from the DNA at the highest dendrimer-DNA charge ratio ($Z_{\pm}$= 1).

EB titration curves of the 14mer–dendrimer system for first three generations (G1, G2 and G3) are portrayed in Figure 3.4 (a-c, right panel). In general for all the three polymers, quenching of EB fluorescence increases sharply with increase in the cationic polymer concentration and attains an imperfect plateau like region, where negligible quenching was observed. The polymer to the oligonucleotides charge ratio at the onset of the plateau like region is considered as the saturation point for the oligonucleotides by the dendrimer. Further addition of the dendrimer to the solution may bind in a minimal amount to the oligonucleotide and therefore, may exclude EB feebly from oligonucleotides. The region below the saturation point represents the coexistence region of unsaturated dendrimer and the saturated oligonucleotide. It is pertinent to mention that the interaction strength of the first three dendrimer generations (G1, G2, G3) with the oligonucleotide can be represented by the observed saturation point.[39] From the figure, it is evidenced that with increase in dendrimer generation, the dendrimer to the 14mer charge ratio value at the saturation point decreases due to the corresponding rise in their surface charge. For example, the observed breaks for the first three generation of PAMAM dendrimers (G1, G2 and G3) at the onset of the plateau like region are 0.30 (Figure 3.4a, right panel), 0.20 (Figure 3.4b, right panel) and 0.07 (Figure 3.4c, right panel) respectively for 1μm oligonucleotide concentration indicated by down arrows.

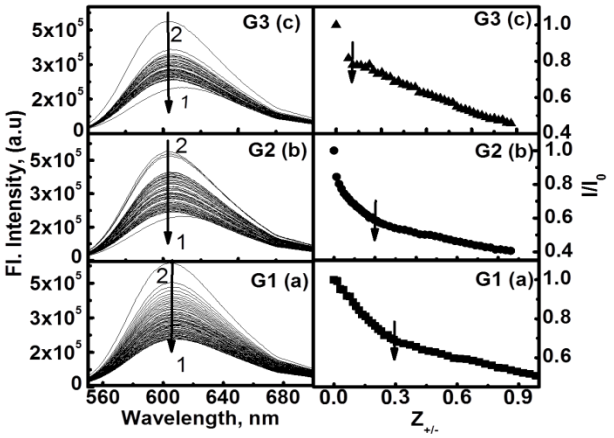

Figure 3.4 EB exclusion experiments for PAMAM dendrimer (a) G1, (b) G2, and (c) G3. Left panels are emission spectra. The down arrows indicate the increment of $Z_{\pm}$. Right panels are I/I_0 vs $Z_{\pm}$ plots. The oligonucleotide concentration was 1 μM in 10 mM sodium phosphate buffer (pH 7.0).

More interestingly, as observed in gel electrophoresis as well as CD experiments, the resulting saturation points from the EB titration curves of G1 and G2 are in good agreement with each other, whereas, in the case of G3 it is more or less same. In these EB titration curves of the oligonucleotide-dendrimer system, the appearance of imperfect plateau region is mostly due to the high charge density of the dendrimer surface in combination with the stiffness of the 14mer helix. As discussed by various researchers,[25,30,33] when a dendrimer molecule is bound to the DNA, the helix cannot bend around it since it is too rigid. Therefore, the rigid rod like single loop oligonucleotide can occupy only a little portion of the dendrimer. The other unoccupied charged sites of the dendrimer provide a high concentration of positive charges and readily attract a second DNA molecule. As the concentration of dendrimer increases, there may be slight rearrangement of the 14mer molecules on the DNA surface due to the existence of high concentration of unsaturated positive charges on the dendrimer surface and consequent feeble EB exclusion. It is also noteworthy that the observed plateau like region in the EB titration curve for dendrimer generation three (Figure 3.4c, right panel) is more imperfect due to its higher positive surface charge density compared to G1 and G2.

3.3.4 Fluorescence studies

Figure 3.5a at the left panel portrays fluorescence emission spectra of the 14mer duplex containing 5'-fluorescein tagged strand I and untagged strand II (D_F) before and after interaction with increasing concentration of PAMAM dendrimer G1. The free oligonucleotides shows emission maximum at 521 nm upon excitation at 490 nm. The 5'-tagged fluorescein of the duplex shows a decrease in the intensity of fluorescence with increase in dendrimer G1 concentration. It is also noteworthy that the fluorescence emission intensity of D_F shows hardly any change after a particular concentration of G1. Such reported increase in the reduction of the duplex (D_F) fluorescence intensity with increasing dendrimer concentration is an indicative of micro environmental change around the fluorescein molecule present in the dendrimer G1-duplex (D_F) system. Additionally, the observed unaltered fluorescence

emission intensity of D_F at a higher G1 concentration is due to the burial of the fluorescein molecule within the cationic polymer assembly evidencing an attainment of saturation. Interestingly, the observed shift in the emission maxima of 5′-fluorescein to higher wavelength (red shift) for each addition of increasing dendrimer concentration indicates the formation of hydrophobic assemblies of the polymer. The fluorescence emission spectra of oligonucleotide (D_F) in the absence and presence of G2 (Figure. 3.5b, left panel) and G3 (Figure. 3.5c, left panel) show a similar behavior as observed in the case of the duplex (D_F)-dendrimer of generation one (G1) system (Figure. 3.5a, left panel). In addition to this, it is also noteworthy that the observed red shift in the emission maxima of 5′-fluorescein in the presence of the polymer increases with increase in polymer generation probably due to the increase in their size.

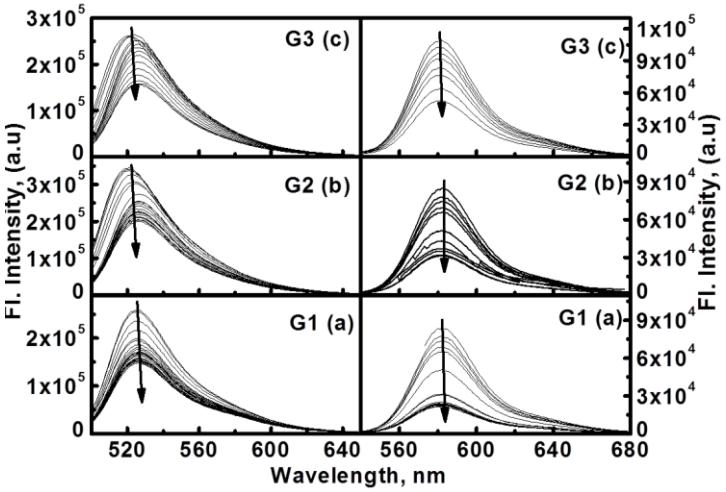

Figure 3.5 Fluorescence emission spectra of oligonucleotide in the left panel D_F (5′-fluoresceins labeled) and right panel D_T (5′-TAMRA labeled) in the absence and presence of increasing concentrations of PAMAM dendrimer (a) G1 (b) G2 and (c) G3. The oligonucleotide concentration was 1 μM in 10 mM sodium phosphate buffer (pH 7.0). The increment of $Z_{\pm}$ is indicated by arrow heads.

The interaction between the oligonucleotide (D_T) containing unlabelled strand I as well as 5′-TAMRA labeled strand II and PAMAM dendrimer of generation one (G1) is shown in Figure 3.5a at right panel. In the absence of G1, the fluorescence emission maximum of the 5′-TAMRA tagged duplex was detected at 582 nm upon excitation at 520 nm. As observed in the case of the duplex D_F-G1 system (Figure. 3.5a, right

panel) here again, the fluorescence intensity of 5′-TAMRA tagged oligonucleotide (D_T) decreases with increase in the concentration of the dendrimer of generation one (G1) indicating micro environmental changes around the fluorophore due to the oligonucleotide-dendrimer interaction. It is worthwhile to mention that a slight blue shift was observed in the intensity maxima of the duplex (D_T) for each increase in dendrimer G1 concentration addition. The behavior of the 5′-TAMRA tagged oligonucleotide in the presence of G2 (Figure. 3.5b, right panel) and G3 (Figure. 3.5c, right panel) was observed to be as similar as D_T-PAMAM G1 system. In the presence of dendrimer, the observed red as well as blue shift in the fluorescence emission maximum of D_F-PAMAM (Figure. 3.5, left panel) as well as D_T-PAMAM (Figure. 3.5, right panel) systems respectively may be interpreted to the change from polar to non-polar environment around the corresponding fluorophores due to the 14mer and dendrimer complexation. The interesting opposite behavior of the two fluorophores 5′-TAMRA (blue shift) and 5′-fluorescein (red shift) was tested by obtaining emission spectra of these free fluorophores in three different solvents, namely, water, methanol as well as hexane and discussed previously by us.[33] In the case of fluorescein, emission maxima were 518, 521, and 524 nm whereas, in the case of TAMRA, emission maxima were 572, 566, and 557 nm in water, methanol and hexane respectively.[33]

3.3.5 FRET studies

Figure 3.6 (left panel) portrays fluorescence emission spectra of the dually tagged oligonucleotide (D_{FT}) by fluorescein and TAMRA at 5′ ends of its strand I and strand II respectively in the absence and presence of the dendrimer of three generations (G1, G2 and G3). From the figure it is evident that two emission maxima are reported for the oligonucleotide (D_{FT}) in the absence of dendrimer of all generations under study. These fluorescence emission maxima were observed as expected one each at 520 and 575 nm corresponding to donor fluorescein and acceptor TAMRA emissions upon excitation at 490 nm respectively. The fluorescence emission intensities decrease in general for donor as well as acceptor for all three generations of PAMAM dendrimer up to certain level of concentration increase. A striking increase in the

emission intensity of TAMRA at higher polymer concentration was seen especially for the dendrimer generations G2 (Figure. 3.6b, left panel) and G3 (Figure. 3.6c, left panel). On the contrary, similar raise in the emission intensity of TAMRA at higher concentrations is not very much obvious for the polymer generation one (G1) (Figure. 3.6a, left panel). Corresponding decrease in the emission intensity of the donor fluorescein for all the generations are reported very moderately in Figure. 3.6 (left panel). Such changes observed in the emission maxima of fluorescein of the dual tagged oligonucleotide are evidencing only very small amount of resonance energy transfer from donor to the acceptor fluorophores.

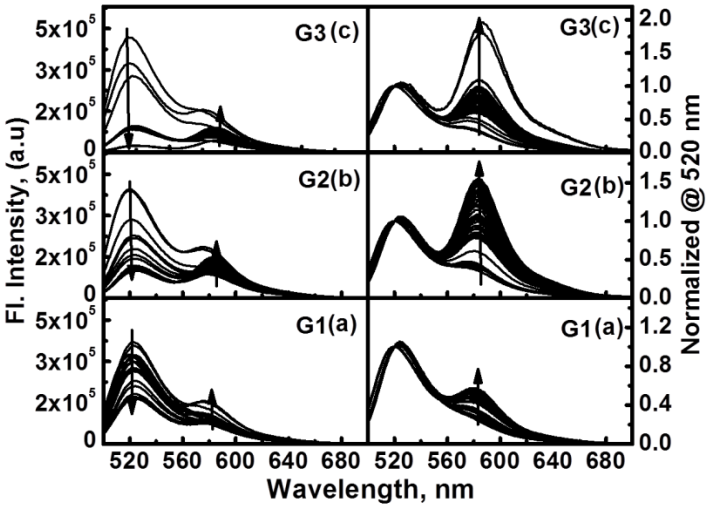

Figure 3.6 Fluorescence emission spectra of the oligonucleotide in the left panel D_{FT} (5'- fluorescein and 5'- TAMRA labeled) and right panel normalized spectra at 520 nm in the absence and presence of increasing concentrations of PAMAM dendrimer (a) G1, (b) G2 and (c) G3. The oligonucleotide concentration was 1 µM in 10 mM sodium phosphate buffer (pH 7.0). The increment of $Z_{\pm}$ is indicated by arrow heads.

In order to bring out the minute differences in the fluorescence energy emission of TAMRA among the three dendrimer generations at higher polymer concentrations more prominently, the corresponding individual spectrum of D_{FT} was normalized at 521 nm in the emission maxima of fluorescein (Figure 3.6, right panel). From Figure 3.6 (right panel) it is clearly evident that initial addition of the polymer does not change the fluorescence intensity of TAMRA with respect to the corresponding fluorescence intensity of fluorescein irrespective of difference in generations. On the other hand, an obvious increase in the fluorescence intensity of TAMRA with respect to fluorescein intensity was seen in Figure 3.6 (right panel) at higher polymer

concentration. More interestingly, the observed raise in the acceptor fluorescence intensity increases with increase in the polymer generation (G1, G2 and G3) especially at higher concentrations. At higher concentration, for every addition of polymer, the observed increase in the acceptor fluorescence intensity with respect to the donor was found to be very huge for G2 (Figure 3.6b, right panel) and G3 (Figure 3.6c, right panel) compared to G1 (Figure 3.6a, right panel). As per our earlier findings, [33] such typical behavior of TAMRA in dual tagged oligonucleic acid (D_{FT}) reveals an absence of energy transfer from donor to acceptor up to initial polymer additions. In contrast after certain levels of polymer concentration, a reduction in either inter or intramolecular distance between the donor as well as the acceptor is expected, due to which there is a resonance energy transfer between fluorescein and TAMRA. Further, the observed obvious differences in the acceptor fluorescence energy emission for PAMAM dendrimer of generation one (G1), two (G2) and three (G3) might be attributed to the difference in the packing of the 14 mer in the DNA-dendrimer complex. It is to be noted that even though G and C unit adjacent to the following probe molecules, 5'-Fluorescein and 5'-TAMRA respectively are fluorescence quenchers but quenching effect of these base units of the short oligonucleotide are not observed to be interfering with the FRET results.

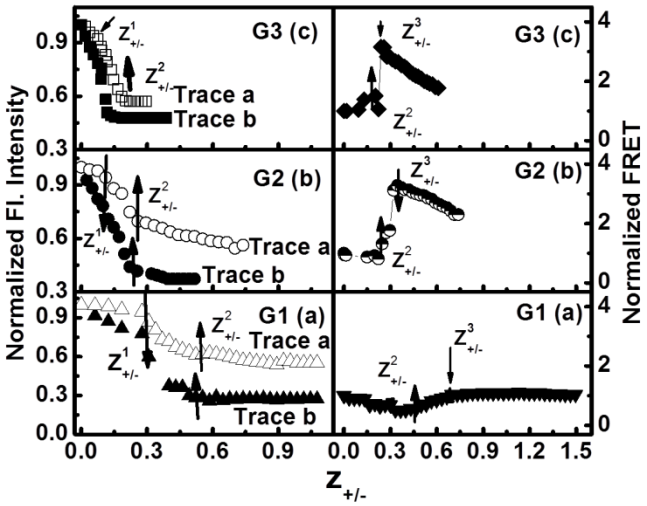

Figure 3.7 Fluorometric titration curves of the oligonucleotides in the left panel; the top traces are D_F (5'-fluorescein labeled) & bottom traces are D_T (5'-TAMRA labeled), and the traces of D_{FT} (5'-fluorescein and 5'-TAMRA labeled) are shown in the right panel in the absence and presence of increasing PAMAM concentration (a) G1, (b) G2 and (c) G3 to oligonucleotide charge ratios. The oligonucleotide concentration was 1 µM in 10 mM sodium phosphate buffer (pH 7.0). Break points $Z^1_{\pm}$, $Z^2_{\pm}$ and $Z^3_{\pm}$ are represented by arrows.

For a detail understanding of the oligonucleotide-dendrimer interactions, observations from fluorescence and FRET investigations (Figure 3.5, and 3.6) are further portrayed as typical fluorometric titration curves of duplexes D_F (Figure 3.7, left panel), D_T (Figure 3.7, left panel) and D_{FT} (Figure 3.7, right panel) with the dendrimer of required generation. In Figure 3.7 (left panel), normalized fluorescence intensity maxima of the duplex D_F in the presence of the PAMAM dendrimer of generation one (G1) (Figure 3.7a, left panel)/ two (G2) (Figure 3.7b, left panel)/three (G3) (Figure 3.7c, left panel) ($I_{521}/I^0_{521,}$ where I_{521} and I^0_{521} are oligonucleotide fluorescence intensities in the presence and absence of the dendrimer of required generation) were plotted as a function of $Z_{\pm}$ (dendrimer to the duplex charge ratio). Additionally, Figure 3.7 (left panel) also portrays normalised fluorescence intensity ($I_{580}/I^0_{580,}$ where I_{580} and I^0_{580} are oligonucleotide fluorescence intensities in the presence and absence of the dendrimer of required generation) of the duplex D_T as a function of dendrimer to D_T charge ratio ($Z_{\pm}$). Figure 3.7a (left panel) reveals existence of two steps in the complex formation between the duplex D_F and the PAMAM dendrimer of generation one (G1) by showing two breaks at $Z_{\pm}$ = 0.28 ($Z^1_{\pm}$) and $Z_{\pm}$ = 0.55 ($Z^2_{\pm}$) in the fluorometric titration curve respectively. It is worth mentioning that the other titration curve correspond to D_T-G1 system also show two breaks at $Z^1_{\pm}$= 0.29 and $Z^2_{\pm}$ = 0.5 further confirming two steps involved in the complexation and the charge ratio values corresponding to two breaks ($Z^1_{\pm}$ and $Z^2_{\pm}$) for the D_T-G1 as well as D_F-G1 systems respectively are found to be the same. Similar to the PAMAM dendrimer generation one, the other dendrimer generations G2 and G3 also show two breaks for each duplexes D_F and D_T at similar charge ratios. For example, D_F-G2 as well as D_T-G2 systems the observed charge ratio values for the break $Z^1_{\pm}$ are 0.11 and 0.1 and $Z^2_{\pm}$ is found at the charge ratio 0.26 for fluorescein as well as 0.25 for TAMRA tagged oligonucleotides respectively. In the presence of G3, for duplexes D_F and D_T the break $Z^1_{\pm}$ exists at 0.096 and 0.095 respectively. Whereas, the break $Z^2_{\pm}$ was seen at the charge ratios 0.18 and 0.12 for D_F-G3 as well as D_T-G3 systems respectively. On a comparative basis, interestingly, these two breaks ($Z^1_{\pm}$ and $Z^2_{\pm}$) indicating two steps in the dendrimer- oligonucleotide complex formation

are observed to be almost the same for the duplexes D_F and D_T for all the three dendrimer generations. Further, the charge ratio values corresponding to the breaks $Z^1_{\pm}$ and $Z^2_{\pm}$ decrease with increase in dendrimer generations. For example, for D_F-G2 system the first break was observed at 0.11 charge ratio and the second was seen at the charge ratio of 0.26. Interestingly, the charge ratio values of these two breaks $Z^1_{\pm}$ and $Z^2_{\pm}$ were further reduced to 0.07 and 0.2 respectively for the duplex D_F in the presence of G3. Such reduction in the break values observed for dendrimers of increasing generations indicate existence of difference in their interaction with the oligonucleotide.

For the dual tagged duplex D_{FT} I_{580}/I_{520} (where I_{580} and I_{520} are the values correspond to the fluorescence maxima observed for fluorescein as well as TAMRA for each dendrimer concentration respectively) values are plotted against the polymer to oligonucleotide charge ratio ($Z_{\pm}$) (Figure 3.7, right panel). These normalised FRET (I_{580}/I_{520}) values are extracted from Figure 3.6 (left panel) for the desired dendrimer generation. In the presence of dendrimer G1, two distinct break points for the fluorometric titration curve of the oligonucleotide tagged with donor as well as acceptor (D_{FT}) were seen. It is noteworthy that during the titration with G1 the observed first break point for the dual tagged oligonucleotide (D_{FT}) at $Z_{\pm}$ is almost in close agreement with the second break $Z^2_{\pm}$ points of both singly tagged duplexes D_F (Figure 3.7a, left panel) and D_T (Figure 3.7a, left panel). As observed in the case of G1, the similarity observed for the first break in the fluorometric titration curves of D_{FT} and the second break $Z^2_{\pm}$ for D_F and D_T is also true in the presence of G2 as well as G3. Hence, hereafter, the first break in the titration curves of D_{FT} is represented as $Z^2_{\pm}$ throughout the text. In the case of G1, after $Z^2_{\pm}$ FRET increased gradually and attained maximum at $Z^3_{\pm}$ and thereafter saturation was seen. The reported FRET increase after $Z^2_{\pm}$ indicates a decrease in distance between the donor fluorescein and the acceptor TAMRA. Further, the FRET maximum found at $Z^3_{\pm}$ is an indicative of the closest possible distance between the donor and acceptor moieties, thereafter which remains unaltered indicating saturation at the titration curve for D_{FT}-G1 system. It is

also noteworthy that in the presence of G1, the highest FRET was observed even before $Z^2_{\pm}$ i.e. at the charge ratio 0.01 (at the first drop of G1) and thereafter decreases to zero at $Z_{\pm}$ = 0.3. The interesting observation below $Z^2_{\pm}$ indicates the aggregation of the D_{FT} molecules due to their competition for the least number of positive sites available at G1 at the lowest concentration. For D_{FT}-G1 system, $Z^2_{\pm}$ and $Z^3_{\pm}$ are observed at 0.49 and 0.69 respectively. It is surprising to observe a raise in FRET for the D_{FT}- G2 system from the charge ratio 0.20 ($Z^2_{\pm}$) and attain a huge maximum at $Z_{\pm}$ = 0.34 ($Z^3_{\pm}$) compared to D_{FT}- G1 system. Interestingly, the obtained maximum FRET at $Z^3_{\pm}$ = 0.34 for D_{FT} in the presence of dendrimer G2 decreases for further raise in $Z_{\pm}$. In the presence of G3, the duplex D_{FT} also showed similar FRET trend as observed in the case of G2. The raise in FRET for G3 begins at the charge ratio ($Z^2_{\pm}$) at 0.1, attains maximum at $Z_{\pm}$ = 0.25 ($Z^3_{\pm}$) and thereafter decreases. On a comparative basis, the highest FRET value was observed for the polymer G2 at the charge ratio $Z^3_{\pm}$ = 0.34 compared to G3 as well as G1. It is noteworthy that normalized FRET intensity value observed for the oligonucleotides D_{FT} in the presence of G3 (3.16) as well as G2 (3.29) is almost three fold higher than the D_{FT}-G1 system (1.06). Such a huge FRET intensity reported in the case of D_{FT}- G2 and D_{FT}- G3 systems is an indicative of the closest packing of oligonucleotides in the corresponding dendriplexes, where either inter- or intra molecular distance between the donor fluorescein and the acceptor TAMRA are expected to be very close to each other. It is pertinent to mention that unlike long DNAs like ct-DNA and plasmid DNA, the rigid and rod structured 14mer oligonucleotide under investigation is most unlikely to undergo bending as well as coiling during the interaction with the dendrimer due to its shorter chain length. Hence during the neutralization process, the intramolecular FRET is ruled out for these 14mer based dendriplexes. The UV melting data on the oligonucleotide (D_0) and PAMAM dendrimer of first three generations (Data not shown) reveal denaturation followed by coiling of the oligonucleotides is highly unlikely in the vicinity of the dendrimer (up to the charge ratio $Z_{\pm}$ = 1).

3.3.6 Dendrimer-DNA interaction mechanism

The fluorescence and FRET investigations on the 14mer based PAMAM dendriplexes of first three generations reveal various steps involved in the dendriplex formation with increase in the polymer concentration. Based on the findings, a schematic representation of the dendriplex formation at increasing dendrimer concentration is displayed in Figure 3.8 for the PAMAM dendrimer of first three generations. For generation one, at first step a simple electrostatic complexation takes place between the cationic PAMAM dendrimer and the phosphate back bone of the 14mer oligonucleotide resulting in dendriplex formation. It is pertinent to recall the first break ($Z^1_{\pm}$) in the fluorometric titration curves of D_F-G1 as well as D_T-G1 systems (Figure 3.7(a), left panel) represents the neutralization point at the charge ratio 0.33. Interestingly, the resulting lowest FRET at this neutralization point (Figure 3.7(a) right panel) is an indicative of largest distance between the oligonucleotide molecules and also indirectly suggestive of 1:1 complexation between the 14mer oligonuclotide and the dendrimer molecule. The formation of monomeric 1:1 complexation at the neutralization point is well reported in literature for siRNA-PAMAM system using silico[42] as well as SAXS[43] studies. After the step I, observed sharp decrease in fluorescence intensity above the charge ratio 0.3 in the fluorometric titration curves of D_F as well as D_T (Figure 3.7(a), left panel) is suggestive for the existence of a strong hydrophobic environment around these fluorophores. Thus, it can be interpreted that at above the neutralization point ($Z_{\pm}$=0.3), the increase in dendrimer concentration causes an addition of new dendrimer molecules into the neutralized dendriplexes followed by an oligonucleotide induced self-assembly to form micellar aggregates. The micellar aggregation of dendrimer in the vicinity of the 14mer represents the step II in the reported schematic diagram (Figure 3.8). As the raise in FRET from the second break ($Z^2_{\pm}$) in the fluorometric titration curve of D_{FT} with G1 (Figure 3.7a, right panel) occurs, it reveals arrangement of the oligonucleotide molecules on the surface of dendrimer aggregates starts from the step II. In the presence of the dendrimer G1, the highest energy transfer observed by FRET experiment reported at the charge ratio 0.6 represents the third step of the 14mer-

G1 interaction (Figure 3.7a, right panel). The obtained FRET profile in the case of D_{FT}-G1 system confirms an increase in the number of loosely held dendrimer aggregates with its concentration followed by a tight fusion of these aggregates. Interestingly, a simultaneous accommodation of the oligonucleotide molecules also takes place effectively around these dendrimer aggregates from the step II and ends at the third step. At the third step, the local concentration of the oligonucleotide along each dendrimer aggregation increases in such a way to attain the closest possible end-to-end distance between two oligonucleotide molecules and manifests a marked raise in the energy transfer at $Z^3_{\pm}$ (Figure 3.7a, right panel).

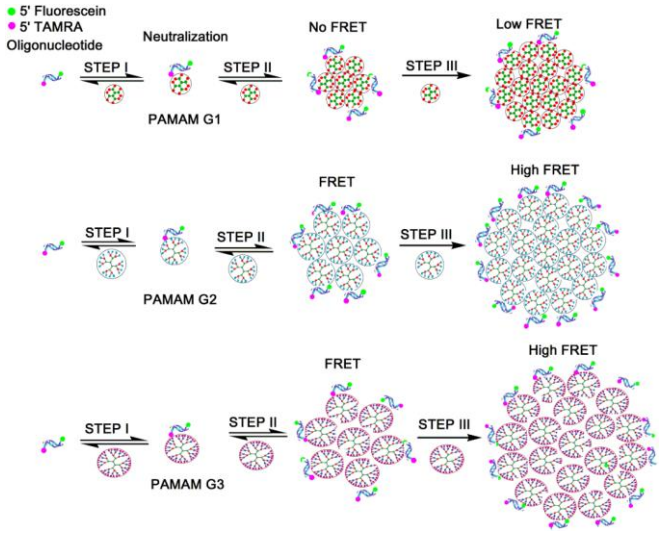

Figure 3.8 Schematic representation of PAMAM dendrimer and oligonucleotide interaction for G1, G2 and G3.

Similar to D_{FT}-G1 system, in the presence of dendrimer generation two (G2) and three (G3), step I corresponds to monomeric complexation between a dendrimer molecule and a 14mer molecule at the neutralization charge ratio 0.18 as well as 0.12 respectively. With increase in dendrimer concentration, the aggregation of dendrimer molecules revealed by the second break ($Z^2_{\pm}$) observed at the fluorometric titration curves for D_F as well as D_T (Figure 3.7, left panel) represents the second step. At the second step, here again the lowest FRET is observed for G2 as well as G3. Most interestingly unlike G1, the highest FRET observed at the only charge ratio 0.33 for G2 and 0.23 for G3 indicates the step III. Further the

observation of sharp decrease in FRET intensity after the step III for the systems D_{FT}-G2 as well as D_{FT}-G3 (Figure 3.7b and 3.7c, right panel) reveals that with increase in dendrimer concentration the local concentration of the 14mer around the dendrimer aggregate decreases due to the increase in the number of micellar aggregates. Additionally, larger size of G2 as well as G3 in comparison with G1 further increase the end-to-end distance between two DNA molecules with increase in the concentration consequently, decreasing the FRET between the donor and acceptor.

3.4 Conclusion

The molecular mechanism of dendriplex formation between the 14mer oligonucleotide and PAMAM dendrimer is successfully elucidated by the fluorescence and FRET investigations. Based on these experimental data, three steps are identified in the dendriplex formation. First step is the neutralization of the 14mer oligonucleotide by the dendrimer molecule in 1:1 ratio. With increase in dendrimer concentration, the oligonucleotide induced self–assembly of dendrimer is considered as step two. The dendrimer aggregation is expected to grow bigger with further raise in its concentration and followed by a fusion of these loosely held dendrimer aggregates at the final step. On the surface of these compact dendrimer aggregates the rigid rod shaped 14mer oligonucleotides are effectively accommodated with the shortest intermolecular distance. The closest packing of the 14 mer molecules on the dendrimer aggregate surface is evidenced by a striking increase in intermolecular FRET between 5'-fluorescein and 5'-TAMRA molecules. Most interestingly, the highest FRET resulted at the aggregates of second generation polymer molecules reveal effective oligonucleotide packing in the dendriplex depends on the dendrimer architecture. Additionally, the observed decrease in the FRET intensities in D_{FT}-G2 as well as D_{FT}-G3 system confirm that there exist a critical dendrimer to oligonucleotide charge ratio for effective dendrimer packing into the dendriplex.

References

1. L. Aagaard, J. J. Rossi. RNAi therapeutics: Principles, prospects and challenges. *Adv. Drugs Deliver. Rev.* **(2007)**, 59, 75–86.
2. I. Sifuentes-Romero, S. L. Milton, A. Garcia-Gasca. Post-transcriptional gene silencing by RNA interference in non-mammalian vertebrate systems: Where do we stand? *Mutat. Res.* **(2011)**, 728,158–171.
3. C. C. Mello, D. Jr. Conte. Revealing the world of RNA interference. *Nature.* **(2004)**, 431, 338–342.
4. A. de Fougerolles, H. P. Vornlocher, J. Maraganore, J. Lieberman. Interfering with disease: a progress report on siRNA-based therapeutics. *Nat. Rev. Drug Discov,* **(2007)**, 6, 443–453.
5. R. S. Christopher, YiqiSeow, J. A. Wood Matthew, *Mol. Ther.* Novel RNA-based Strategies for Therapeutic Gene Silencing. **(2010)**, 18, 466-476.
6. Scott M. Hammond, A. Amy Caudy, J. Gregory Hannon. Post-Transcriptional Gene Silencing By Double Stranded RNA. *Nat. Rev. Genet.* **(2001)**, 2, 110-119.
7. A. Potti, R. L. Schilsky, J. R. Nevins. Refocusing the war on cancer: The critical role of personalized treatment. *Sci. Transl. Med.* **(2010)**, 2, 1-3.
8. J. Nguyen, F. C. Szoka. Nucleic acid delivery: The missing pieces of the puzzle? *Acc. Chem. Res.* **(2012)**, 45, 1153–1162.
9. D. J. Gary, N. Puri, Y.Y. Won. Polymer-based siRNA delivery: Perspectives on the fundamental and phenomenological distinctions from polymer-based DNA delivery. J. Control. Release. *J. Control. Release,* **(2007)**, 121, 64–73.
10. H. Shen, T. Sun, M. Ferrari. Nano vector delivery of siRNA for cancer therapy. *Cancer Gene Ther.* **(2012)**, 19, 367–373.
11. S. Nimesh, N. Gupta, R. Chandra. Cationic polymer based nanocarriers for delivery of therapeutic nucleic acids. *J. Biomed. Nanotechnol.* **(2011**), 7, 504–520.

12. I. Posadas, F.J. Guerra, V. Nonviral vectors for the delivery of small interfering RNAs to the CNS. *Nanomedicine*. **(2010)**, 5, 1219–1236.

13. Y. Gao, L. X. Liu, X. R. Li. Research progress on siRNA delivery with nonviral carriers. *Int. J. Nanomed.* (**2011)**, *6*, 1017–1025.

14. M. Jafari, M. Soltani, S. Naahidi, D. N. Karunaratne, P. Chen. Nonviral approach for targeted nucleic acid delivery. *Curr. Med. Chem.* **(2012)**, 19, 197–208.

15. R. S. Dias, B. Lindman, *DNA Interaction with Polymers and Surfactants,* Eds. John Wiley and Sons: Hoboken. NJ., 2008.

16. C. Dufes, I. F. Uchegbu, A. G. Schatzlein. Dendrimers in gene delivery. *Adv. Drug Deliv. Rev.* **(2005)**, 57, 2177–2202.

17. Y. Gao, G. Gao, Y. He, T. Liu, R. Qi. Recent advances of dendrimers in delivery of genes and drugs. *Mini Rev. Med. Chem.* **(2008)**, 8, 889–900.

18. S. Biswas, P. Vladimir Torchilin. Dendrimers for siRNA Delivery. *Pharmaceuticals,* **(2013)**, 6, 161-183.

19. D. G. Shcharbin, B. Klajnert, M. Bryszewska. Dendrimers in Gene Transfection. *Biochemistry (Moscow).* **(2009)**, 74, 1070-1079.

20. K. Wada, H. Arima, T. Tsutsumi, Y. Chihara, K. Hattori, F. Hirayama, K. Uekama. Improvement of gene delivery mediated by mannosylated dendrimer/alpha-cyclodextrin conjugates. *J. Control. Release.* **(2005)**, 104, 397-413.

21. R. Q. Huang, Y. H. Qu, W. L. Ke, J. H. Zhu, Y. Y. Pei, C. Jiang. Efficient gene delivery targeted to the brain using a transferrin-conjugated polyethyleneglycol-modified polyamidoamine dendrimer. *Faseb J.* **(2007)**, 21, 1117-1125.

22. M. L. Ainalem, R. A. Campbell, S. Khalid, R. J. Gillams, A. R. Rennie and T. Nylander. On the Ability of PAMAM Dendrimers and Dendrimer/DNA Aggregates To Penetrate POPC Model Biomembranes. *J. Phys. Chem. B.* **(2010)**, 114, 7229–7244.

23. S. Monteagudo, F. C. PérezMartínez, M. D. Pérez-Carrión, J. Guerra, S. Merino, M. P. Sánchez-Verdú and V. Ceña, *Nanomedicine*. **(2012)**, 7(4), 493–506.

24. Y. Yang, S. Sunoqrot, C. Stowell, J. Ji, C. W. Lee, J. W. Kim, S. A. Khan and S. Hong, *Biomacromolecules,* 2012, **13**, 2154−2162.

25. K. Fant, E. K. Esbjo¨rner, P. Lincoln, B. Norde´n. DNA Condensation by PAMAM Dendrimers: Self-Assembly Characteristics and Effect on Transcription. *Biochemistry.* ***(*****2008)**, 47, 1732-1740.

26. E. Vuorimaa, A. Urtti, R. Seppa¨nen, H. Lemmetyinen and M. Yliperttula. Time-Resolved Fluorescence Spectroscopy Reveals Functional Differences of Cationic Polymer-DNA Complexes. *J. Am. Chem. Soc*., 2008, **130**, 11695–11700.

27. O. Taratula, O. B. Garbuzenko, P. Kirkpatric, P. Pandya, I. R. Savla, V. P. Pozharov, H. He, T. Minko. Surface-engineered targeted PPI dendrimer for efficient intracellular and intratumoral siRNA delivery. *J. Control. Release,* 2009, **140**, 284–293.

28. S. Spagnou, A. D. Miller, M. Keller. Differences in the formulation, cellular uptake, and delivery with plasmid DNA. *Biochemistry,* 2004, **43**, 13348–13356.

29. Gary, D. J.; Puri, N.; Won, Y. Y. Polymer-based siRNA delivery: Perspectives on the fundamental and phenomenological distinctions from polymer-based DNA delivery. J. Control. Release. 2007, 121, 64–73.

30. Jensen, L. B.; Pavan, G. M.; Kasimova, M. R.; Rutherford, S.; Danani, A.; Nielsen, H. M.; Foged, C. Elucidating the molecular mechanism of PAMAM-siRNA dendriplex self-assembly: Effect of dendrimer charge density. Int. J. Pharm. 2011, 416, 410–418.

31. Xin-Cheng, Shen.; Jiehua, Zhou.; Xiaoxuan, Liu.; Jiangyu, Wu.; Fanqi, Qu.; Zhi-Ling, Zhang.; Dai-Wen, Pang.; Gilles, Qu´el´ever.; Cheng-Cai, Zhang.; and Ling,

Peng. Importance of size-to-charge ratio in construction of stable and uniform nanoscale RNA/dendrimer complexes. Org. Biomol. Chem. 2007, 5, 3674–3681.

32. Perez, A. P.; Romero, E. L.; Morilla, M. J. Ethylendiamine core PAMAM dendrimers/siRNA complexes as in vitro silencing agents. Int. J. Pharm. 2009, 380, 189-200.

33. D. Santhiya.; S. Maiti. An investigation on interaction between 14mer DNA oligonucleotide and CTAB by fluorescence and fluorescence energy transfer studies. J. Phys. Chem. B, 2010, 114, 7602-7608.

34. Tomalia, D. A.; Christensen, J. B.; Boas, U. Dendrimers, dendrons, and dendritic polymers: discovery, applications and the future. Cambridge University Press. 2012, 29-33.

35. Marky, L. A.; Blumenfeld, K. S.; Kozlowski, S.; Breslauer, K. Salt-dependent conformational transitions in the self-complementary deoxydodecanucleotide d(CGCAATTCGCG): evidence for hairpin formation. J. Biopolym. 1983, 22, 1247-1257.

36. Kaur, H.; Arora, A.; Wengel, J.; Maiti, S. Thermodynamic, Counterion, and Hydration Effects for the Incorporation of Locked Nucleic Acid Nucleotides into DNA Duplexes. Biochemistry. 2006, 45, 7347-7355.

37. Waring, M. J. Complex formation between ethidium bromide and nucleic acids. J. Mol. Biol. 1965, 13, 269-282.

38. Fried, M.; Crothers, D. M. Equilibria and kinetics of lac repressor-operator interactions by polyacrylamide gel electrophoresis. Nucleic Acids Res. 1981, 9, 6505-6525.

39. Jadhav, V. M.; Valaske, R.; Maiti, S. Interaction Between 14mer DNA Oligonucleotide and Cationic Surfactants of Various Chain Lengths. J. Phys. Chem. B. 2008, 112, 8824−8831.

40. LePecq, J. B.; Paoletti, C. A fluorescent complex between ethidium bromide and nucleic acids. Physical-chemical characterization. J. Mol. Biol. 1967, 27, 87-106.

41. Armitage, B.; Yu, C; Devadoss, C.; Schuster, G. B. Cationic Anthraquinone Derivatives as Catalytic DNA Photonucleases: Mechanisms for DNA Damage and Quinone Recycling. J. Am. Chem. Soc. 1994, 116, 9847-9859.

42. Pavan, G. M.; Albertazzi, L.; Danani, A. Ability to adapt: Different generations of PAMAM dendrimers show different behaviors in binding siRNA. J. Phys. Chem. B. 2010, 114, 2667–2675.

43. Jensen, L. B.; Mortensen, K.; Pavan, G. M.; Kasimova, M. R.; Jensen, D. K.; Gadzhyeva, V.; Nielsen, H. M.; Foged, C. Molecular Characterization of the Interaction between siRNA and PAMAM G7 Dendrimers by SAXS, ITC, and Molecular Dynamics Simulations. Biomacromolecules. 2010, 11, 3571–3477.

CHAPTER 4

INVESTIGATION ON PAMAM DENDRIMER AND 14MER OLIGONUCLEOTIDES PACKING KINETICS BY STOPPED-FLOW FLUORESCENCE SPECTROSCOPY

4.1 Introduction

Gene therapy signifies correction of genetic defects against several neurodegenerative disorders, viral infections and cancer. But it is pertinent to mention that promise of successful therapeutic gene therapy is still limited by several barriers. Prominent disputes still remains undefeated particularly in the cell targeted specific delivery and systematic gene delivery [1-4]. It is noteworthy that the significance of short oligonucleotides is recently realized as RNAi, siRNA and antisense oligonucleotides [2]. Usually, the process of RNAi involves the enzymatic cleavage of long dsRNA transcripts into micro RNA and small interfering RNA (siRNA)[2]. Fascinatingly, both antisense/synthetic oligonucleotides and RNAi-based gene therapy target mRNA to conquer transcription of an over expressing endogenous gene or a cancer-causing oncogene, by selectively inhibiting the undesirable protein expressionss[2-4]. The short/antisense oligonucleotides generally ranges from 14–30 nucleotides and block translation of the disease-causing protein after complementarily hybridizing to their target messenger RNA (mRNA) and degrading them by activating RNaseH. Usually, siRNAs have increased nuclease stability and gene silencing efficiency, as well as reduced immune responses. However, on the contrary, in order to avoid off-target effects and minimize certain sequence motifs deliberate selection and design of siRNA sequence is required [1-3]. Regardless, the apparent ease of designing siRNAs a number of problems still persists than compared to popular DNA-based antisense oligonucleotides[2]. It has been depicted by many groups that naked oligonucleotides incorporate poorly through cells [5] and quite essentially, these oligonucleotides dispose to localize in

other areas of the cell like endosomes/lysosomes which are of non-targeted sites [6-8]. Even though, several techniques have been introduced by researchers to ameliorate the cellular uptake of oligonucleotides [2], there exist a numerous hurdles [1]. However, for successful clinical applications, there is need of a systemic administration of these nucleic acids into cells, which mostly depends on the use of efficient carriers commonly viral or non-viral vectors.

Even though, viral vectors have high gene transfection efficiency than non-viral vectors, non-viral vector based gene delivery is being in use to avoid their insertional mutagenesis and immunological problems [3]. It is also pertinent to mention that non-viral carrier systems are mostly constructed systematically and biocompatible using innovative fabrication approaches for safer delivery of the therapeutic gene cargo into the cells. There exixt a variety of non-viral cationic vectors like liposomes, poly L-lysine, PAMAM (polyamidoamine) dendrimers and so on [9-11]. The non-viral cationic gene vectors like PAMAM dendrimer is an interesting nano carrier due to their synthetically tunable molecular structures, sizes, surface charges as well as their functionalities [12-15]. Additionally, PAMAM-DNA complexes have been proven not only for their highly soluble and stable nature and also do their resistsance towards nuclease digestion in all the physiological conditions [6]. Interestingly, The pioneering studies on therapeutic nucleic acids binding PAMAM dendrimers demonstrated that these multivalent polycationic carrier molecules can form a strong and stable binding with phosphate (polyanionic) groups present on DNA/oligonucleotides through strong electrostatic interactions[16-18] and further lead to successful therapeutic gene delivery through oral, ocular, parenteral and transdermal routs of administration [19-21]. It is pertinent to mention that dendrimer cytotoxicity increases with increase in generation number [22, 23] and recently importance of lower generation dendrimers are highlighted in rapidly growing arena of RNAi therapeutics[24]. Interestingly, efficient pDNA transfection of unmodified low generation PAMAM dendriers into CHO-K1 and HaCaT cells lines is successfully demonstrated by us for transdermal gene delivery applications [25].

As we all know, the first and most significant in vitro barrier of non-viral nucleic acid delivery is the size and negative charge of the oligonucleotides. Hence, it is extremely crucial to draw the information regarding association of the gene vehicles with therapeutic nucleic acids and quantifying their capability in condensing or packing the nucleic acid molecules. It is pertinent to mention that the deficiency of tight cationic ligand association with nucleic acid may leads to endosomal/ lysosomal entrapment of these molecules, which further leads to less/poor transfection at the target sites [24, 26-28]. Hence it becomes very important to predict gene transfection efficiency on the physicochemical characteristics of these nucleic acid based complexes. In particular, among usual physicochemical interaction studies, it is essential to investigate a clear definition of kinetic pathway and associated critical parameters that characterize the formation of DNA-cationic carrier complexes and subsequent unpacking of the complex for the successful therapeutic delivery at the target site [29]. Literature reveals a numerous experimental [30, 31] and simulation techniques [32, 33] are used to understand the interaction between cationic vectors and nucleic acids. Stopped flow fluorescence is one of the modern attractive techniques to study the kinetic parameters of the nucleic acid based complexes with relaxation times down to 1-2 ms. This attractive stopped flow fluorescence technique is widely used to understand kinetics of DNA-cationic ligand interactions [34-37]. It is noteworthy that, short oligonucleotide (14-30 nucleotides) complexation with cationic vehicle is quite different with huge DNA molecules. For example, recently, our projection on the 14mer oligonucleotide and low generation dendrimer interactions using fluorescence and Förster resonance energy transfer (FRET) techniques evidences systematic 14 mer oligonucleotide packing in dendriplex in spite of their condensation. In the present investigation, we extended our findings to investigate the important kinetic parameters to characterize the complexation of lower generation PAMAM dendrimers with 14 mer short oligonucleotides by using stopped-flow spectrofluorometric technique.

4.2 Materials and Methods

PAMAM (starburst) Dendrimers of lower generations -1, 2 & 3 (cationic polymers) of highest purity (>99%) were obtained from Sigma Aldrich. The 14mer short DNA oligonucleotide of strand 1 (5'-GATGTTCACTCCAG-3') and strand 2 (5'-CTGGAGTGAACATC-3') were obtained from SBS-Genetech. As manufacturer indicated that the GC content of the oligonucleotide was 50%. The concentration of the oligonucleotide was calculated based on the optical density (OD) values provided by the manufacturer.

The DNA duplex have been prepared by mixing equimolar concentration of both the oligonucleotide strands and then heated to 95°C for 10 minutes and cooled to room temperature for 4-6 h. Here 1 μM 14mer oligonucleotide is equivalent to a 26 μM (as 14mer single strand oligonucleotides will have 13 phosphate groups) phosphate charge.

Ethidium bromide (3,8-diamino-5-ethyl-6-phenylphenanthridium bromide, EB) was purchased from Sigma Aldrich and used without further purification. The stock solution of EB was prepared by dissolving 2.2 mg in 1 mL of 10 mM phosphate buffer, and the concentration was determined by using a UV–visible spectrophotometer (ε= 5600 M^{-1} cm^{-1} at 480 nm). Ethidium bromide solutions were stored in the dark at 4 °C before use.

4.2.1 Steady state Fluorescence spectroscopic studies

In order to understand the dendrimer-based short oligonucleotide delivery system, ethidium bromide (EB) exclusion studies were carried out as follows: fluorescence spectra of the oligonucleotide–EB complexes were recorded in the absence and presence of the desired generation of PAMAM dendrimer from 500 to 700 nm at an excitation wavelength (λex) of 480 nm using a spectrofluorometer (JobinYvon FluoroMax 3) with a Peltier thermostat. A 14 mM concentration of EB was mixed with a 1 mM concentration of the oligonucleotide solutions (1EB : 1 base pair) in 10 mM sodium phosphate buffer as well as in 41 mM Na^+ salt concentration in sodium phosphate buffer at pH 7.0 and equilibrated for 10 min at 20 °C. For these

experiments, a stock EB solution was prepared by dissolving 1.97 mg of EB in 1000 mL of water, and the corresponding stock concentration was determined using a Cary 100 UV-visible spectrophotometer assuming a molar extinction coefficient of 5600 L mol1 cm1 at 480 nm [38] 300 mL of this oligonucleotide–EB mixture was taken in a fluorescence cuvette, and increasing amounts of the required concentration of the cationic polymer were added to the mixture. After each addition of the polymer, the contents of the fluorescence cuvette were incubated for 10 min before recording each spectrum. The concentrations of the dendrimer stock solutions were prepared in such a way that the maximum dilution of the oligonucleotide–EB complex was maintained well within 10% due to the dendrimer addition. The dilution factors considered for the calculation were related to the final charge ratios.

4.2.2 Gel Electrophoresis Studies

The electrophoretic mobilities of PAMAM dendrimer of generations 1, 2 & 3 duplex DNA oligonucleotide (14 mer) complexes at various charge ratios $Z_{(\pm)}$ were determined by using 15% native-PAGE. Gel electrophoresis experiments were carried out in a buffer consisting of 45 mM Tris-borate and 1 mM EDTA at pH 8.0. In these studies, in order to prepare oligonucleotide-dendrimer complex of required charge ratio, 1 μM concentration of oligonucleotide (equivalent to 26 μM phosphate unit) was mixed with various concentrations of the desired dendrimer generations (1, 2 & 3) solution and incubated for 30 min. Polyacrylamide gels were run at 120 V for 4 h at 4 °C using the oligonucleotide-dendrimer complexes of various charge ratios. Further, the corresponding dendriplex bands were visualized under UV illumination after staining the gels with ethidium bromide for 30 min at room temperature.

4.2.3 Stopped-Flow Fluorescence Spectroscopic Studies

The kinetic measurements were performed using a SFA-20 rapid kinetics accessory (HI-Tech Scientific) in Jobin Yvon Fluorolog with a Peltier thermostat. The concentration of both DNA and ethidium bromide in the 14 mer DNA−EB complex solution was 1 μM, and four different concentrations of the dendrimer solutions were used for the stopped-flow kinetic study to obtain the charge ratio of the

resultant solutions as Z+/−= 0.3, 0.6, 0.9 and 1.2 respectively, upon mixing of equal volume of two solutions. The excitation and emission monochromator were set to 480 and 590 nm, respectively. During the experiment, two separate syringes of the stopped-flow were filled up with DNA−EB complex and dendrimer solutions, and in each run, an equal volume of both solutions was injected at once into the sample chamber. The emission spectra were monitored continuously both before (t = 0 s) and after the injection. The dead time of the instrument was determined from the test reaction described elsewhere and was found to be 5 ms for a 1:1 mixing. Required control experiments were carried out by mixing a DNA−EB solution and buffer solutions. the fluorescence signal of DNA-EB complex was found to be unchanged within the time of the measurement. The stopped-flow kinetic study were also performed with increasing concentration of short oligonucleotide as 1 μM, 3 μM, 5 μM, 7 μM and 10 μM with PAMAM dendrimer generation three to obtain the charge ratio of the resultant solutions as Z± = 0.6.

4.3 Results and Discussion

In order to understand the interaction between therapeutic short oligonucleotide and PAMAM dendrimer of lower generations (G1, G2 and G3) steady-state fluorescence spectroscopic as well as gel electrophoresis studies were carried out. Figure 4.1 left panel, portrays the fluorescence emission spectra of free EtBr (Trace 1) solution, EtBr intercalated 14 mer short oligonucleotides (trace 2) and oligonucleotide-PAMMAM dendrimer complexes of first three generation (a) G1, (b) G2 and (c) G3 with increasing charge ratios ($Z_{\pm}$) in 10 mM sodium phosphate buffer (containing 16 mM Na^{+} concentration) at pH 7.0. From the figure, Intercalation of EB with 14mer oligonucleotides is clearly evidenced by a significant raise in fluorescence emission spectrum of the DNA-EB complex at 608 nm, upon excitation at 480 nm (Trace 2) compared to free EB (Trace 1). Interestingly, for all three generations, an increase in fluorescence quenching is evidenced for oligonucleotide-EtBr complex with increase in the addition of dendrimer concentration in general, which is

indicated by a down arrow. The observed fluorescence quenching clearly indicates efficient release of EtBr from the 14mer molecules by the addition of positively charged dendrimer molecules. For example, in the case of G1 (Table I), as the charge ratio ($Z_{+/-}$) increases from 0.41 to 1.12 percentage EtBr release raises from 69.08% to 93.69%. From Table I interestingly, the amount of EtBr released from the short oligonucleotides increases with increase in dendrimer generation G1 to G3 for almost similar charge ratios. For example, percentage EtBr release is reported 47.7% for G1, 58.4% for G2 and 62.1% for G3 at the charge ratio ($Z_{+/-}$) 0.14. The observed increase in dendrimer interaction strength on oligonucleotides with the dendrimer generation number is mainly due to the corresponding rise in their surface charge.

Tabel III: The percentage of EtBr release upon increasing charge ratio ($Z_{\pm}$) of PAMAM dendrimers of lower generations G1, G2 and G3 in 16 mM Na+ buffer concentration at pH 7.0. The concentration of the oligonucleotide was 1 µM.

PAMAM Dendrimer	$Z_{\pm}$	% EB Release
G1	0.138	47.74
	0.41	69.06
	1.02	90.69
	1.12	93.69
	1.15	99.64
G2	0.14	58.35
	0.23	68.32
	0.56	83.28
	0.85	95.01
	0.86	98.69
G3	0.14	52.47
	0.48	75.66
	0.77	98.85

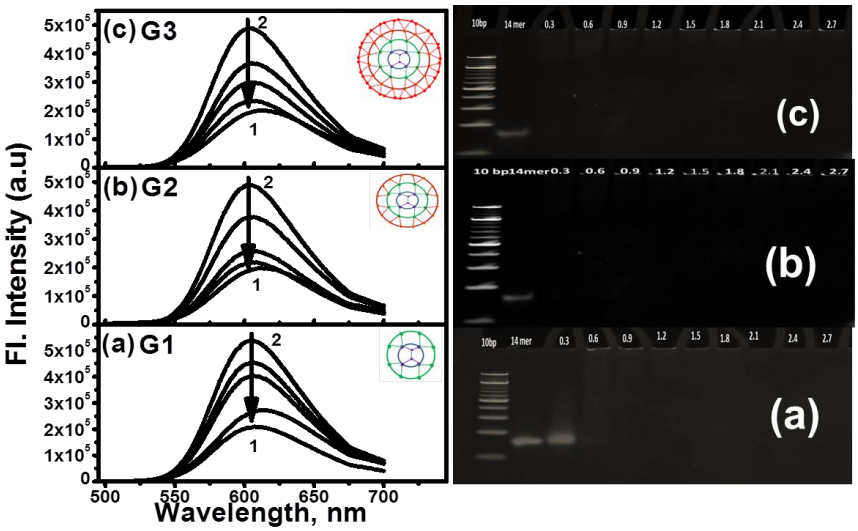

Figure 4.1 Panel A, shows EtBr fluorescence spectra for PAMAM dendrimers of lower generations (a) G1, (b) G2 and (c) G3. Traces 1 and 2 in each plot are fluorescence emission spectra of free EtBr and EtBr bound to 14 mer DNA oligonucleotide. The down arrows indicate the increase of Z ±. The 14 mer DNA oligonucleotide concentration was 1 µM in 10 mM sodium phosphate buffer at pH 7.0. Panel B, Gel electrophoresis assay. 15% non-denaturing PAGE was run with complexes of PAMAM dendrimer (a) G1 (b) G2 and (c) G3 at various PAMAM dendrimer to oligonucleotide charge ratios (as mentioned on the corresponding lanes). The gel was run in buffer consisting of 45 mM Tris-borate and 1 mM EDTA at pH 8.0, at 120 V for 60 min at 4°C. The gels were visualized under UV illumination after staining with ethidium bromide at room temperature.

In order to visualize the interaction between the 14 mer DNA oligonucleotide and the PAMAM dendrimer of first three generations gel electrophoresis were carried out. It is pertinent to recall that the migration level of positively charged dendrimer associated with negatively charged oligonucleotide determines partial or complete neutralization of the corresponding nucleic acid. The migration of partially or completely neutralized oligonucleotides molecules by the cationic ligands either slowed down or completely hindered through the gel. Figure 4.1 right panel, portrays the before and after interaction of oligonucleotide with PAMAM dendrimer of (a) G1, (b) G2 and (c) G3. The first and second wells of all the three gel images represent the migration of the 10 bp molecular weight marker as well as free 14 mer DNA oligonucleotides respectively. On the other hand, the following wells of the three PAGEs indicate the migration of dendriplexes with increasing dendrimer to oligonucleotide charge ratio ($Z_{\pm}$) from 0.3 to 2.7. In figure 4.1 (a) right panel, the migration of oligonucleotide in the presence of dendrimer G1 is seen upto the

charge ratio ($Z_{\pm}$) 0.3. From figure, the It is also important to refer that smearing and reduction in the band intensity corresponding to 14mer-G1 complex at $Z_{\pm}$= 0.3 compared to bare oligonucleotide ($Z_{\pm}$ = 0). Interestingly, the migration of the short oligonucleotide is completely invisible from the charge ratio 1.2 to 2.7. These observations indicate upto the charge ratio ($Z_{\pm}$) 1.2 there exist partial neutralization of the oligonucleotides and thereafter complete saturation of the molecules is achieved. In case of G2 and G3 (figure 4.1 right panel (b) and (c) respectively), smearing of oligonucleotide is feebly seen up to the charge ratio ($Z_{\pm}$) 0.6 suggesting the existence of partially neutralized oligonucleotide in trace quantities. Further DNA migration is completely retarded from $Z_{\pm}$ = 0.9 to Z± = 2.7. Interestingly, representative wells of the PAGE (b) as well as (c) are observed to comprise a perturbed oligonucleotide-dendrimer complex for both the generations G2 ($Z_{\pm}$ = 0.6 to $Z_{\pm}$ = 2.7) and G3 (Z± = 0.6 to $Z_{\pm}$ = 2.7). It is also noteworthy that in case of both G2 and G3, the effective neutralization of the oligonucleotide by the dendrimer is suggested by the disappearance of the DNA band even at lower charge ratio (Z± = 0.3) compared to G1. Most interestingly, the eminently visible retarded 14mer molecules in the wells indicate the availability of the stain within the dendriplex, which may discloses the lack of compaction ability of 14 mer DNA oligonucleotides by the cationic dendrimer molecules. These observations on short oligonucleotide and PAMAM dendrimer of lower generations (G1, G2 and G3) interactions by steady-state fluorescence spectroscopy and gel electrophoresis are in good agreement with our earlier observations [36,39, 40].

4.3.1 Kinetic data analysis

Based on the successful observation on the complexation of 14mer oligonucleotide with PAMMAM dendrimer of lower generation by **Steady state fluorescence spectroscopic as well as gel electrophoresis studies,** the binding kinetics of dendrimers (G1, G2 and G3) with short oligonucleotide molecules were monitored by using stopped-flow fluorescence spectroscopic technique as function of time. The figure 2a, depicts the normal fluorescence intensity decay of EtBr observed on G1

binding on short oligonucleotide at dendrimer to oligonucleotide charge ratio (Z±) 1.2 as a function of time, in the presence of 26 mM Na^+ ion concentration at pH 7.0. As per the previous report [34], in the present study also the obtained fluorescence decay kinetic curve was analysed by considering it as a super-position of exponentials terms given below:

$$I(t) = \sum_{i=1}^{i} A_i \exp(-t/\tau_i) \quad \textbf{(1)}$$

Where I is the fluorescence at time t, A_i is the prefactors, and τ_i is the pseudo-first-order time constants. The reciprocal of time constant is the relative rate constant of the 14mer-oligonucleotide binding reaction (k_i). The Nelder−Mead simplex method for minimizing eq 1 was used for the entire kinetic data analysis. Here, the number of exponentials was gradually increased until no systematic deviation of the residual was found (Figure 4.2b). Interestingly, it was observed that three exponential functions (i = 3) were found sufficient to depict the fluorescence decay kinetics of EtBr upon G1 binding to the short oligonucleotide. Considering these observations, the following are proposed fundamental reaction scheme in three steps for the cationic dendrimer binding on short oligonucleotides.

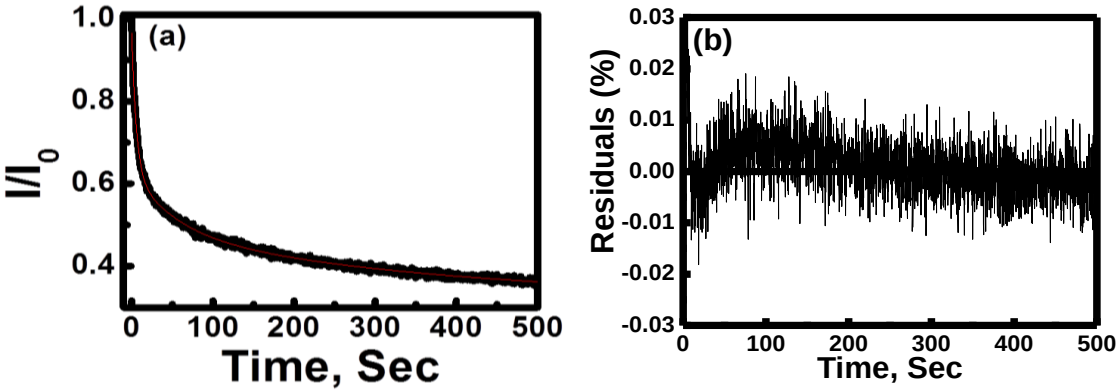

Figure 4.2 Stopped-flow data corresponding to the fluorescence intensity decay of EB observed upon PAMAM generation 1 binding to short DNA at Z ± = 1.2, as a function of time. The short DNA concentration was 1 µM in 10 mM NaCl salt conc, sodium phosphate buffer (pH 7.0). The smooth line in panel (a) shows the fitting obtained with eq 1 and panel (b) shows the residuals of the fit.

$$ON{-}EtBr \rightleftharpoons ON^{-} + EtBr \quad (2)$$

$$ON^{-} + D^{+} \rightleftharpoons ON{-}D(c) \quad (3)$$

$$ON{-}D\,(c) \underset{k_2}{\overset{k_1}{\rightleftharpoons}} ON{-}D\,(ma) \underset{k_3}{\rightleftharpoons} ON\text{-}D\,(ra) \quad (4)$$

Where 'c' stands for 1:1 complexation of oligonucleotides with PAMAM dendrimer, 'ma' refers the interaction of micellar aggregated dendrimer molecules with oligonucleotides and 'ra' represents further rearrangement of the dendriplex. Based on our recent findings via FRET investigations on 14mer-dendrimer interactions [39] the above said reaction scheme is explained as follows: initially there exists simple 1:1 electrostatic binding of negatively charged phosphate back bone of oligonucleotides molecules with the positively charged amino surface groups of the PAMAM dendrimer. The formation of monomeric 1:1 complexation of oligonucleotides-PAMAM at the neutralization point is in good agreement with literature for siRNA-PAMAM system using silico[41] as well as SAXS [42] studies. Followingly, there results a 14 mer induced self-assembly to form an aggregation of PAMAM dendrimer molecules. Finally, at the third step a rearrangement of these loosely held dendrimer aggregates in term of their size and shape leads to a tight aggregate fusion and is also followed by a simultaneous accommodation of oligonucleotides molecules around these cationic aggregates (Figure 4.3).

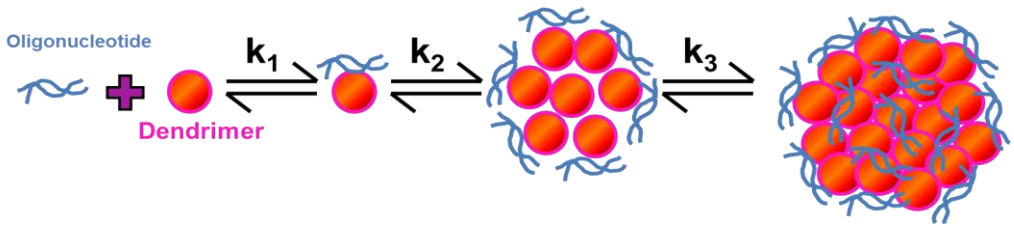

Figure 4.3 Schematic representation of the proposed lower generation PAMAM dendrimer binding mechanism and DNA compaction. The different components are not at scale.

It is important to note that by considering the above mechanism, it is most likely that the relative rate constants vary with dendrimer to oligonucleotides charge ratio, the ionic strength of the medium as well as with the dendrimer generations of under

study (G1, G2 and G3). The latter, having an impact on the shape and size of the micelles, can affect oligonucleotides packing as well its associability.

4.3.2 Effect of charge ratio on binding kinetics

Figure 4.4(a) shows EtBr fluorescence intensity decay kinetics observed upon PAMAM dendrimer of generation G1,G2 and G3 binding individually onto the 14mer oligonucleotide at various charge ratio ($(Z_{+/-})$ 0.3, 0.6, 0.9 and 1.2), in the presence of 10 mM sodium phosphate buffer at 25 °C. Similar to Figure 4.2(a), the EtBr fluorescence emission spectrum on oligonucleotide-dendrimer interaction fits well into a triexponential function as given in eq. 1, indicating the existence of the 14 mer binding interactions with PAMAM molecules in three steps. The obtained rate constant values, k_1, k_2 and k_3 for the PAMAM dendrimers understudy correspond to the binding process of the dendrimer to oligonucleotide to form complexation in 1:1 ratio followed by micellar aggregation of dendrimer molecules in the vicinity of the 14 mer and further rearrangement of the dendriplexes respectively. The obtained three relative rate constants (k_1, k_2 and k_3) were plotted against various charge ratios ($(Z_{+/-})$ 0.3, 0.6, 0.9 and 1.2), as shown in Figure 4.4(b).

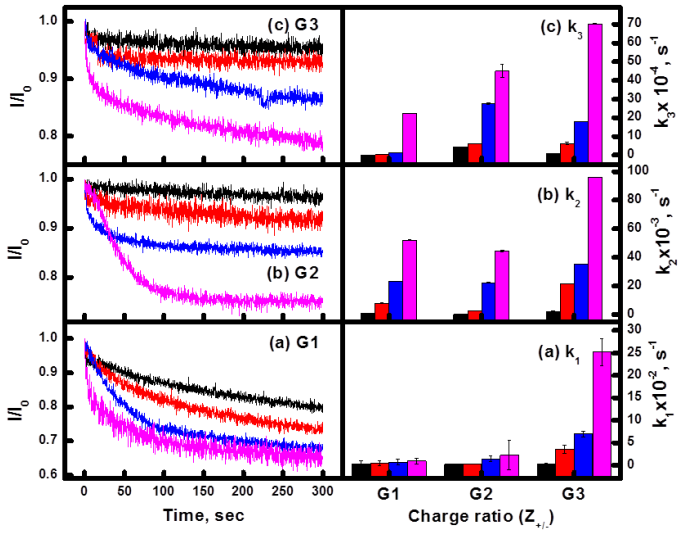

Figure 4.4 Fluorescence intensity as a function of time for (a) PAMAM dendrimer G1, (b) PAMAM dendrimer G2 and (c) PAMAM dendrimer G3 binding to short oligo-DNA at $Z_{\pm}$ = 0.3 (black), 0.6 (red) and 0.9 (blue) and 1.2 (Magenta). The oligonucleotide concentration was 1 µM in 10 mM sodium phosphate buffer (pH 7.0).

Here, each rate constant is an average of three independent kinetic experiments. Interestingly, it is pertinent to note that for the dendrimers of the first three generations (G1, G2 and G3), all the three relative rate constants are well separated, by at least an order of magnitude, and, in general, increase with increasing in dendrimer to oligonucleotide charge ratio (Z±). In detail, the relative rate constant k1 of very first step (eq. (3)) corresponds to the electrostatic binding of the positively charged dendrimer on the 14 mer molecule, which is a diffusion-driven process and also in general found to be faster with increase in the dendrimer to oligonucleotide charge ratio (Z±). Interestingly, the reported the first rate constant (k1) is observed to be very different for the first three dendrimer generations under study, which clearly indicates the existence of differences in the interaction of PAMAM dendrimer molecules as per the generations with the short oligonucleotide. In detail, for G1, G2 there is hardly any difference found in the magnitude of the first rate constant values obtained for the various charge ratios under study. On the other hand for G3, there exists a significant difference in the reported k1 values with increase in G3 to oligonucleotides charge ratio from (Z± = 0.3 to 1.2). It is also noteworthy that the value of k1 is almost 10 times higher at Z± = 1.2 in comparison with Z± = 0.9 for G3. These striking differences in the first relative rate constant of the first three generations understudy certainly suggest that binding of individual dendrimer on the 14 mer molecules are not simple diffusion. In order to understand the observed difference in the 1:1 complexation rate of dendrimer and oligonucleotide it is pertinent to recall that in PAMAM dendrimer structure, the active terminal primary amine that becomes positively charged at physiological conditions doubles with the generation number as follows, G1 contains 8, G2 contains 16 and G3 contains 32. More importantly as we move, G1 to G3 exposure of amino functional groups on the surface becomes the highest for G3. Hence, the magnitude of rate constant (k1), for a given generation increases with the increase in the amount of dendrimer as well as with the increase in the generation number. For example, the reported fastest rate

constant (k1= 25.2) for G3 at Z± = 1.2 is not only due to the highest concentration used but also due to its highest exposure in cationic surface charge.

In the case of second rate constant (k_2), in general the magnitude increases with increase in the dendrimer to oligonucleotide charge ratio for all the three dendrimer generations used. In contrast to G3, the reported values of k_2 at various charge ratios are more or less similar for G1 and G2. For instance, at the charge ratio (Z±) 1.2 the reported k_2 values are 51.1 s^{-1}, 44.4 $s^{-1}$and 95.1 s^{-1} respectively. This is probably because the relatively smaller size of the G1 and G2 dendrimer resulted in a larger surface area and therefore a lower charge density compared to G3. In detail, since the second step corresponds to the micellar aggregation of the PAMAM dendrimer molecules in the vicinity of the 14 mer oligonucleotides, the observed weaker binding of G1 as well as G2 micellar aggregates on the oligonucleotides can be attributed to the lower dendrimer surface charge density compared to G3. Here it is pertinent to recall that the dendrimer aggregation number decreases roughly by factor of 2 with each increment of generation number, which is in line with a two-fold increase in dendrimer surface charge upon an increase in the generation number.

Similar to k_1 and k_2 the relative rate constant (k_3) of the third step also in general increases with increase in the dendrimer to oligonucleotides charge ratio. On the other hand, the observed irregularity in the rearrangement rates (k_3) for G1 and G2 at the entire charge ratio under study is due to the consequence of their smaller size leading to larger surface area and therefore results a lower charge density that enabled the formation of well-structured dendriplexes. Interestingly, with increase in dendrimer to the 14mer charge ratio (Z±), G3 reports a significance rise in the rearrangement rate (k_3) for its tight fusion of molecular aggregate followed by the oligonucleotide packing due to the available higher surface charge density in comparison with G1 and G2. The proposed three steps in PAMMAM dendrimer-oligonucleotide interaction is portrayed in figure 4.3.

4.3.3 Effect of salt concentration:

(a) Steady state fluorescence spectroscopic studies:

In order to investigate effect of ionic strength on the dendrimer binding to the oligonucleotide, EtBr, a cationic dye, is premixed with the 14 mer with increasing concentration of Na^+ ions (16 mM and 41 mM(shown in figure 4.5)) and titrated with dendrimer of required generation (Figure 4.6 left panel (16 mM Na^+) right panel (41 mM Na^+). Here, 16 mM Na+ refers to the concentration of sodium ions in 10 mM sodium phosphate buffer. It is pertinent to recall that the ethidium ion intercalates into the 14 mer and dramatically increases its fluorescence efficiency. The addition of the dendrimer into the oliegonucleotide-EB complex solution results in the removal of the intercalated EB from the 14 mer molecule, and a quenching of fluorescent intensity is observed.

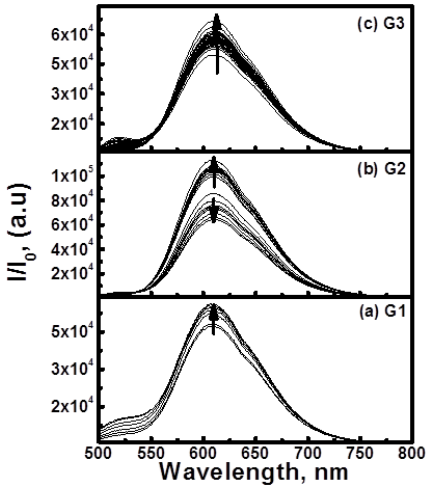

Figure 4.5 EB fluorescence spectra for PAMAM dendrimers of lower generations (a) G1, (b) G2 and (c) G3. Traces 1 and 2 in each plot are fluorescence emission spectra of free EB and EB bound to 14 mer DNA oligonucleotide. The up arrows indicate the increase of Z ±. The 14 mer DNA oligonucleotide concentration was 1 µM in 25 mM NaCl salt concentration in sodium phosphate buffer at pH 7.0.

In general, in presence of Na^+ ions, the fluorescent intensity of 14mer-EB premix solution decreases with increase in the dendrimer to oligonucleotide charge rato (*Z*±) and portrays a distinct characteristic break in *Z*± values, (represented by arbitrary arrow heads) for 16 mM and 41 mM Na^+ concentration. It is also pertinent to note

that the rate of quenching in fluorescence intensity decreases with increase in Na^+ concentration from 16 mM to 41 mM Na^+ ions. In contrast, quenching of EtBr fluorescence intensity increased with increase in dendrimer generation G1 to G3.

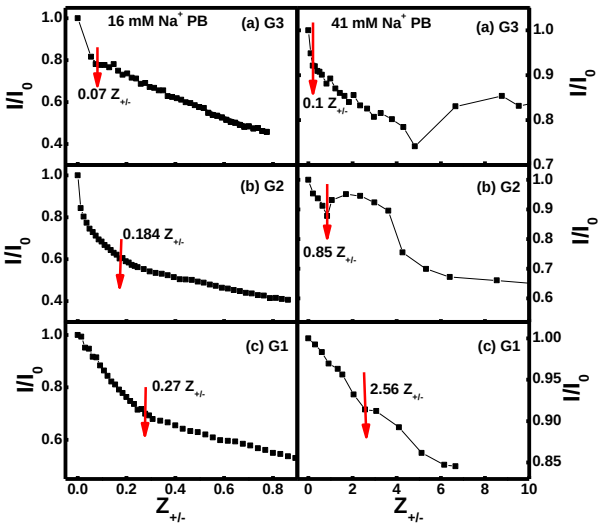

Figure 4.6 Ethidium bromide exclusion experiments for oligonucleotide at various generations of PAMAM dendrimer (a) G3, (b) G2 and (c) G1 to oligonucleotide charge ratios in the absence of NaCl (Left panel) and in the presence of 41 mM NaCl (Right panel). Arrow heads represent arbitrary saturation points in the displacement of EB from the oligonucleotide by lower generation PAMAM dendrimers. The oligonucleotide concentration was 1 μM in 10 mM sodium phosphate buffer (pH 7.0).

It is also noteworthy that generally for all the three generations, EtBr exclusion was reported very steeply up to the reported characteristic charge ratio (represented by arbitrary arrow heads) at which the oligonucleotide is almost saturated with dendrimer molecules and further very feeble dendrimer binding to oligonucleotide was noticed on further addition of the polymer to the solution and, therefore, less exclusion of EtBr from oligonucletides could be observed at both the salt concentrations. Interestingly, with increase in the concentration of Na^+ ions from 16 mM to 41 mM the characteristic saturation value *Z*± also increases, which is again attributed to the screening effect of Na+ ions on the oligonucleotide and the increased oligonucleotide stability. It is worth to recall that, in the fluorometric titration of oligonucleotides with G1, G2 and G3 (Figures 4.6) in the presence of 16mM and 41 mM Na^+, the charge neutralization values (*Z*±) were increased from 0.07, 0.184 and 0.27 to 0.01, 0.85 and 2.56 respectively (Figures 4.6).

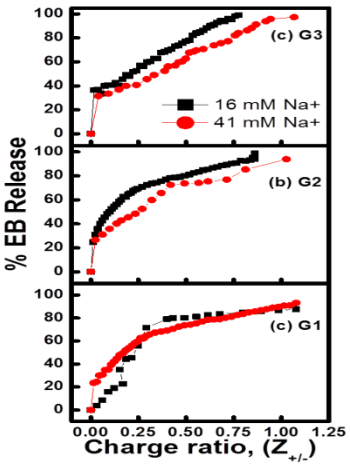

Figure 4.7 EB exclusion experiments. Percentage of EB released from the DNA as a function of $Z_{\pm}$ in absence of NaCl (black) and in presence of 41 mM NaCl (red) for PAMAM dendrimer generation (a) G3, (b) G2 and (c) G1. The oligonucleotide concentration was 1 µM in 10 mM sodium phosphate buffer (pH 7.0).

(b) Effect of Salt Concentration on Kinetics

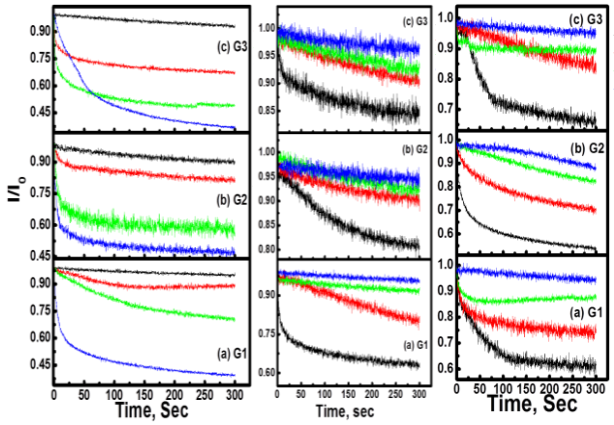

Figure 4.8 Fluorescence intensity as a function of time for (a) PAMAM dendrimer G1, (b) PAMAM dendrimer G2 and (c) PAMAM dendrimer G3 binding to short oligo-DNA at Z± = 0.3 (black), 0.6 (red) and 0.9 (green) and 1.2 (blue). The oligonucleotide concentration was 1 µM in 26 mM NaCl (left panel), 41 mM NaCl (middle panel) and 66 mM NaCl (right panel) salt concentration in phosphate buffer (pH 7.0).

The effect of increasing salt concentration (16 mM, 26 mM, 41 mM and 66 mM) on the kinetics of oligonucleotides-PAMAM dendrimer binding at various charge ratio ((Z±) 0.3, 0.6, 0.9 and 1.2), in the presence of 10 mM sodium phosphate buffer at 25 °C is portrayed in Figure 4.9 (a) to (c) for the generations G1, G2 and G3. Similar to Figure 4.4 here again for the dendrimers of the first three generations (G1, G2 and G3), all the three relative rate constants (k_1, k_2 and k_3) are well separated, by at least

an order of magnitude. In general, all the three relative rate constants of G1 and G2 are independent of salt concentration as well as the dendrimer to oligonucleotides charge ratio understudy indicating weaker interaction of lower generation dendrimers with the 14 mer molecules. Once again, the observed insignificancy of G1 and G2 rate constants is probably due to the consequence of their smaller size leading to larger surface area and therefore results a lower charge density that enabled the formation of well-structured dendriplexes [43-45]. Interestingly, for G3 there is a decrease in first two relative rate constants k_1 *and* k_2 upto 41 mM Na^+ concentration for all the charge ratio under investigation and thereafter the relative rate constants become more or less similar to each other. Here, the highest magnitude of k_1 *and* k_2 at the highest charge ratio (Z±) as well as the lowest ionic strength (16 mM) indicating significant interaction of G3 with the oligonucleotides compared to G1 and G2. In contrast for G3, the relative rate constant k_3 at various ionic strength as well as charge ratio remains almost very similar indicating almost similar and the slowest further rearrangement of the compacted dendriplex.

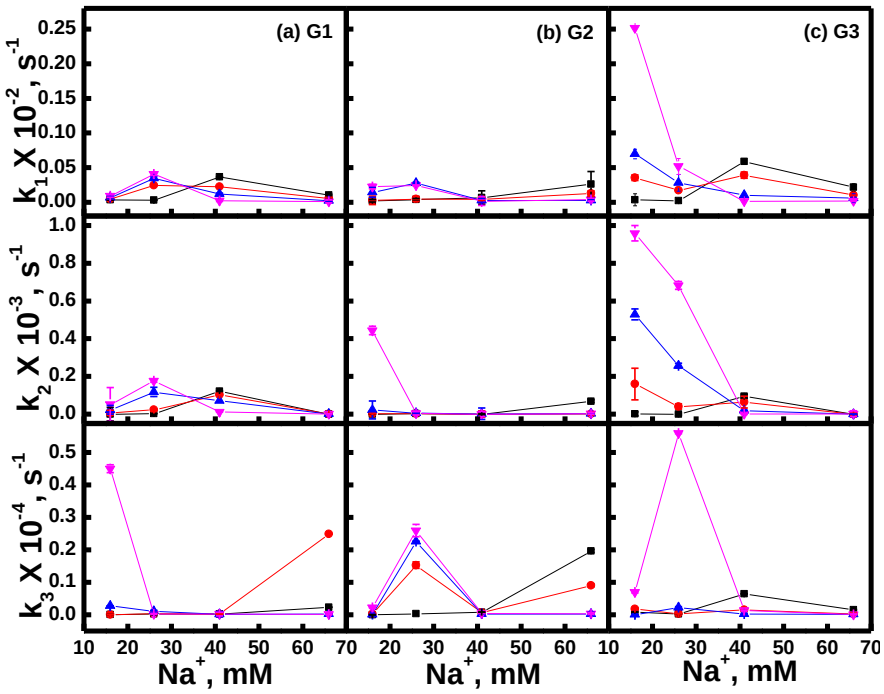

Figure 4.9 First, second and third relative rate constants (k_1, k_2 and k_3) for PAMAM dendrimer generation (a) G1, (b) G2 and (c) G3 binding to short DNA oligonucleotide, respectively, as a function of Na^+ concentration at various charge ratios 0.3 (black), 0.6 (red), 0.9 (blue) and 1.2 (magenta). The DNA oligonucleotide concentration was 1 µM in 10 mM sodium phosphate buffer (pH 7.0).

Table IV: Relative Rate Constants for the Different Generations of PAMAM dendrimer Binding to short-DNA Oligonucleotide as a Function of the Charge Ratio (Z±), for Different Na+ concentrations.

Salt concentration	$Z_{\pm}$	PAMAM DENDRIEMR G1			PAMAM DENDRIEMR G2			PAMAM DENDRIEMR G3		
		k_1*10^{-2}	k_2*10^{-3}	k_3*10^{-4}	k_1*10^{-2}	k_2*10^{-3}	k_3*10^{-4}	k_1*10^{-2}	k_2*10^{-3}	k_3*10^{-4}
16 mM Na^+	0.3	0.00341 ± 5.48E-04	0.000645823 ± 0.03596	0.00063063 ± 3.00E-04	0.00203 ± 0.00178	0.000127525 ± 2.26E-04	0.000130663 ± 7.20E-06	0.0035 ± 0.0087	0.00176 ± 0.0106	0.00859 ± 5.10E-04
	0.6	0.00482 ± 6.11E-04	0.00787 ± 0.0131	0.000483879 ± 2.90E-04	0.00271 ± 0.00603	0.00271 ± 3.13E-05	0.00271 ± 6.50E-06	0.03539 ± 0.00411	0.15982 ± 0.0834	0.01814 ± 0.00176
	0.9	0.00684 ± 0.00205	0.02323 ± 0.02339	0.02762 ± 3.50E-04	0.0142 ± 0.00694	0.02233 ± 0.0471	0.00106 ± 5.11E-04	0.06984 ± 0.0068	0.5289 ± 0.0287	0.000626732 ± 6.10E-04
	1.2	0.009 ± 0.00175	0.05187 ± 0.08977	0.45037 ± 0.0124	0.02233 ± 0.00327	0.44374 ± 0.0221	0.02233 ± 0.00174	0.25173 ± 0.00199	0.95879 ± 0.0407	0.07022 ± 0.003
26 mM Na^+	0.3	0.00292 ± 1.90E-04	0.00292 ± 5.69E-08	0.00292 ± 0.0038	0.0039 ± 0.00172	0.0039 ± 0.0021	0.0039 ±	0.00221 ± 7.40E-04	0.000792349 0.0052	0.00221 ± 1.21E-04
	0.6	0.02452 ± 0.00114	0.02452 ± 2.17EE-05	0.0038 ± 1.78E-04	0.00477 ± 0.00368	0.00304 ± 0.00368	0.15301 ± 0.0102	0.01711 ± 6.10E-04	0.04059 ± 0.01422	0.00355 ± 1.72E-04
	0.9	0.03452 ± 0.00196	0.1179 ± 0.02456	0.01102 ± 0.00289	0.02764 ± 0.00106	0.00595 ± 0.00229	0.22615 ± 3.46E-04	0.02814 ± 0.01202	0.2573 0.01262	0.02281 ± 0.00216
	1.2	0.04048 ± 0.00182	0.1773 ± 0.00801	0.00278 ± 0.00172	0.02431 ± 7.19E-04	0.00465 ± 0.00932	0.25936 ± 0.019	0.05177 ± 0.01142	0.68213 ± 0.0209	0.0216 ± 0.00144
41 mM Na^+	0.3	0.03651 ± 4.96E-04	0.12229 ± 0.0023	0.00257 ± 0.00481	0.00658 ± 0.00968	0.000337087 ± 0.003	0.00821 ± 3.85E-05	0.05884 ± 0.00423	0.09523 ± 0.0092	0.06487 ± 2.20E-04
	0.6	0.02252 ± 4.79E-04	0.10252 ± 3.93E-08	0.00252 ± 9.70E-04	0.0041 ± 0.00187	0.000468042 ± 0.016	0.00674 ± 7.43E-05	0.03894 ± 0.00435	0.0642 ± 0.0313	0.01515 ± 1.60E-04
	0.9	0.01214 ± 0.00104	0.07214 ±	0.00214 ± 0.0082	0.00262 ± 0.00277	0.00262 ± 0.03092	0.00262 ± 7.22E-04	0.01024 ± 0.0028	0.02002 ± 1.50E-04	0.00277 ± 0.0012
	1.2	0.00228 ± 0.00128	0.01228 ± 6.52E-09	0.00228 ± 0.00587	0.00162 ± 0.0061	0.000577063 ± 0.014	0.00454 ± 6.07E-09	0.00128 ± 0.00201	0.00153 ± 0.00191	0.0138 ± 7.50E-05
66 mM Na+	0.3	0.01049 ± 8.52E-04	0.00012921 ± 1.69E-08	0.02321 ± 3.20E-04	0.02594 ± 0.01842	0.06882 ± 0.00686	0.19683 ± 0.00411	0.02147 ± 0.00549	0.000577063 ± 5.29E-04	0.01515 ± 0.0014
	0.6	0.00567 ± 5.98E-07	0.0019 ± 0.00175	0.24897 ± 4.04E-04	0.01257 ± 0.00376	0.00182 ± 0.0079	0.09036 ± 0.0043	0.01038 ± 8.70E-04	0.000468042 ± 0.00401	0.00229 ± 0.00251
	0.9	0.00221 ± 0.00175	0.00221 ± 5.98E-07	0.00221 ± 4.62E-04	0.00272 ± 0.00145	0.00272 ± 0.00116	0.00272 ± 0.00549	0.00577 ± 0.00655	0.000337087 ± 3.26E-04	0.00152 ±
	1.2	0.00115 ± 0.00217	0.00215 ± 1.75E-08	0.00215 ± 8.90E-04	0.00369 ± 0.0021	0.00369 ± 0.00411	0.00369 ± 0.00238	0.00185 ± 0.00339	0.00262 ± 0.0149	0.00127 ± 1.00E-03

4.3.4 Effect of oligonucleotide concentration on Kinetics

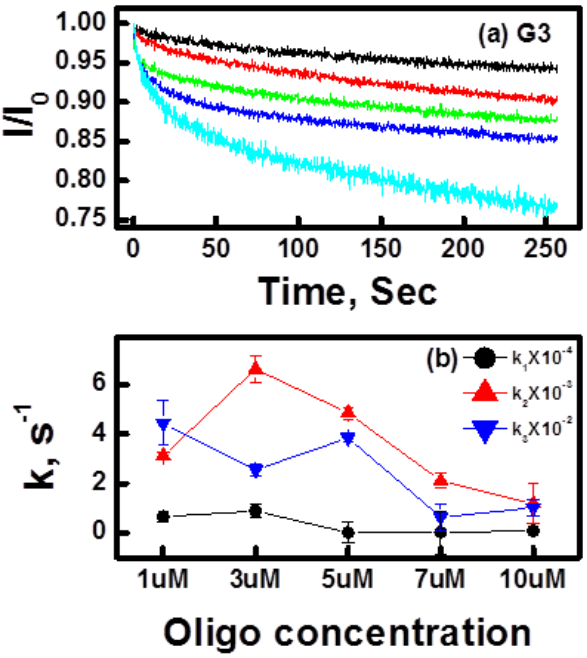

Figure 4.10 (a) Fluorescence intensity as a function of time for PAMAM dendrimer G3 binding to short oligo-DNA at various concentrations of 1 µM (black), 3 µM (red) and 5 µM (green), 7 µM (blue) and 10 µM (cyan) and (b) First, second and third relative rate constants k_1 (black), k_2 (red) and k_3 (blue) for PAMAM dendrimer G3 binding to short DNA oligonucleotide. The dendrimer to oligonucleotide concentration charge ratio (Z±) was 0. 6 in 10 mM phosphate buffer (pH 7.0).

Figure 4.10 portrays EtBr fluorescence intensity decay kinetics observed upon PAMAM dendrimer of generation G3 binding onto the 14mer oligonucleotide at increasing concentrations (1 µM to 10 µM) in the presence of 10 mM sodium phosphate buffer at 25 °C. It is noteworthy that for each oligonucleotide concentration understudy corresponds to the following charge ratio Z± 0.6. Here again, it is noteworthy that all the three relative rate constants (k_1, k_2 and k_3) are well separated, by at least an order of magnitude. It is noteworthy that the relative rate constant k_1 remains almost similar with increase in the 14mer concentration by which there is a drastic decrease in the charge ratio. Interestingly, the observed similarity in k_1 with increasing oligonucleotides concentration confirms the possibility of 1:1 complexation between G3 and the oligonucleotides. The relative rate constant of the second step (k_2) decreases with increasing oligonucleotide concentration indicating weaker interaction of the oligonucleotides with micellar aggregated

dendrimer molecules suggestive of decreasing dendrimer to oligonucleotide charge ratio. Similarly, the magnitude of k_3, which refers to a tight fusion of dendrimer micellar aggregation, followed by a simultaneous oligonucleotides rearrangement around these cationic aggregates also decreases with increase in oligonucleotide concentration.

4.4 Conclusion

The molecular packing mechanism of dendriplex formation between the 14mer oligonucleotide and PAMAM dendrimer is successfully elucidated by the FRET investigations in chapter three. The binding affinity of these lower generation dendrimers is also furtherly confirmed by stopped-flow kinetic experiments. Based on stopped-flow experimental data, three step dendriplex packing are identified. First step is the simple neutralization of the 14mer oligonucleotide by the dendrimer molecule in 1:1 ratio. With increase in dendrimer concentration, the oligonucleotide induced self–assembly of dendrimer is considered as step two. Following, dendrimer aggregation is expected to grow bigger with further raise in its concentration and followed by a fusion of these loosely held dendrimer aggregates at the final step. On the surface of these compact dendrimer aggregates the rigid rod shaped 14mer oligonucleotides are effectively accommodated with the shortest intermolecular distance. The architecture of the PAMAM dendrimer was found to have a significant impact on the kinetics of the dendriplex formation. Among the first three generations of PAMAM dendrimers, G2 and G3 exhibited significantly faster binding kinetics compared to the G1 dendrimers.

References

1. L. Aagaard and J. J. Rossi, RNAi therapeutics: Principles, prospects and challenges Adv. Drug Delivery Rev., 2007, 59, 75–86.
2. Rudolph L. Juliano SURVEY AND SUMMARY The delivery of therapeutic oligonucleotides 6518–6548 Nucleic Acids Research, 2016, Vol. 44,

3. Elsabahy, M, Nazarali, A and Foldvari, M (2011). Non-viral nucleic acid delivery: key challenges and future directions. Curr Drug Deliv 8: 235–244.

4. In Vivo Gene Delivery by Nonviral Vectors: Overcoming Hurdles? Yuan Zhang, Andrew Satterlee and Leaf Huang, Molecular therapy: the journal of the American Society of Gene Therapy, 2012, 20, 7, 1298-304.

5. Dan Luo and W. Mark Saltzman Synthetic DNA delivery systems NATURE BIOTECHNOLOGY VOL 18 JANUARY 2000 33-37.

6. Johannes Winkler, Oligonucleotide conjugates for therapeutic applications Ther Deliv. 2013 July ; 4(7): 791–809. doi:10.4155/tde.13.47.

7. Dirin M, Winkler J. Influence of diverse chemical modifications on the ADME characteristics and toxicology of antisense oligonucleotides. Expert Opin. Biol. Ther. 2013; 13(6):875–888.

8. R.L. Juliano, Xin Ming, Kyle Carver, and Brian Laing Cellular Uptake and Intracellular Trafficking of Oligonucleotides: Implications for Oligonucleotide Pharmacology NUCLEIC ACID THERAPEUTICS 24 (2), 2014

9. Targeted Delivery Systems for Oligonucleotide Therapeutics Bo Yu, Xiaobin Zhao, L. James Lee, and Robert J. Lee The AAPS Journal, Vol. 11, No. 1, March 2009 195-203

10. M. Jafari, M. Soltani, S. Naahidi, D.N. Karunaratne and P. Chen, Current Medicinal Chemistry, 2012, 19, 197-208 197 0929-8673/12 $58.00+.00 © 2012 Bentham Science Publishers Nonviral Approach for Targeted Nucleic Acid Delivery.

11. Yan Gao Xin-Ling Liu Xiao-Rong Li Research progress on siRNA delivery with nonviral carriers. Int. J. Nanomed., 2011, 6, 1017–1025.

12. Dufes, C.; Uchegbu, I. F.; Schatzlein, A. G. Dendrimers in gene delivery. Adv. Drug Deliv. Rev. 2005, 57, 2177–2202.

13. Gao, Y.; Gao, G.; He, Y.; Liu, T.; Qi, R. Recent advances of dendrimers in delivery of genes and drugs. Mini Rev. Med. Chem. 2008, 8, 889–900.

14. Swati Biswas.; Vladimir P. Torchilin. Dendrimers for siRNA Delivery. Pharmaceuticals. 2013, 6, 161-183.

15. D. G. Shcharbin.; B. Klajnert.; M. Bryszewska. Dendrimers in Gene Transfection. Biochemistry (Moscow), 2009, 74, 1070-1079.

16. C. S. Braun, J. A. Vetro, D. A. Tomalia, G. S. Koe, J. G. Koe and C. R. Middaugh, Structure/function relationships of polyamidoamine/DNA dendrimers as Gene Delivery vehicles, J. pharm. Sci. 2005, 94, 423-436.

17. R. Esfand and D. A. Tomalia, Poly(amidoamine) (PAMAM) dendrimers: From biomimicry to drug delivery and biomedical applications, Drug Discov. Today 2001, 6, 427–436.

18. A. U. Bielinska, J. F. Kukowska-Latallo and J. R.Baker, Jr. The interaction of plasmid DNA with polyamidoaminedendrimers: mechanism of complex formation and analysis of alterations induced in nuclease sensitivity and transcriptional activity of the complexed DNA, Biochim. Biophys. Acta. 1997, 1353, 180–190.

19. S. Svenson and D. A. Tomalia, Dendrimers in biomedical applications – reflections on the field, Adv. Drug Deliv. Rev. 2005, 57, 2106–2129.

20. Q. Xu, C.H. Wang and D. W. Pack, Polymeric Carriers for Gene Delivery: Chitosan and poly(amidoamine) dendrimers. Curr. Pharm. Des. 2010, 16, 2350–2368.

21. Y. Cheng, Z. Xu, M. Ma and T. Xu, Dendrimers as drug carriers: Applications in different routes of drug administration, J. Pharm. Sci. 2008, 97, 123–143.

22. J. F. Kukowska-Latallo, A. U. Bielinska, J. Johnson, R. Spindler, D. A.Tomalia and J. R. Baker, Jr. Efficient transfer of genetic material into mammalian cells using Starburst polyamidoamine dendrimers, Proc. Natl. Acad. Sci. U. S. A. 1996, 3, 4897−4902.

23. Y. Cheng, L. Zhao, Y. Li and T. Xu, Design of biocompatible dendrimers for cancer diagnosis and therapy: current status and future perspectives. Chem. Soc. Rev. 2011, 40, 2673−2703.

24. P. Kesharwani, S. Banerjee, U. Gupta, M. C. I. M. Amin, S. Padhye, F. H. Sarkar and A. K. Iyer, PAMAM dendrimers as promising nanocarriers for RNAi therapeutics Mater. Today 2015, 18, 565–572.

25. Role of Unmodified Low Generation PAMAM Dendrimers in Efficient NonToxic Gene Transfection: HemaKumariAlajangi, Poornemaa Natarajan, ManikaVij, MuniaGanguli and DeenanSanthiya, **Chemistry Select 2016**, 1, 5206- 5217.

26. R. S. Dias, B. Lindman, Eds. John Wiley and Sons: Hoboken. NJ., 2008.

27. Meredith A. Mintzer and Eric E. Simanek. Nonviral Vectors for Gene Delivery Chem. Rev. 2009, 109, 259–302.

28. José A González-Masiá, Damián García-Olmo, Dolores C García-Olmo. Circulating nucleic acids in plasma and serum (CNAPS): applications in oncology, OncoTargets and Therapy 2013:6 819–832.

29. Schaffer DV, Fidelman NA, Dan N, Lauffenburger DA. Vector unpacking as a potential barrier for receptor-mediated polyplex gene delivery. Biotechnol Bioeng. 2000 Mar 5; 67(5):598-606.

30. Niven, R.; Pearlman, R.; Wedeking, T.; Mackeigan, J.; Noker, P.; Simpson-Herren, L.; Smith, J. G. J. Pharm. Sci. 1998, 87, 1292–1299. Le Nevy, A-L. M.; Lee, C. T. J. Am. Chem. Soc. 2006, 128, 6400.

31. Mel'nikov, S. M.; Sergeyev, V. G.; Takahashi, H.; Hatta, I. J. Phys.Chem. 1997, 107, 6917. (a) Mel'nikov, S. M.; Sergeyev, V. G.; Yoshikawa, K. J. Am. Chem. Soc. 1995, 117, 9951. (b) Me´szaro´s, R.; Varga, I.; Gilanyi, T. J. Phys. Chem.B 2005, 109, 13538.

32. (a) Pattarkine, M. V.; Ganesh, K. N. Biochim. Biophys. Res. Commun. 1999, 263, (b) Rosa, M.; Dias, R.; Miguel, M. G.; Lindman, B. Biomacromolecules 2005, 6, 2164.

33. (a) Sarraguca, J. M. G.; Pais, A. A. C. C. Chem. Phys. Lett. 2004,398, 140. (b) Smith, P.; Lynden-Bell, R. M.; Smith, W. Phys. Chem. Chem.Phys. 2000, 2, 1305.

34. E.; Grueso E.; Roldan and F. Sanchez, Kinetic Study of the Cetyltrimethylammonium/DNA interaction, J. Phys. Chem. B 2009, 113, 8319−8323.

35. D. Dey, S. Kumar, S. Maiti and D. Dhara, Stopped-flow kinetic studies of poly(amidoamine) dendrimer−calf thymus DNA to form dendriplexes, J. Phys. Chem. B 2013, 117, 13767−1377.

36. D. Santhiya, R. Dias. S. Dutta P. K. Das, M. G. Miguel, B. Lindman and S. Maiti, Kinetic studies of amino acid-based surfactant binding to DNA, J. Phys. Chem. B 2012, 116, 5831-5837.

37. P. C. A. Barreleiro and B. Lindman. The Kinetics of DNA-Cationic Vesicle Complex Formation J. Phys. Chem. B 2003, 107, 6208-6213

38. Waring, M. J. Complex formation between ethidium bromide and nucleic acids. J. Mol. Biol. 1965, 13, 269-282.

39. Hema Kumari Alajangi and Deenan Santhiya. Fluorescence and Forster resonance energy transfer investigations on DNA oligonucleotide and PAMAM dendrimer packing interactions in dendriplexes. Phys.Chem.Chem.Phys. (2015), 17, 8680-8691.

40. D. Santhiya and S. Maiti. An investigation on interaction between 14mer DNA oligonucleotide and CTAB by fluorescence and fluorescence energy transfer studies. Journal of physical chemistry B 2010, 114(22), 7602-7608.

41. G. M. Pavan, L.Albertazzi, A.Danani. Ability to Adapt: Different Generations of PAMAM Dendrimers Show Different Behaviors in Binding siRNA J. Phys. Chem. B. (2010), 114, 2667–2675.

42. L. B. Jensen, K. Mortensen, G. M. Pavan, M. R. Kasimova, D. K. Jensen, V. Gadzhyeva, H. M. Nielsen, C. Foged. Molecular Characterization of the

Interaction between siRNA and PAMAM G7 Dendrimers by SAXS, ITC, and Molecular Dynamics Simulations. Biomacromolecules, 2010, 11, 3571–3477.

43. Ainalem, M. L.; Carnerup, A. M.; Janiak, J.; Alfredsson, V.; Nylander, T.; Schillen, K. Condensing DNA with Poly(amido amine) Dendrimers of Different Generations: Means of Controlling Aggregate Morphology. Soft Matter 2009, 5, 2310−2320.

44. Evans, H. M.; Ahmad, A.; Ewert, K.; Pfohl, T.; Martin-Herranz, A.; Bruinsma, R. F.; Safinya, C. R. Structural Polymorphism of DNA−Dendrimer Complexes. Phys. Rev. Lett. 2003, 91, 75501−75504.

45. Golan, R.; Pietrasanta, L. I.; Hsieh, W.; Hansma, H. G. DNA Toroids: Stages in Condensation. Biochemistry 1999, 38, 14069−14076.

CHAPTER 5

ROLE OF UNMODIFIED LOW GENERATION PAMAM DENDRIMERS IN EFFICIENT NON-TOXIC GENE TRANSFECTION

5.1 Introduction

A new paradigm in medicine called gene therapy involves altering of genes entailed in disease by delivering therapeutic gene (nucleic acid based drugs). Delivering such therapeutic gene to the specific target site is an irresistible challenge to drug delivery scientists. However, the polyanionic nature of DNA limits the cellular membrane interactions. Hence, successful therapeutic DNA based gene delivery highly relies on the efficient extracellular and intracellular delivery of DNA molecules for empowering target interaction.[1—5] Non-viral vectors are being used in improving potential therapeutic effect of DNA because they are safe and non-immunogenic as compared to viral vectors. Even though lower transfection efficiency of non-viral vectors are proven compared to viral-mediated gene transfection, the observed shortcomings could be overcome by appropriate structural designing of carriers like cationic polymers or lipids. For example, non-viral vectors can easily be targeted to a target tissue or cell by coupling of cell- or tissue-specific targeting moieties on the carrier. Additionally, by controlling the size of DNA-cationic vector complex the bio-distribution, cellular internalization and intracellular trafficking of the micro- or nanoparticle can be influenced. Most importantly, the success of the non-viral gene therapy is dependent on the various extra- and intracellular barriers that affect the efficiency of all gene delivery systems, including cellular uptake, endosomal escape, nuclear uptake and gene expression.[6--8] Poly cationic vector such as poly (amidoamine) (PAMAM) dendrimer is one of the versatile non-viral based gene delivery systems for efficient targeted delivery of DNA amongst numerous other cationic vectors.[9--11] In particular, PAMAM dendrimer is shown as a potential vehicle

especially through several routes of administration, including oral, ocular, parenteral and transdermal.[9,12,13] The uniqueness of these dendrimers are that they are monodisperse, hyper branched and of controlled size and molecular weight, possessing number of terminal groups with the increasing generation number.[14] More interestingly, PAMAM-DNA complexes have been found to be highly soluble and stable in almost all the physiological conditions and also observed to be resistant to nuclease digestion by Bielinska *et al.*[15] These distinctive characteristics of PAMAM dendrimer coupled with their architecture has attracted attention of several research groups and their applications in biology and medicine have been explored.[9,16--18]Additionally, various research groups also commenced to determine dendrimer toxicity and immunogenicity and reported that cytotoxicity increases with increase in generation number i.e. smaller the generation of PAMAM dendrimer less the chances of cytotoxicity.[19, 20] In spite of high cost and high cytotoxicity, there exist enormous successful targeted transfection reports using unmodified and modified dendrimers of higher generations.[10, 20--22] It is pertinent to mention that even though PAMAM dendrimer-based gene transfection reagents such as Superfect and Priofect are already commercially available, these products are based on toxic high generation dendrimers and also not cost effective.[23]

In spite of numerous attempts made for efficient gene transfection using surface engineered lower generation dendrimers,[24-26] there are also a few remarkable recent highlights on the possibility of using unmodified lower generation dendrimer in skin penetration[27] as well as in the rapidly growing area of dendrimer mediated RNAi therapeutics.[28] Therefore, there is a necessity to focus on the systematic control of the physicochemical properties of less toxic and cost effective low-generation dendrimers for successful gene transfection. A careful review on literature reveals that only a few researchers used unmodified lower generation PAMAM dendrimer for gene transfection. One decade ago, Braun *et al.*[29] beautifully demonstrated a structure-function relationship between the biophysical properties of dendrimer/pDNA complexes (Plasmid DNA pMB 290(4.9 kbp)) of various generation and the corresponding *invitro* transfection efficiencies into CHO-K1 cells.

Based on the experiments it was observed that G4 at 1--10 charge ratio and G7 at 2--10 charge ratios showed remarkable biological activity among dendrimers of generation G2, G4, G7 and G9. It is noteworthy that Haensler and Szoka[30] investigated transfection of a series of PAMAM dendrimer generation from G1 to G10 into CV1 cells and reported that charge ratio and diameter of the dendrimer are the key factors for the transfection. More interestingly, Tajarobi[31] observed highest *in-vitro* transfection of PAMAM dendrimer generation G4 across Madin Darby Canine Kidney cells followed by G1 or G0, G3, G2. It is also noteworthy that low generation, G2 and G3, poly(propylenimine) dendrimers have been evaluated successfully for the potential cellular delivery of antisense oligonucleotides (ODNs) targeting the epidermal growth factor receptor (EGFR) in A431 epidermoid carcinoma cells.[32] Based on various interesting review articles on dendrimers in gene transfection[10, 12, 21] it has been seen that there is a lack of systematic analysis on gene transfection studies with the unmodified PAMAM dendrimer especially from the generation G1 to G3. Very recently, the representative low generation PAMAM dendrimers (G1, G2 and G3) were investigated systematically by us for short oligonucleotide packing in dendriplex mediated gene delivery by projecting a direct insight on the 14mer oligonucleotide and dendrimer interactions using fluorescence and FRET techniques.[33]

It is very important to highlight here that a systematic study on skin penetration of cationic PAMAM dendrimers (G1 to G6) using iontophoresis was shown as inversely related to the dendrimer molecular weight by Perumal.[34] Hong and co-workers[35] showed smaller dendrimers penetrate the skin better than larger ones, that is, the skin permeation and penetration depth of G2 are superior to those of G4. Further recent review on dendrimer -mediated drug delivery to the skin confirms the successful possibility of lower dendrimers to deliver therapeutic genes for treating genetic abnormalities, infections and skin cancer. The observed success in therapeutic delivery through the skin is evidenced mainly due to its larger size, easy accessibility and extensive characterization both at cellular and molecular levels.[36] Most importantly, the skin was shown to contain less nucleases compared to other

routes of delivery.[37] Apart from these, such transdermal treatments provide various other benefits over the conventional methods, including reduced side effects, non-invasiveness, improved patient compliance, bypassing first-pass metabolism, imparting prolonged drug delivery properties and most importantly if needed, the treatment could be easily withdrawn immediately.[38] It is pertinent to mention that several researchers used modified PAMAM dendrimers and successfully transfected therapeutic gene *in-vitro*. However, the efficiency of these modified/synthesized dendrimers was low and nonspecific in *in-vivo.*[39, 40, 41]

To the best of our knowledge, the unmodified lower generation PAMAM dendrimer carriers have not been used to transfect pDNA into HaCaT cells which is known for its difficulty for pDNA transfection due to its slow growth rate. Additionally, based on a careful review on literature, it has also been noticed that there is a lack of systematic analysis on *in-vitro* gene transfection studies with the unmodified PAMAM dendrimer especially from the generation G1 to G3. These polymers are non-toxic, serum stable, efficient in cellular uptake, condense and release DNA easily, easy to modify as compared to the higher generation dendrimers.[18] Therefore, our study can have immense importance and can add to the literature as evidence for application of low generation dendrimers. Considering together lower cytotoxicity and skin penetrability of lower generation PAMAM dendrimers, we have explored pDNA condensation using PAMAM dendrimers of first three generations G1, G2 and G3 by agarose gel as well as ethidium bromide (EtBr) condensation assays and subsequent DNA release is observed by EtBr release assay. Further, in order to understand dendrimer binding on DNA, stopped-flow fluorescence experiments are performed. *In vitro* DNA uptake and endosomal escape are demonstrated in CHO-K1 cells using flow cytometry and confocal microscopy. Additionally, transfection efficiency of pDNA into the nucleus is also observed by luciferase assay in CHO-K1 cells in the presence as well as in the absence of endosomotropic agents like bafilomycin A1 and chloroquine. Cytotoxicity of these lower generation dendrimers is determined by MTT assay in CHO-K1 cells. Further, these observations are extended in human skin cell line, HaCaT as an application for gene delivery to check

whether the low generation PAMAM dendrimers can deliver DNA into the human skin cells and the corresponding cytotoxicity is also tested. In addition to these, in order to explore the possibility of usage of the lower generation based dendriplexes in future for *in-vivo* gene therapeutic studies, serum stability assays are carried out by exposing the dendriplexes to different concentrations of fetal bovine serum.

5.2 Materials and methods

5.2.1 Materials

Starburst PAMAM dendrimer of generation one, two and three (G1, G2 and G3) of highest purity (> 99 %) (Figure 5.1) were purchased from Sigma-Aldrich. The plasmids pEGFP-C1, 4.7 kb (Clonetech) and pMIR-REPORT™Luciferase, 6.47 kb (Ambion) were amplified in E.coli DH5-α and purified using GenElute HP Endotoxin-Free Plasmid MaxiPrep Kit (Sigma). Luciferase assay and Cell Titre GLO kit was purchased from Promega. Label IT® Tracker Fluorescein Kit for labeling pDNA was purchased from Mirus Bio Corporation. All other chemicals and cell culture media were procured from Sigma unless stated otherwise. All the other reagents used were of AR grade purity. Milli-Q water was used for all the experiments.

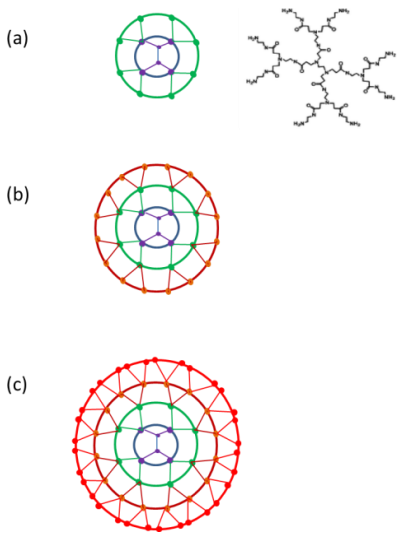

Figure 5.1 Chemical structure of poly (amidoamine) (PAMAM) dendrimer of Generation 1 (G1) and Schematic representation of first three PAMAM dendrimer generations (a) G1, (b) G2 and (c) G3. Color Code: Purple: Core; Green: Generation 1; Brown: Generation 2; Red: Generation 3.[33]

5.2.2 Preparation on PAMAM dendrimer – DNA complex (dendriplex)

Dendriplexes were prepared depending on the calculation of electrostatic charge present on each constituent i.e. at different charge ratios ($Z_{\pm}$) expressed as the ratio (N/P) of the concentration of cationic charge of the dendrimer (N) to that of the DNA phosphate groups (P). Stock solutions of the PAMAM dendrimers of 1, 2 and 3 generations were prepared by dissolving the required amount of dendrimer of the desired generation in a known volume of milli-Q water and the corresponding concentrations were determined gravimetrically and stored at 4 $^{\circ}$C until required. Final concentration of plasmid DNA used was 20–50 ng/µL and added drop-wise to an equal volume of the appropriate dendrimer dilution while continuous vortexing. Before performing every experiment the dendriplexes were incubated for 30 min at room temperature to ensure complex formation.

5.2.3 DNA condensation assays

5.2.3 (a) Gel condensation assay-The electrophoretic mobilities of the PAMAM dendrimer-pDNA complexes of generation 1, 2 and 3 at various charge ratios ($Z_{\pm}$) were determined using agarose gel electrophoresis. Gel electrophoresis experiments were carried out in a buffer solution consisting of 1× TAE buffer (pH 7.4) for 30 min at 100 V. In these studies, in order to prepare the dendriplex of the required charge ratio, 20 µl of the dendriplex having 200 ng total DNA was loaded in each well onto 1 % agarose gel containing ethidium bromide.

5.2.3 (b) Ethidium bromide (EtBr) condensation assay- pDNA condensation was also measured from the inhibition of DNA-intercalated EtBr fluorescence signal in the presence of respective generation of PAMAM dendrimer. The assay was carried out in black 96-well format plates (Nunc) where 4.22 µL EtBr (10 ng/µL) and 20µL DNA (20 ng/µL) i.e., one EtBr molecule per 6 base pairs of DNA, was dispensed in each well and incubated in dark for 5 min at room temperature. 20 µL of dendrimer solution at increasing charge ratio was then added and the plate incubated for another 10 min in dark. The fluorescence was recorded at the emission wavelength of 595 nm upon excitation at 535 nm using microplate reader (Infinite 200 Pro, Tecan

Inc., Maennedorf, Switzerland). The fluorescence of DNA with EtBr was taken as the maximum, i.e. 100 % and the relative percentage decrease in fluorescence signal was calculated at increasing charge ratio and plotted as percentage of maximum.

5.2.3 (c) Kinetic studies of dendriplex formation by using Stopped flow fluorescence spectroscopy-The kinetic measurements were performed using a SFA-20 rapid kinetics accessory (HI-Tech Scientific) in JobinYvonFluorolog with a Peltier thermostat. The concentration of both pDNA and ethidium bromide in the pDNA−EtBr complex solution was 20 ng/µL, and two different (the charge ratios were chosen from agarose gel electrophoresis and EtBr assays at which most efficient condensation observed) concentrations of the dendrimer solutions were used for the stopped-flow kinetic study to obtain the charge ratio of the resultant solutions as $Z_{+/-}$ = 5 and 10 respectively, upon mixing of equal volume of two solutions. The excitation and emission monochromator were set to 480 and 590 nm, respectively. During the experiment, two separate syringes of the stopped-flow were filled up with pDNA−EtBr complex and dendrimer solutions, and in each run, an equal volume of both solutions was injected at once into the sample chamber. The emission spectra were monitored continuously both before (t = 0 s) and after the injection. The dead time of the instrument was determined from the test reaction described elsewhere[42] and was found to be 20 ms for a 1:1 mixing. All the experiments were carried out using 10 mM sodium phosphate buffer.

5.2.4 DNA release/ Stability of dendrimer-pDNA complex

The stability of the dendriplexes against the anionic molecules was studied by checking the amount of DNA released with EtBr molecules. In a 96 well black plates (Nunc), the increasing amounts of heparin (0.1 to 50 heparin : 1 dendrimer) (wt/wt) was added followed by addition of the 20 µL of dendriplex and 10 µL EtBr (4.22 ng/µL) and incubated at room temperature in the dark for 15 min. The fluorescence of DNA with EtBr was taken as 100 % and the relative percentage increase in fluorescence signal was calculated at increasing concentration of heparin using microplate reader (Infinite 200 Pro, Tecan Inc., Maennedorf, Switzerland).

5.2.5 Determination of particle size, zeta potential by DLS

Size of the particle and zeta potential of dendriplexes prepared at different charge ratios at 50 ng/µL of DNA concentration in deionized water were measured by Zetasizer Nano ZS (Malvern Instruments, UK) at a fixed angle of 173° at 25 °C. Minimum of 3 readings were recorded for each sample with replicates.

5.2.6 Morphology of the dendriplexes by AFM

The morphologies of the different dendriplexes were analyzed using Atomic Force Microscopy (AFM). The dendriplexes were prepared at two different charge ratios (5 and 10) and incubated for 30 min. The dendriplex (4 µL) was loaded between two freshly cleaved pieces of mica to ensure even spreading of solution on mica surface, kept for 2 min and dried in air. Imaging was carried out with 5500 Scanning Probe Microscope (Agilent Technologies, Inc., AZ) using AAC mode in air with 225 µm long silicon cantilevers (Agilent Technologies, Inc.) with resonance frequency of around 75 kHz and force constant of 2.8 N/m. Scan speed used was 1 line/s. Image analysis was performed using Pico Image software.

5.2.7 (a) Transfection efficiency measurement using luciferase assay

Chinese hamster ovary cells (CHO-K1) and HaCaT cells (Adult human keratinocytes maintained in Ham's F-12K media supplemented with 10 % (v/v) Fetal bovine serum (Life Technologies, USA) and DMEM-F12 respectively at 37 °C and 5 % CO2 in humidified incubator. Cells were seeded 24 h before transfection in 24-well plates. Dendriplexes were prepared with final pDNA concentration of 20 ng/µL (pMIR-Report™Luciferase) and incubated for 30 min at room temperature. 100 µL of dendriplex (2 µg DNA/well) was added to cells (approx. 70% confluency) in serum free media (OptiMEM, Invitrogen). To study the effect of bafilomycin A1 and chloroquine, cells were pretreated with either at a final concentration of 100 nM and 100 µM for 15 min in 300 µL opti-MEM respectively. After 5 h of incubation at 37 °C, the media was removed; cells were washed with phosphate buffered saline (PBS, pH 7.4) and appended with 500 µL complete growth medium. After 24 h or 48 h, cells

were washed with PBS and lysed with 100 µL of cell culture lysis buffer (1× CCLR, Promega). 50 µL of cell lysate supernatant was evaluated for luciferase expression using the luciferase assay substrate (Promega) as a function of light emission by integration over 10 s in Orion microplate luminometer (Berthold Detection System, Germany). Luciferase activity was normalized with total protein content of the cells calculated using BCA protein assay (Pierce). Transfection in presence of serum was also carried out in growth medium containing various percentages of serum (10 %, 25 % and 50 %) as per the above procedure. Transfection efficiency is expressed as mean value ± SD and all experiments were performed thrice with duplicates.

5.2.7 (b) Transfection efficiency of pEGFP-C1 with dendrimer based complexes

HaCaT cells were seeded at density of 58,000 cells/well in a 24 well plate. After 24h, when 70% confluency was attained, complete media was replaced by 300µl OPTI-MEM. Following this, 100µl of complexes prepared using G1, G2 or G3 dendrimer and EGFP-C1 plasmid DNA (20ng/µl) at charge ratio 5, 10 and 20 respectively were added to each well (2µg plasmid DNA per well). After 4h of incubation at 37°C, the incomplete media was replaced by complete media DMEM-F12 and cells were kept for further incubation at 37°C and 5% CO_2. After 24 h of treatment, cells were washed with 500µl of ice cold 1X phosphate buffered saline (PBS) followed by trypsinization (100µlof0.25%trypsin) and centrifugation at 2500 rpm for 5 minutes at 4°C. The pellet was resuspended in 500µl of ice cold 1X phosphate buffered saline (PBS) and again centrifuged at 2500rpm for 5 minutes. The cellular pellet obtained was suspended in 200µl of 1X PBS and kept in ice. Flow cytometry measurements were performed using BD Accuri flow cytometer (Becton Dickinson). Lipofectamine 2000^{TM} was taken as positive control for the study. Data was plotted as percentage EGFP positive cells and values were represented as Mean ± S.D.

5.2.8 Cellular uptake studies

***5.2.8 (a) Flow cytometry assay*.** Cellular uptake was studied by FITC labelled pEGFPC1 plasmid (labelled using Mirus, Label IT Tracker Fluorescein Kit at a ratio of

0.75:1 according to the manufacturer's protocol). Dendriplexes were prepared using this labeled pDNA at different charge ratios. After attaining 70 % confluency of CHO-K1 cells in the 24 well plate, cells were treated with labeled dendriplexes for 4 h and incubated at 37 °C in the provided Opti-MEM (Invitrogen) media. After 4 h incubation, the media containing dendriplexes was aspirated and cells were washed twice with PBS supplemented with heparin (1 mg/mL) followed by 0.4 % trypan blue in PBS wash and PBS alone. The cells were then collected by trypsinization (0.25 % trypsin) and washed with ice cold PBS. Finally, the cells are resuspended in PBS having 1 % BSA and then analyzed by using flow cytometer BD Accuri^{TM} C6. The FITC labeled dendriplexes were excited using 488 nm laser and detected with 530/30 nm (FL1) band pass filter. Experiments were performed in triplicates and total 10,000 events were acquired in each case.

5.2.8 (b) Confocal microscopy. CHO-K1 cells were seeded at a density of 1.2×10^5 in 35 mm μ-dishes (ibidi, Germany) and incubated for 24 h. FITC labeled dendriplexes of G2 and G3 were prepared at $Z_{+/-}$ of 10 and 5 added to the cells (2 μg pDNA per dish) in 500 μL Opti-MEM respectively. After 3.5 h, Hoechst 33342 (Invitrogen) was added at a final concentration of 330 ng/μL and incubated for another 30 min, the media was removed and cells were washed at least 3 times with 1× PBS followed by 1x PBS containing 1 mg/mL heparin (to remove extracellular bound dendriplexes from the cells). Imaging was done using a Nikon TiE motorized inverted fluorescence microscope equipped with a 60X, 1.4 N.A. plan apochromat oil immersion objective using a Plan-Apochromat 63 × 1.4 N.A. lens and the 405, 488 and 543 nm laser lines.

5.2.9 Cell viability assay

The percentage of viable cells was determined by MTT (Promega) assay according to manufacturer's protocol. The quantification of dendrimer-mediated toxicity was done using MTT assay after incubating the CHO-K1 cells in the presence of varying concentrations of dendrimer for 4 to 24 h. Briefly, CHO-K1 cells were seeded 1 day before treatment into 96-well plate. Cells were treated with a 20 μL of dendriplexes at charge ratio at which transfection was carried out for each generation of PAMAM

dendrimer in serum-free media for 4 h and then cell viability was evaluated at 4 h. For an assay at 24 h, the dendriplexes were incubated for 5 h; the media was replaced with 100 µL complete growth medium. Thereafter, cell viability was evaluated after the 24 h according to the manufacturer's protocol. The data is represented as formazan absorbance at 540 nm, untreated cells were considered as 100 % viable in cell viability assay. Further, cell viability was also confirmed independently by cell titer assay. For this assay, cells were seeded in a 96 well plate at a density of 5000 cells per well for both HaCaT and CHO-K1 in independent experimental set ups. After 24 h when cells attained 70-80 % confluency, complete media in each well was replaced with 80 µL of Opti-MEM (Invitrogen). Following this 20 µL of dendriplexes (with final plasmid DNA concentration of 200 ng/well) was added to the cells. Cell viability was analyzed after 4 h and 24 h of incubation at 37 °C (in the latter case media was replaced with complete media after 4 h) using Cell Titre GLO method (Promega) according to manufacturer's protocol for both CHO-K1 and HaCaT cell lines. In the case of HaCaT cell line the time points were extended to 72 h and 96 h. Measurements were recorded using microplate reader (Infinite 200 Pro Tecan) and plotted as percentage cell viability. Untreated wells were taken as 100 % viable cells. All experiments were conducted in triplicate and averaged.

5.2.10 Serum stability assay

In vivo pDNA protection ability of the dendrimer was examined by exposing the dendriplexes to different concentrations of fetal bovine serum (Invitrogen). 40 µL of dendriplexes containing 800 ng of DNA (final concentration) were prepared at the charge ratio at which transfections are performed for each of the generation ($Z_{+/-}$ = 5 for G3 and 10 for G2) and incubated with different serum concentrations (10 %, 25 % and 50 %) for 2 h at 37 °C. To inactivate the nucleases and other serum components, the samples were incubated at 75 °C for 15 min. The samples were subsequently subject to heparin release (20:1 wt of heparin: wt of dendrimer) to completely release pDNA from the dendriplex. The integrity of the released DNA was analyzed by running the samples in 1 % agarose gel at 120 V in 1X TAE buffer for 50 min.

5.3. Results and discussion

As we know, one of the key factors for poor efficiency of DNA transfection to the target cells is premature cargo release in the blood stream when administered *in-vivo*. Such early release of DNA from the DNA-cationic complexes is known to be responsible for rapid degradation of the nucleic acid by serum nuclease.[43] In order to overcome this crucial difficulty of premature DNA release, it becomes essential to balance physicochemical interactions between the nucleic acid and the cationic vector. The *in-vitro* and *in-vivo* gene transfection efficiency can then be correlated to the size and charge of the complex, which can be controlled by the suitable architecture and concentration of the cationic vehicle.[44] Hence to bring out the required preliminary understandings in pDNA-PAMAM dendrimer (G1, G2 and G3) interactions for the corresponding gene transfection studies the following pDNA condensation and release assays were carried out.

5.3.1 DNA condensation

The efficiency of pDNA condensation with PAMAM dendrimers can be demonstrated by EtBr assay and also by agarose gel electrophoresis. In EtBr assay, EtBr a well-known fluorescent probe intercalates the DNA molecule. Such intercalation of the fluorescent dye into free DNA increases its fluorescence quantum yield to 10 fold greater as compared to its free state. Due to dendrimer-pDNA complex (dendriplex) formation, there is exclusion of intercalated EtBr from the DNA molecules and consequently fluorescence intensity decreases. The observed reduction in the EtBr fluorescence intensity is directly correlated to pDNA condensation which also draws information to understand the competition between the EtBr and the co-solutes. Figure 5.2a shows EtBr intercalation assay for pDNA condensation using PAMAM dendrimer of first three generations (G1, G2 and G3). From the figure it is evident that in general fluorescence intensity of intercalated EtBr decreases drastically (from 100 %) with increase in the dendrimer to pDNA charge ratio. In the presence of G1, a drastic decrease in fluorescence intensity from 100 % to 24.2 % was observed from the charge ratio ($Z_{\pm}$) 0 to 0.5 and thereafter attained plateau till $Z_{\pm}$=3. After $Z_{\pm}$ =3, a

slight increase in the fluorescence intensity was seen in the case of G1 with increase in the charge ratio. Interestingly, in the presence of G2, the fluorescence intensity of EtBr showed a reduction in the intensity from 100 % to 15.9 % from $Z_{\pm}$= 0 to 0.5 respectively and remained more or less constant till the charge ratio of 10. Thereafter, only a negligible fluorescence increase is observed from the charge ratio 10 to 20. Similarly for G3, the lowest fluorescence intensity 21.1 % was observed at $Z_{\pm}$ =1 and remained more or less same as observed in the case of G2. The lowest fluorescence intensity observed at the $Z_{\pm}$= 0.5 to 3 for G1, 0.5 to 10 for G2 and 1 to 10 for G3 revealed electrostatic interaction of pDNA by the dendrimer of respective generation at those charge ratios. In comparison, more or less similar displacement of EtBr by all the three dendrimers from the charge ratio $Z_{\pm}$= 1 to 3 indicates the corresponding dendrimer binding affinity to the DNA molecules is almost same. Beyond charge ratio 3 to 10, the dendrimers of generation G2 and G3 show greater affinity with the DNA compared to G1 whereas, at higher charge ratios after $Z_{\pm}$= 10, the third generation dendrimer shows greatest affinity to complex with the DNA molecule among G2 and G1. The observed slight increase in fluorescence intensity of EtBr above $Z_{\pm}$ =3 compared to G2 and G3 could be explained as follows: In general, the accessibility of DNA to EtBr decreases with increasing dendrimer concentration until neutralization is reached mainly due to a decrease in the number of binding sites per nucleotide for EtBr binding with increasing amount of dendrimers. This observation further indicates that dendrimer binding on DNA is sufficiently strong that dendrimers cannot be displaced by added EtBr. At neutralization point, the dendriplex consists of “tightly bound DNA” regions and “linker DNA” regions, where the “linker DNA” regions are open for EtBr binding [(45)]. Obviously, as size of dendrimer molecules increases with the dendrimer generation, availability of linker DNA regions for EtBr binding decreases. Above neutralization point, the increase in dendrimer concentration causes an addition of new dendrimer molecules into the neutralized dendriplexes followed by a DNA induced self-assembly to form micellar aggregates.[(33)] Here again, tightly bound as well as linker DNA regions are expected and their availability varies with the size of the micellar aggregates. The observed

increase in the fluorescence for dendriplexes of G1 when $Z_{\pm}$ 3 could be correlated to the increase of linker DNA regions for EtBr binding due to the aggregation of dendrimer molecules in the vicinity of DNA above the neutralization point. These observations indicate that, the dendriplex formation by dendrimers of first three generations is not only depending on the generation but also on the dendrimer to DNA charge ratio ($Z_{\pm}$) and is in good agreement with previous findings.[29,33,45]

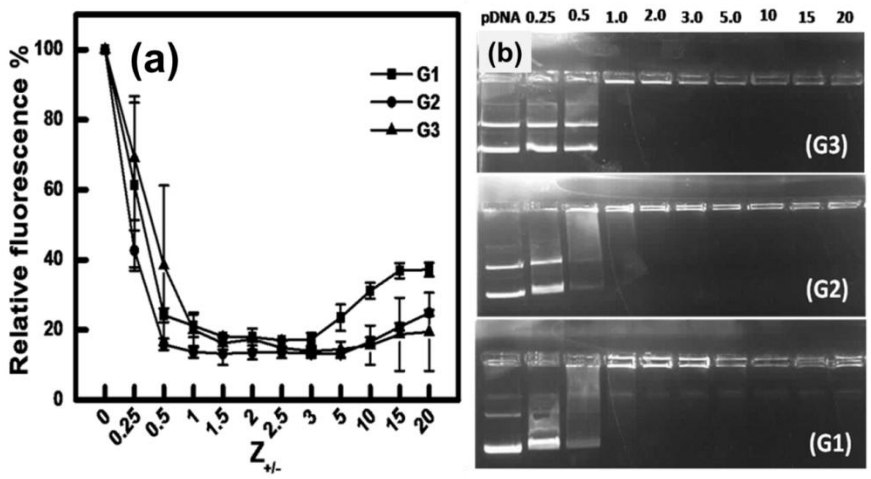

Figure 5.2 (a) EtBr intercalation assay for pDNA condensation. DNA condensation was measured by a decrease in the fluorescence upon increasing $Z_{\pm}$ for first three generations. The fluorescence of free uncomplexed DNA with EtBr was set as maximum i.e. 100%. (b) Agarose gel condensation images. 1% agarose gel containing ethidium bromide (one EtBr molecule per 6 base pairs of DNA), was run with dendriplexes of G1, G2 and G3at various dendrimer to pDNA charge ratios ($Z_{\pm}$) (as mentioned on the corresponding lanes). The gel was run in buffer consisting of 1X TAE at pH 7.4, at 120 V for 30 min.

5.3.2 Gel condensation assay

DNA condensation by the cationic vector can be visualized through gel condensation assay. The electrostatic binding interaction between the cationic vector and the negatively charged DNA results in partial or complete condensation of the corresponding nucleic acid. The observed condensation of DNA in the presence of the cationic ligand decreases the relative mobility of the nucleic acid as observed through agarose gel electrophoresis. Hence, the extent of DNA migration determines the DNA condensation by the ligand. Gel condensation studies were carried out on pDNA before and after the interaction of PAMAM dendrimers G1, G2 and G3 (Figure

5.2b).The first lane in each case corresponds to the migration of free pDNA, whereas subsequent wells of the gel represent the migration of pDNA-dendrimer complexes at increasing PAMAM dendrimer to the pDNA charge ratio (from $Z_{\pm}$= 0.25 to $Z_{\pm}$ = 20). From the figure it is evident that for dendrimer of generation 1 (G1), the migration of free DNA was visualized up to the charge ratio 0.5 and thereafter DNA mobility was partially retarded in the wells indicating the condensation of DNA by the dendrimer from the $Z_{\pm}$= 1. It is also noteworthy that smearing and reduction in the intensity of bands corresponding to the pDNA-G1 complex at charge ratio 0.25 and 0.5 was observed compared to free pDNA ($Z_{\pm}$ = 0) suggesting the existence of DNA in both partially as well as completely neutralized state. It is to be noted that in the presence of G1, slight visibility of pDNA band continues even in the range of the charge ratio 0.5 to $Z_{\pm}$=20 indicating incomplete condensation of DNA by G1. More or less similar condensation behavior of DNA was observed for G2 upto the DNA to dendrimer charge ratio ($Z_{\pm}$) =1 and thereafter interestingly pDNA migration through the agarose gel is completely retarded and perturbation of DNA-G2 complex is visualized in the corresponding wells of the gel. Interestingly, in the presence of G3, the complete condensation of pDNA by the dendrimer was observed from the charge ratio ($Z_{\pm}$) =1, whereas, the intensity of pDNA bands appear to be the same for the charge ratios 0.25 and 0.50 in comparison with the free pDNA. The observed disappearance of the DNA band above the charge ratio ($Z_{\pm}$) = 0.5 for G2 and G3 is suggestive of effective neutralization of the DNA with dendrimer of generation two (G2) and three (G3) compared to G1 due to increase in the positive surface charge density of the PAMAM dendrimer with increase in generation. Further, in the presence of G2 and G3, prominently visible retarded DNA at the wells indicates the accessibility of the stain inside the dendriplex, which may also reveal inability of the pDNA to undergo very tight compaction. This interesting observation of Figure 5.2b suggests for the existence of highly cooperative interactions between the pDNA as well as the corresponding dendrimer and the results are in good agreement with EtBr assay (Figure 5.2a). Further, the observed migration behavior of pDNA through agarose gel in the presence of PAMAM dendrimer is also in line with our recent studies on the 14mer mobility in 15 % native PAGE before and after interaction with PAMAM dendrimer of three generations G1, G2 and G3.[33]

5.3.3 Binding kinetics of DNA-dendrimer

Even though, the condensation of pDNA by the dendrimers of first three generations are demonstrated successfully by EtBr as well as gel condensation assays (Figure 2 (a) and (b)), investigation on pDNA-dendrimer binding kinetics is also equally essential to understand the pDNA compaction mechanism.[42,46-48] Herein, the essentiality of the binding kinetics arises mainly due to our aim in releasing the therapeutic pDNA from the lower generation based dendriplex (G1, G2 and G3) into the cytoplasm of the target cell. It is also noteworthy that these lower generation dendrimers are observed for poor transfection in comparison with dendrimers of higher generation by various researchers in last decade.[10,20-22,29] On the other hand, the success of these lower generation dendrimers is being realized in the current era.[24,27,28] Here again, most classic works where computational/experimental techniques have been used to focus on higher generation dendrimers. Even though, few recent publications focus on lower generation dendrimers, the existing literature have mostly used huge CT-DNA [47] molecules and the corresponding rate constants cannot be correlated with our present work where we have used much smaller plasmid DNA. Hence, it becomes important to draw DNA-dendrimer binding information from the stop-flow kinetics, which is known for understanding fast reactions, where rapid mixing of reactant solutions is necessary.[49] The resulting information on dendrimer-DNA interaction pathways plays an extremely vital role in gene transfection, involving the cargo release kinetics from the vector at the target site.[50] Figure3 shows kinetic plots of EtBr fluorescence intensity decay observed upon PAMAM dendrimer of generation G1, G2 and G3 binding to pDNA at $Z_{\pm}$ 5 as well as 10, in the presence of 10 mM sodium phosphate buffer. Here, the analysis of the kinetic data were carried out as per previous report [46] by assuming the resulting fluorescence decay curve is a superposition of exponentials terms, according to

$$I(t) = \sum_{i=1}^{i} A_i \exp(-t/\tau_i) \qquad \textbf{(5.1)}$$

Where I is the fluorescence at time t, A_i is the prefactors, and τ_i is the pseudo-first-order time constant. The reciprocal of time constant is the relative rate constant of the reaction (k_i). The Nelder–Mead simplex method for minimizing eq 5.1 was

applied. The quality of the fit was assessed from the R^2 value. The number of exponentials was increased until no systematic deviation of the residual was found (data not shown). It was found that three exponential functions (i=3) were sufficient to describe the fluorescence decay kinetics of EtBr upon dendrimer binding to pDNA (data not shown). Based on these observations, the following interaction mechanisms are proposed for dendrimer-pDNA interaction.

$$^{+}\mathbf{D} + \mathbf{pDNA} - \mathbf{EtBr} \rightleftharpoons \mathbf{pDNA} - \mathbf{D} + \mathbf{EtBr} \qquad \textbf{(5.2)}$$

The above EtBr displacement interactions of dendrimer with pDNA can be divided into four steps as follows:

$$\mathbf{pDNA} - \mathbf{EtBr} \rightleftharpoons \mathbf{pDNA} + \mathbf{EtBr} \qquad \textbf{(5.3)}$$

$$\mathbf{pDNA + D^{+} \rightleftharpoons pDNA\text{-}D\ (rc)} \qquad \textbf{(5.4)}$$

$$\mathbf{pDNA\text{-}D(rc) \rightleftharpoons pDNA - D\ (cs) \rightleftharpoons pDNA\text{-}D(ra)} \qquad \textbf{(5.5)}$$

Where 'rc' stands for random coil, 'cs' and 'ra' refer to compacted state and further rearrangement of the complex, respectively. The fluorescence decay curves were fitted to eq 5.1 and also plotted against charge ratios, as shown in Figure 5.3. For each generation of dendrimer three relative rate constants k_1, k_2 and k_3 (the reciprocal of the time constants, τ_1, τ_2 and τ_3 respectively) are found at two different charge ratios ($Z_{\pm}$) 5 and 10 (Table V). The relative rate constants k_1, k_2 and k_3 correspond to the binding process of the dendrimer to pDNA to form random pDNA coils followed by DNA compaction and further rearrangement respectively. In general, the reported EtBr displacement mechanism from pDNA by the dendrimer is very similar to earlier studies [47, 48] and the value of relative rate constants are found to vary with dendrimer to pDNA charge ratio as well as the dendrimer generation. Each rate constant shown in Table V is an average of three independent kinetic experiments. From Table V, it is evident that for dendrimers of three generations under study, all the three relative rate constants are well separated mostly, by at least an order of magnitude, and, in general, increases with increasing charge ratio for G2 and G3. Based on the previous report,[42, 47] the first step (eq. (5.4)) is due to

the electrostatic binding of the dendrimer on the pDNA molecule, which is a diffusion-driven process and also faster with increase in the amount of dendrimer concentration.

Interestingly, the first rate constant k_1 is observed to be very different for the first three dendrimer generations under study indicating occurrence of association and aggregations of the dendrimer molecules in the vicinity of DNA initially. It is to be pointed out that only simple diffusion followed by binding of individual dendrimer on the DNA molecule would not lead to such large differences in the relative rate constant of the different generations. In the case of second rate constant (k_2) for G2 and G3 a striking decrease is observed with increase in the dendrimer to DNA charge ratio by clearly indicating a delay in the condensation of pDNA due to the possible slower internal rearrangement of the dendrimer molecules at $Z_{\pm}$=10 compared to $Z_{\pm}$=5 during DNA condensation. In contrast to k_1 and k_2 values of G2 and G3, k_3 does not show any specific trend due to the irregularity in further rearrangement of the compacted dendriplex. On the other hand, very closely placed rate constants of G1 (k_1, k_2 *and* k_3) are observed for the charge ratios under study clearly showing the weakest interaction of G1 with pDNA molecules.

Table V. Relative Rate Constants for the First Three PAMAM Dendrimer Generations Binding to pDNA as a Function of the Charge Ratio ($Z_{\pm}$) at a Fixed Concentration of pDNA and Temperature.

PAMAM Dendrimer	$Z_{\pm}$	k_1 (s^{-1})	k_2 (s^{-1})	k_3 (s^{-1})
G3	5	5.00E-02	1.78E-04	2.09E-01
	10	9.89E-02	9.90E-02	5.03E-01
G2	5	5.93E+00	3.34E-01	1.37E-02
	10	9.53E+01	7.95E-02	1.21E-02
G1	5	1.42E-01	9.56E+01	2.61E-01
	10	2.76E-01	2.57E-01	1.87E+01

The observed insignificancy of G1 rate constants is probably due to the consequence of its smaller size leading to larger surface area and therefore results a lower charge density that enabled the formation of well-structured dendriplexes.[50-52] The above described dendrimer-pDNA binding kinetic pathways is in good agreement with the earlier findings on CT-DNA binding with amino acid based surfactants[42] as well as PAMAM dendrimer (G1, G2, G3 and G4)[47] and further supports the findings on EtBr and gel condensation assays (Figure 5.2).

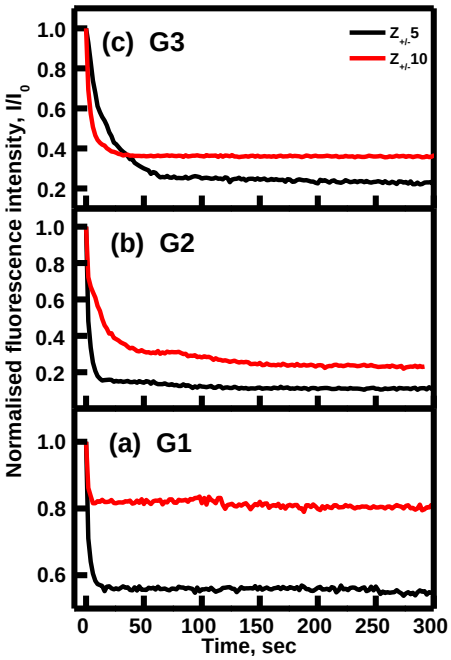

Figure 5.3 Stopped-flow data corresponding to the fluorescence intensity decay of ethidium bromide observed upon PAMAM dendrimer of the first three generations binding to pDNA at $Z_{\pm}$= 5 (black line) and 10 (red line), as a function of time. The pDNA concentration was 20 µM in 10 mM sodium phosphate buffer (pH 7.0).

5.3.4 DNA release assays

In this study, pDNA release from the corresponding dendriplex is tested in the presence of heparin-an anionic challenger. Observations on DNA release with anionic challenger are essential to understand the stability of DNA-cationic vector complex in the presence of intracellular and extracellular anionic agents during *in-vivo* delivery. Herein, the ability of the dendriplex to release DNA was investigated by EtBr inclusion assays in the presence of increasing concentrations of heparin at a

fixed dendrimer to DNA charge ratio ($Z_{\pm}$) 10. Figure 5.4 shows EtBr inclusion assay in the presence of increasing heparin to dendrimer wt/wt ratio for the dendriplexes of first three generations of PAMAM dendrimer at $Z_{\pm}$= 10. In this experiment, in the presence of heparin, extent of EtBr intercalation into the destabilized DNA is determined by fluorimetry. From Figure 5.4 it is evident that for the dendrimer of generation one (G1), the DNA release from the dendriplex is observed in the presence of increasing wt/wt ratio of heparin.

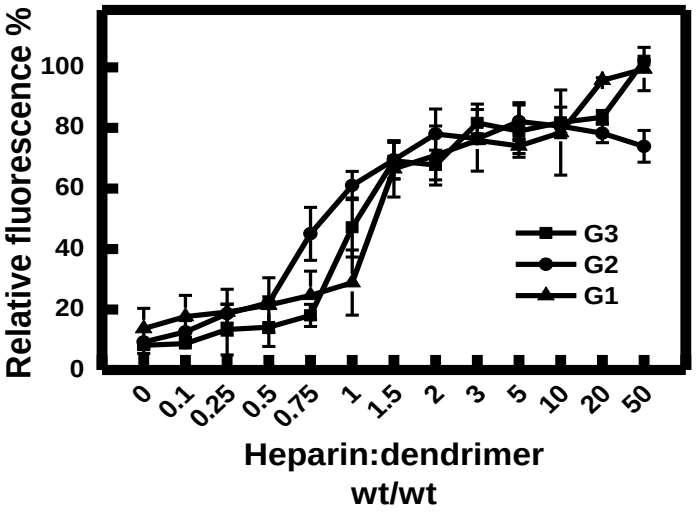

Figure 5.4 Relative stability of dendriplexes at charge ratio ($Z_{\pm}$) 10 against different concentrations of heparin (0.1 to 50 heparin: 1dendrimer) (wt/wt). Amount of DNA released was measured by increase in the fluorescence due to EtBr intercalation. Values are plotted as percentage of maximum ± S.D.

The DNA release from the cationic vector was gradual upto 1 (wt:wt ratio of heparin) and reported to be 28.8 % fluorescence of EtBr, thereafter a steep raise in DNA release was seen from 1 to 1.5 (almost 66.4^%) wt:wt ratio of heparin. Beyond 1.5, DNA release increased slowly with increase in heparin concentration and finally almost 100^% DNA was released at the highest wt:wt ratio of heparin (50 wt/wt). A similar DNA release trend is observed for G2 and G3 with increase in wt:wt ratio of heparin. As heparin concentration increases, dendriplex made of G2 and G3 releases almost similar amount of pDNA upto 2 wt:wt ratio of heparin. On the other hand, around 75 % of pDNA is released from pDNA-G2 complex where as 100 % pDNA release was found in the case of G3 based dendriplex at 50 wt:wt ratio of heparin.

Overall, pDNA release profile for G2 and G3 are better at the wide range of heparin to dendrimer wt:wt ratio compare to G1 and are in good agreement with pDNA condensation assay (Figure 5.2).

5.3.5 Transfection efficiency of dendriplexes

Before testing transfection efficiency of dendriplexes, their size, charge were analyzed using DLS and also dendriplex morphologies were viewed under AFM. The results were observed to be suitable for transfection and the corresponding data are Shown in Table VI and Figure 5.5.

Table VI. Zeta potential as well as zeta size of various dendriplexes

Dendriplex	Zeta potential (mV)	Zeta size (nm)	PDI for zeta size
G1 Z± = 5	-0.091±0.01	2427	1
G1 Z± = 10	-0.187±0.02	1665	1
G2 Z± = 5	18±1.23	119.3	0.133
G2 Z± = 10	21.3±0.09	125.5	0.108
G3 Z± = 5	19.2±1.23	129.5	0.124
G3 Z± = 10	23±0.87	118.5	0.106

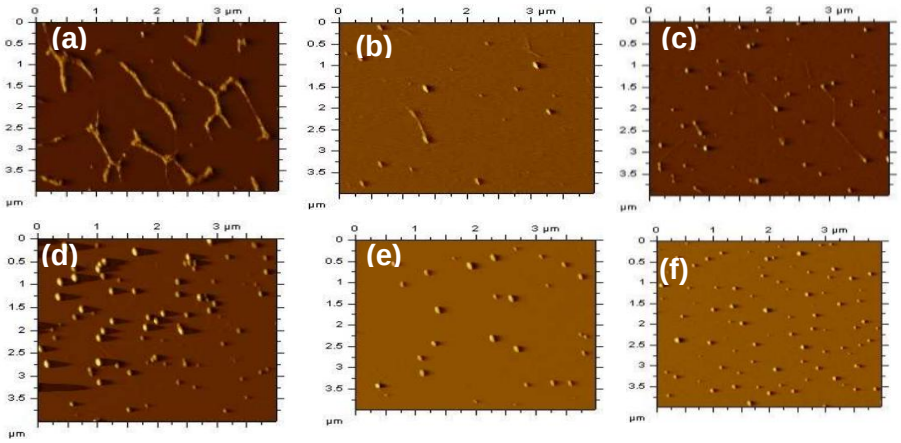

Figure 5.5. AFM images of various dendriplexes (a) only pDNA (b) G1 at $Z_{\pm}$ = 5 (c) G1 at $Z_{\pm}$ = 10 (d) G2 at $Z_{\pm}$ = 5 (e) G2 at $Z_{\pm}$ = 10 (f) G3 at G1 at $Z_{\pm}$ = 10.

Figure 5.6 shows *in-vitro* transfection efficiency of dendriplexes (PAMAM dendrimers of first three generation-pDNA) at various charge ratios into CHO-K1 cells at the post transfection time points (a) 24 h and (b) 48 h. It is pertinent to recall that here transfection was carried out using luciferase reporter gene (pMIR-REPORT™ Luciferase, 6.47 kb). In the case of dendrimer generation G1, for the charge ratio 5 to 20 at 24 h time point transfection was quantified to be about 10^5 RLU/mg protein. Interestingly, at the charge ratio ($Z_{\pm}$) 50 transfection was increased to 10^6 RLU/mg protein. When the time point is increased to 48 h, there was not much change in the transfection efficiency 10^5 RLU/mg protein) of G1 from the charge ratio 5 to 50 as compared to 24 h time point. In general, the transfection efficiency of G1 based dendriplexes were increased with increase in the charge ratio at both the time points 24 h and 48 h. In the case of G2, transfection efficiency was observed to be more or less similar for all the charge ratios (5 to 50) at both the time points 24 h as well as 48 h (about 10^6 RLU/mg protein).

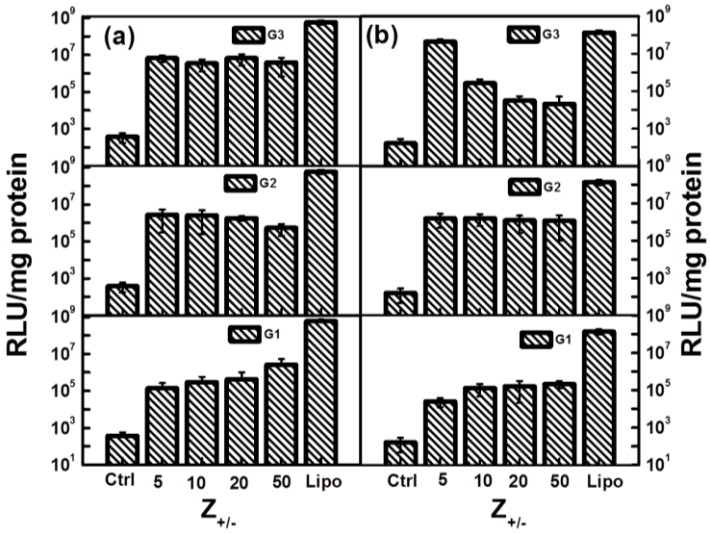

Figure 5.6 *In vitro* transfection efficiency of pDNA in CHO-K1 cells after complexing with PAMAM dendrimer of the first three generations (G1, G2 and G3) at (a) 24 h and (b) 48 h. A negative (only Opti-MEM medium) as well as positive control (Lipofectamine™ 2000) are also shown for the comparative analysis of dendriplex transfection efficiency.

But an exception is observed in the case of G2 at charge ratio 50 at 24 h time point, where transfection was about 10^5 RLU/mg protein which is lesser than an order of magnitude in comparison with the other charge ratios. In the case of G3 at 24 h,

dendriplex transfection was reported to be in the order of 10^6 RLU/mg protein for all the charge ratios studied. On the other hand, at 48 h time point, G3 based dendriplex at charge ratio 5 showed significant transfection efficiency in the order of 10^7 RLU/mg protein compared to lipofectamine (10^8 RLU/mg protein). Thereafter a slight decrease in transfection efficiency of G3 was observed with increase in the charge ratio from ($Z_{\pm}$) 10 to 50, which is in the order of 10^5 to 10^4 RLU/mg protein. Based on these observations, we conclude that the dendrimers of generation G2 at charge ratio 10 (10^6 RLU/mg protein) and generation G3 (10^8 RLU/mg protein) at the lowest charge ratio 5 both at 24 h as well as 48 h time point were observed to show the most efficient transfections. These interesting observations of *in-vitro* G2 based dendriplex transfection into CHO-K1 cells are in contrast to the early observation of Braun *et al.,*[29] where it showed poor transfection ability of G2 compared to G4 and G7. These observations might be due to more focus towards the applicability of higher generation dendrimers G4) compared to the lower generation in gene transfection. It is also noteworthy that *in-vitro* transfection of G3 based dendriplexes were not experimented by Braun *et al.*[29]

Being an attractive gene carrier PAMAM dendrimers possess ethylenediamine nucleus and methyl acrylate and ethylenediamine branching (Figure 5.1).[9] Our observation based on gel condensation (Figure 5.2) and release assay (Figure 5.4) confirm the effective condensation of pDNA by PAMAM dendrimers via electrostatic interactions to form a dendriplex above dendrimer to pDNA charge ratio ($Z_{\pm}$) 1 and subsequent 80 % DNA release is observed from $Z_{\pm}$=3 to 50. On the other hand, it becomes important to highlight that comparative efficiency of pDNA condensation (Figure 5.2) and release (Figure 5.4) among the first three PAMAM dendrimer generations are not able to be distinguished by these usual assays. On the other hand, stop-flow dendrimer-pDNA binding kinetics (Figure 5.3) clearly distinguishes the efficient DNA condensation of G2 and G3 compared to G1. More importantly, the occurrence of association and aggregations of the dendrimer molecules in the vicinity of DNA is realized in stop-flow kinetics, which is known to be concentration dependent. Hence, the dendriplex results in size control which is suitable for gene

transfection as revealed by zeta sizer (Table VI). Such dendrimer molecular aggregation in the vicinity of DNA is recently visualized by us, where the molecular mechanism of dendriplex formation between the 14mer oligonucleotide and PAMAM dendrimer was explored by the fluorescence and FRET investigations.[33] The observed 100 % cellular entry of G2 and G3 based dendriplexes by the flow cytometry (Figure 5.7) as well as the significant gene transfection data (Figure 5.5) for the dendrimers of generation G2 at charge ratio 10 (10^6 RLU/mg protein) and generation G3 (10^8 RLU/mg protein) at the lowest charge ratio 5 both at 24 h as well as 48 h time point might be due to the suitable size of the corresponding dendriplexes obtained. Such efficient internalization of DNA when associated with polycationic vectors were released from the endosomes after cellular entry by the well-known 'proton sponge effect.[15, 19, 29, 30] In detail, herein, an interaction of the excess positive charges of the dendriplex with negatively charged cell-surface groups result in adsorptive endocytosis and membrane destabilization as proposed by Behr for cationic liposomes-DNA complexes.[53]

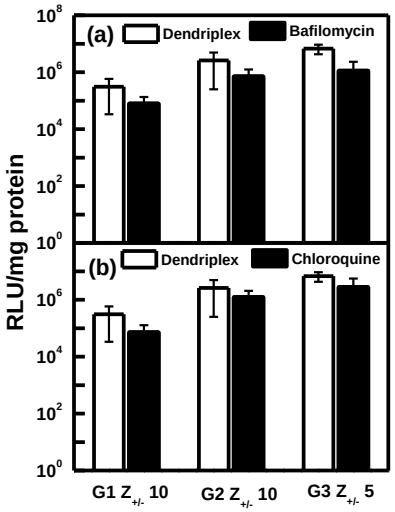

Figure 5.7 *In vitro* transfection efficiency of pDNA in CHO-K1 cells after complexing with PAMAM dendrimer of the first three generations in presence and absence of bafilomycin and chloroquine at various dendrimer to pDNA charge ratio ($Z_{\pm}$).

After evidencing the successful pDNA transfection using G3 as well as G2 into the CHO-K1 cell line (Figure 5.6), transfection studies were further extended in the presence of endosomotropic agents like bafilomycin A1 and chloroquine. Bafilomycin

A1 can inhibit the acidification of endosomes, thus preventing their maturation and fusion into lysosomes.[54,55] Chloroquine is another molecule that accumulates in endosomes/lysosomes and causes the swelling and disruption of endocytic vesicles by osmotic effects.[56] Figure 5.7 portrays *in-vitro* transfection efficiency of low generation PAMAM dendrimers in the presence and absence of bafilomycin (Figure 5.7a) and chloroquine (Figure 5.7b) in CHO-K1 cells at various $Z_{\pm}$. Interestingly, in the presence of these agents, transfection efficiency of the lower generation dendrimers (G1, G2, and G3) were retained compared to the transfection efficiency obtained in their absence. These observations indicate that dendrimers of lower generation at charge ratio 10 for G1 as well as G2 and at charge ratio 5 in the case of dendrimer generation 3 are capable to transfect the cells and overcome the endosomal barrier easily and reach the nucleus. From the above findings it could be concluded that there exists other non-endosome associated entry mechanisms involved in the entry of PAMAM dendrimers. Hence, herein the addition of either bafilomycin A1 or chloroquine does not significantly increase the transfection efficiency. This could mean the unlike what was originally thought, endosomal escape is probably not the rate limiting step in this process.

5.3.6 Cellular uptake.

For a successful gene transfection, the cellular uptake and intracellular localization of a gene carrier play important roles. Herein, cellular uptake studies were carried out using FITC labeled pDNA and both the fluorescence positive cells and the mean fluorescence intensity of the population were estimated using flow cytometry in CHO-K1 cells at 37°C. The corresponding data indicating percentage of fluorescence positive cells and their mean intensity are portrayed in Figure 5.8a along with the control experiment. Interestingly, at 37°C, for dendriplexes made up of G2 at charge ratio 10 and G3 at charge ratio 5, cellular entry of the corresponding dendriplex is observed to be almost 100 %. Subsequently the uptake of dendriplexes (G2 at $Z_{\pm}$=10 and G3 at $Z_{\pm}$=5) containing labeled DNA were also checked using fluorescence microscopy and portrayed in Figure 5.8b1-8b4 and 5.8c1-8c4 for G2 at $Z_{\pm}$=10 and G3 at $Z_{\pm}$=5 respectively.

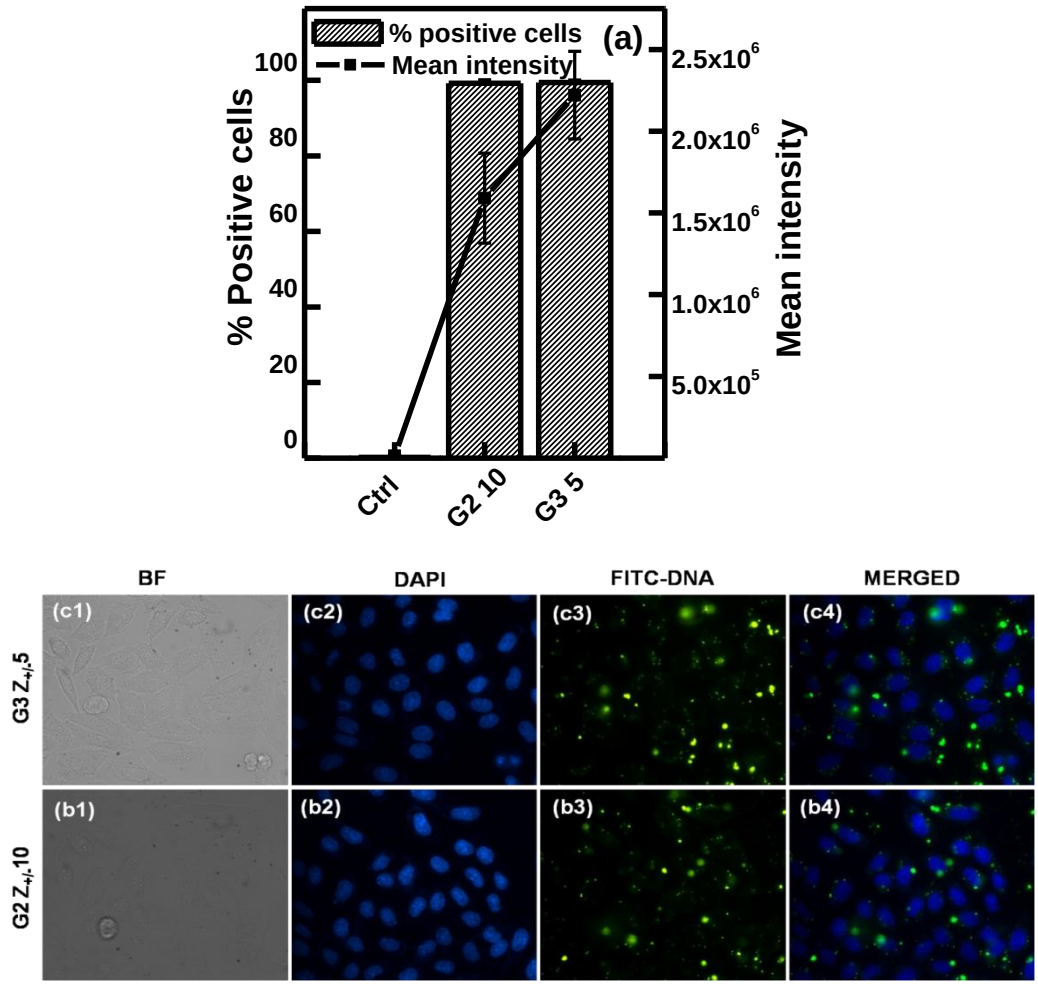

Figure 5.8 Cellular uptake of the dendriplexes. (a) Percentage of fluorescence positive cells (bars) and their mean intensity (line) measured using flow cytometry. CHO-K1 cells incubated for 4 h with dendriplexes formed using G2 at $Z_{\pm}$ 10 and G3 at $Z_{\pm}$ 5 with FITC labeled pDNA. The data are shown as the mean ± S.D. Confocal images of live CHO-K1 cell obtained after pDNA transfection using PAMAM dendrimer (b1-b4) G2 at $Z_{\pm}$ 10 (Bottom lane)and (c1-c4) G3 at $Z_{\pm}$5 (top lane). In confocal images blue color arose from the nuclear dye DAPI; green color arose from fluorescein units.

The observed fluorescence of FITC in the displayed images indicate that dendriplexes made up of G2 at charge ratio 10 and G3 at charge ratio 5 were successfully up-taken into the cells and reached the periphery of the corresponding nucleus. These confocal images further confirm almost 100 % uptake data observed by the flow cytometry. To the best of our knowledge, the observed interesting data is reported by us for the first time in CHO-K1 cells.

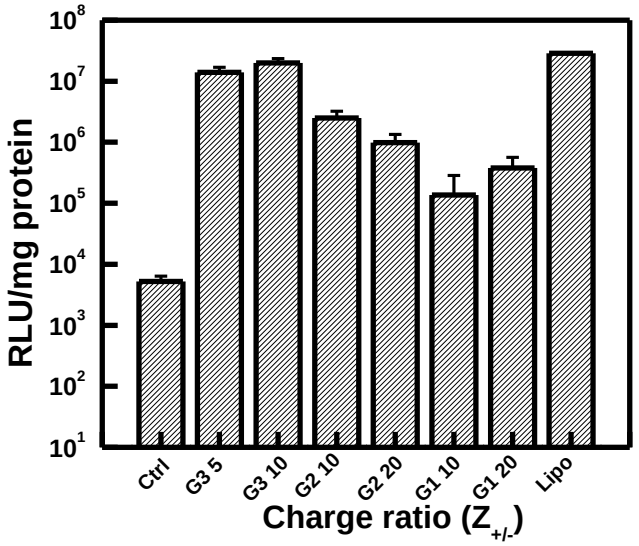

Figure 5.9 *In vitro* transfection efficiency of pDNA in HaCaT cells after complexing with PAMAM dendrimer of the first three generation at 24 h. A negative (only opti MEM medium) as well as positive control (Lipofectamine™ 2000) are also shown for the comparative analysis of dendriplex transfection efficiency.

Based on the above interesting observations in the pDNA transfection and uptake into CHO-K1 cells, these studies are also extended to find its application into the HaCaT cells to target skin. Herein, HaCaT cells are chosen for *in-vitro* transfection based on the recent interesting observations of lower generation dendrimers in skin penetrations.[57] Interestingly, *in-vitro* transfection studies (Figure 5.9) revealed that the highest transfection efficiency was observed for G3 based dendriplexes at both the charge ratios ($Z_{\pm}$) 5 and 10 compared to the dendriplexes made up of G2 and G3. Additionally, transfection efficiency of dendrimer complexes was confirmed using another reporter plasmid EGFP-C1 in HaCaT cell line that is usually considered difficult to transfect. We treated these cells with G1, G2, G3 complexes prepared at different charge ratios as mentioned in luciferase transfection and observed EGFP expression after 24 h (Figure 5.10).

It was seen that both G2 and G3 based complexes exhibit ~40 % EGFP positive cells at charge ratio 20 and 5 respectively whereas G1 based complexes exhibit slightly less transfection efficiency, with only 25 % EGFP positive cells at lower charge ratio 10. Comparison with the commercial transfection agent Lipofectamine 2000™ shows

that dendriplexes are not as efficient in cellular transfection but it seems G2 might achieve the similar transfection efficiency at higher charge ratio owing to its proportional increase in percentage positive cells at increasing charge ratios.

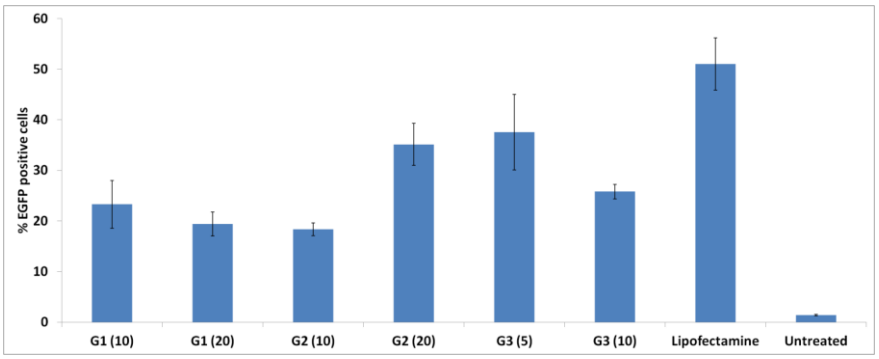

Figure 5.10 Quantitative analysis of EGFP expression in HaCaT cells following treatment with G1, G2, G3 dendrimer-DNA complexes was carried out using flow cytometry. The percentage EGFP positive cells were recorded. The data are shown as Mean ± S.D. Lipofectamine 2000™ was taken as positive control for the study.

Furtherly, cellular uptake of dendrimer complexes of G2 at $Z_{\pm}$ 10 and G3 at $Z_{\pm}$ 5 with FITC labeled pDNA in HaCaT cells (Figure 5.11) reveals that almost 100 % of fluorescence positive cells are observed both in the case of G2 at $Z_{\pm}$ 10 and G3 at $Z_{\pm}$ 5 and the corresponding mean intensity measured using flow cytometry also indicate successful entry of the dendriplexes into the nucleus of HaCaT cells. All these transfection experiments with various pDNA into the HaCaT cells are evidencing that lower generation dendrimers especially G2 and G3 are successful gene carriers for transdermal treatments.

It is pertinent to note that as per the demonstration of Hong *et al.,*[58] PAMAM dendrimers can enter cells by creating transient pores (in case of G7) or by expanding already existing surface defects/ holes (in case of G5) in the cell membrane. Further this ability of the PAMAM dendrimers to interact with lipid bilayers is probably the reason behind the enhanced transfection efficiency in skin cell lines that are rich in lipid components, and this needs to be explored in future studies. Even though, skin penetration studies in tissue would be interesting but requires detailed experimentation which is beyond the scope of the current manuscript and would be reported separately.

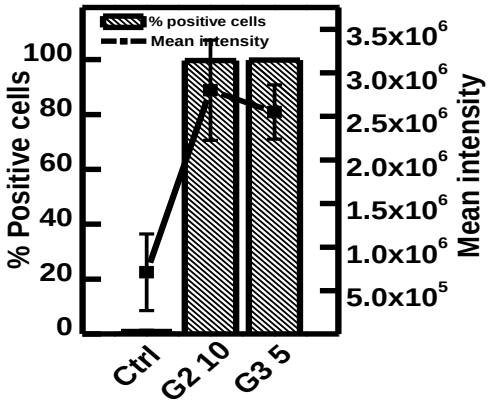

Figure 5.11 Cellular uptake of the dendriplexes in HaCaT cells. Percentage of fluorescence positive cells (bars) and their mean intensity (line) measured using flow cytometry. HaCaT cells incubated for 4 h with dendriplexes formed using G2 at $Z_{\pm}$ 10 and G3 at $Z_{\pm}$ 5 with FITC labeled pDNA. The data are shown as the mean ± S.D.

5.3.7 Cell viability assay

MTT assay was carried out for G1, G2 and G3 in the presence of a corresponding dendriplex at required charge ratio after 4 h and 24 h in CHO-K1 (Figure 5.12) as well HaCaT (Figure 5.13) cells. In general, the MTT assay resulted in negligible cytotoxicity for all the dendrimers under investigation. In the case of CHO-K1 cells, cell viability was around 80 % at 4 h in the presence of dendriplex and was in good agreement with lipofectamine data.

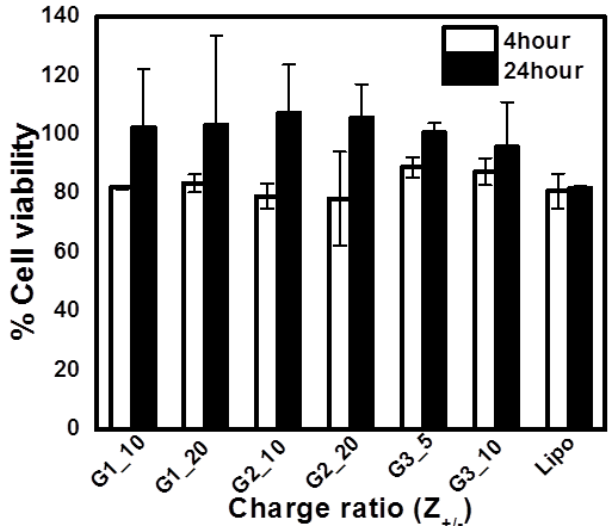

Figure 5.12 MTT cell viability assay in presence of dendriplexes at various charge ratios ($Z_{\pm}$) at 4 h and 24 h in CHO-K1 cell line. Untreated cells were defined as 100% viable. lipo=Lipofectamine™ 2000.

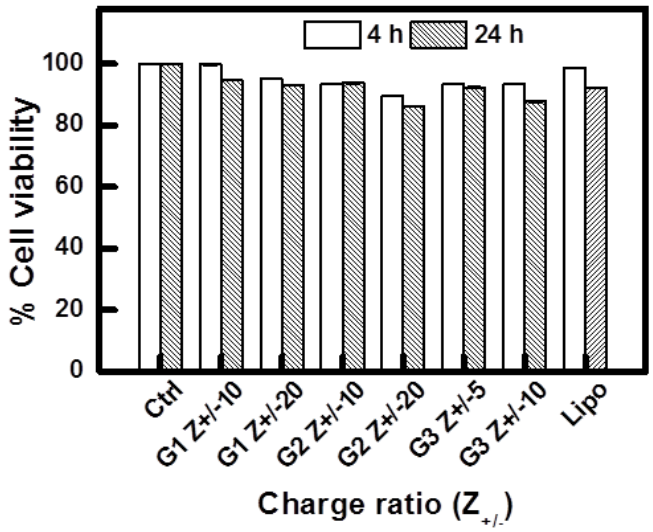

Figure 5.13 MTT Cell viability assay in presence of dendriplexes at various charge ratios at 4 h and 24 h in HaCaT (human skin) cell line. Untreated cells were defined as 100% viable. lipo=Lipofectamine™ 2000. The SD values are not visible in the graph due to very low values.

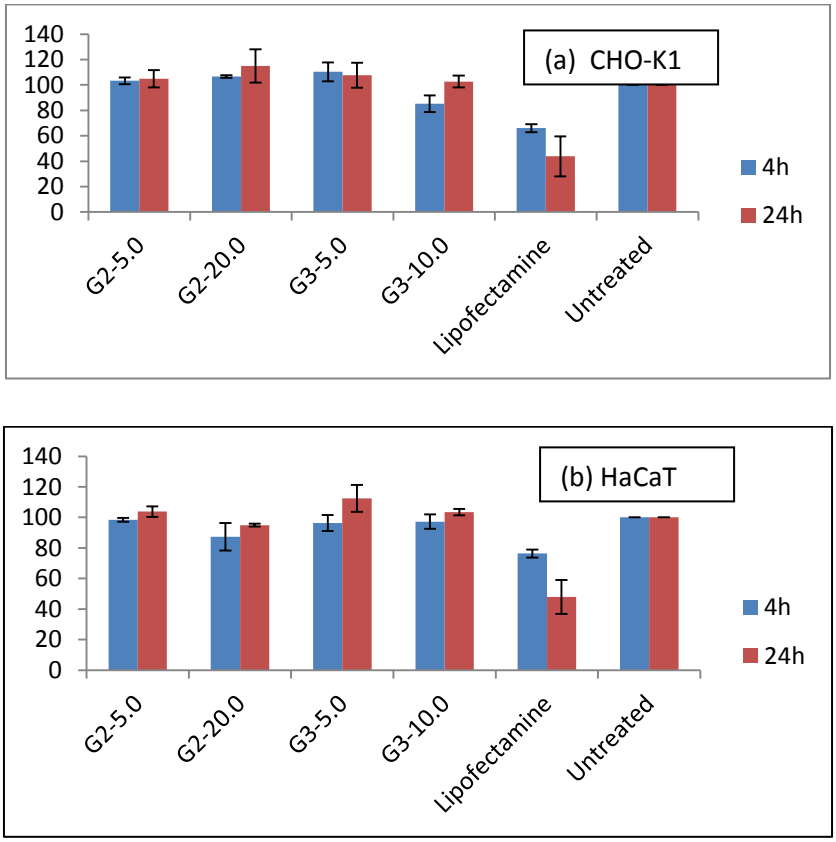

Figure 5.14 Cell Titer assay in presence of dendriplexes at various charge ratios at 4 h and 24 h in (a) CHO-K1 and (b) HaCaT (human skin) cell line. Untreated cells were defined as 100% viable. Lipofectamine=Lipofectamine™ 2000.

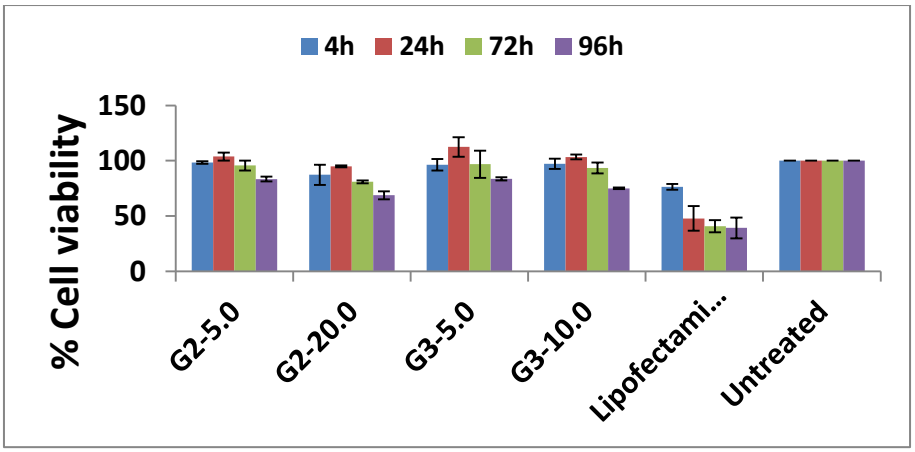

Figure 5.15 Cell titer assay in presence of dendriplexes at various charge ratios at 4 h, 24 h, 72 h and 96 h in HaCaT (human skin) cell line. Untreated cells were defined as 100% viable. Lipofectamine=Lipofectamine™ 2000.

On the other hand, in the presence of dendriplex at 24 h, 100 % CHO-K1 cell growth was observed in comparison with lipofectamine, which showed around 80 % cell viability for the same time point. The observed variations in cell growth compared to control could probably be explained as follows: MTT assay measures the metabolic activity of the cells. The optical density (OD) of CHO-K1 cell samples treated with required dendriplexes are compared with the OD of the untreated CHO-K1 cell samples (control) and a relative % of cell viability is calculated considering the control samples to be 100 % viable. If by chance the dendriplex treated samples have more number of cells than the control samples at 24 h time point, this will be reflected as viability greater than 100 % in calculation (the OD of dendriplex treated samples is higher than the control). This could imply that there is no toxicity posed by the dendriplex and considered as cells continue to proliferate at a level comparable to that of untreated cells (Control). Mostly, variability comes here due to the uncertainty in the cell proliferation at longer durations. Interestingly, cell viability data for HaCaT cells indicate healthy cell growth for all the dendriplexes used and were in close agreement with lipofectamine. Overall, the absence of cytotoxicity indicates PAMAM dendrimer of first three generations as good transfection agents for pDNA delivery into CHO-K1 and HaCaT cells. Non-toxicity of the dendrimers was also confirmed by independent cell titer assay for both CHO-K1 and HaCaT cell lines

for 4 h and 24 h (Figure 5.14 (a and b)) for CHO-K1 and HaCaT cell lines respectively). Interestingly, reported cell cytotoxicity data (shown in Figure 5.15) at higher time points (72 h and 96 h) also indicated negligible cytotoxicity by portraying more than 80 % of cell viability.

5.3.8 Serum stability and transfection efficiency of the dendriplexs in the presence of serum.

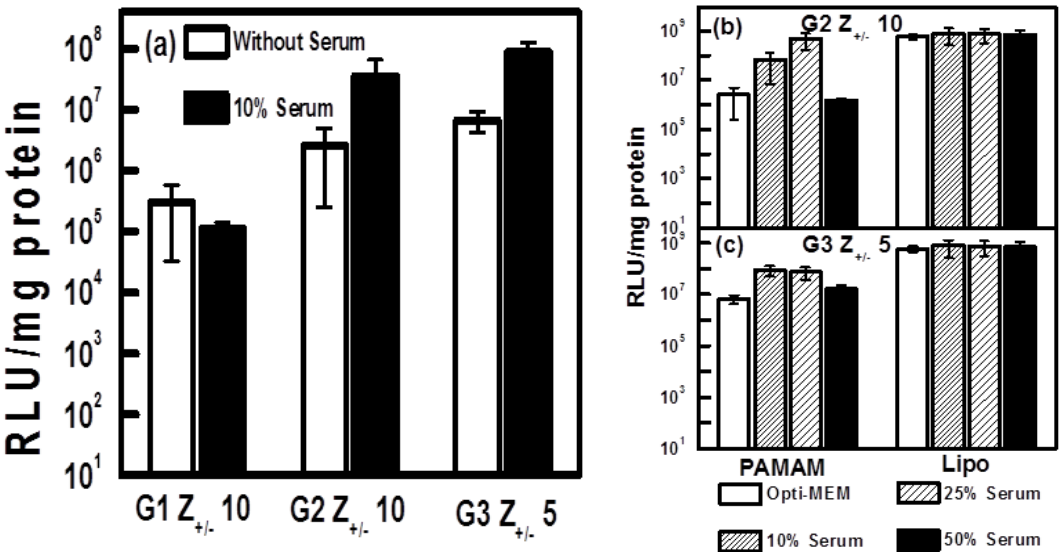

Figure 5.16 *In vitro* transfection efficiency of (a) pDNA based dendriplexes of the first three generations (at the lowest charge ratio in which good transgene expression was observed) was checked in the presence of lower serum (10%), (b) G3 in the presence of various concentration of serum (10%, 25% and 50 %) and (c) G2 in the presence of various concentration of serum (10%, 25% and 50 %) in CHO-K1 cells. A negative (only Opti-MEM medium) as well as positive control (Lipofectamine™ 2000) are also shown for the comparative analysis of dendriplex transfection efficiency.

Apart from transporting the cargo to the target, cationic vectors used in *in-vivo* gene delivery should also protect the therapeutic pDNA from serum degradation. In order to verify if these low generation dendrimers can transfect cells efficiently in the presence of serum, the transfection efficiency of G1 ($Z_{\pm}$=10), G2 ($Z_{\pm}$= 10) and G3 ($Z_{\pm}$= 5) was checked in medium containing 10 % serum initially (Figure 5.16a). The transfection efficiency of G2 and G3 PAMAM was retained even in this condition. This prompted us to check the transfection efficiency of G2 (Figure 5.16b) and G3 (Figure 5.16c) PAMAM at higher serum concentrations (25 % and 50 %). The

transfection by G3 is maintained even at 50 % serum and is comparable to the level of transfection obtained in OPTI-MEM while the transfection efficiency of G2 at this condition is slightly lesser.

To further verify, if this persistent level of transfection even in the presence of such high serum concentrations is due to the dendriplexes stability in serum, G2 and G3 dendriplexes were subject to serum stability test in agarose gel. Figure 17 shows agarose gel images of DNA release in the presence of the anionic challenger, heparin for (a) G3 at $Z_{\pm}$ 5 and (b) G2 at $Z_{\pm}$ 10. Lane 1 and 2 of agarose gel images show the mobility of naked pDNA and DNA complexed by dendrimers respectively. Lanes 3-6 represent dendriplexes incubated with increasing % of serum followed by heparin release. Though the intensity of released pDNA from the denriplexes is decreasing with increasing percentage of serum to an extent, major amount of pDNA is released and is found intact too (the amount of released pDNA corresponds to the amount of pDNA that was protected by the dendrimer from degradation by the components in the serum). Thus dendriplexes are not completely destabilized in the presence of serum and they are still entering the cells efficiently resulting in transgene expression.

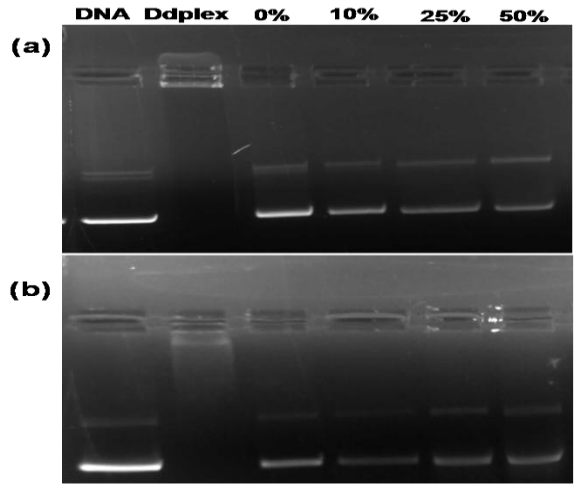

Figure 5.17 Serum stability of pDNA was estimated after dendriplex formation (a) at $Z_{\pm}$ 5 with G3 and (b) at $Z_{\pm}$10 with G2 at different concentrations of serum on agarose gel. Lane 1 - Ctrl (only plasmid DNA), Lane 2 - only dendriplex, Lane 3 - 5, dendriplex with 10%, 25% and 50% concentrations of serum respectively. Here, pDNA was released from the dendriplex by heparin challenge.

5.4 Conclusion

The optimized efficient pDNA transfection using PAMAM dendrimer into the CHO-K1 cells at lower charge ratio 10 for G2 and 5 for G3 is appreciable as the toxicity of dendrimers is mostly influenced by generation (size) and/or dose dependence. The successful demonstration of pDNA transfection using G2 and G3 into HaCaT cells with negligible toxicity indicated a versatile platform for cell-specific nucleic acid therapeutics for skin disorder. Finally, the observed serum stability of G2 as well as G3 based dendriplexes in CHO-K1 cells promises for *in-vivo* gene delivery applications without extrinsic serum inhibition. Overall, we emphasize our systematic observations on lower generation dendrimer carriers might pave way for a convenient, versatile and possibly patient compliant approach to deliver large hydrophilic macromolecules like nucleic acids across skin in a non-toxic manner.

References

1. W. F. Anderson, Human gene therapy, *Science* 1992, **256,** 808-813.
2. R. C. Mulligan, The basic science of gene therapy, *Science* 1993,**260,** 926-932.
3. H. A Magid, Gene therapy for cancer: present status and future perspective, *Mol. Cell. Ther*. 2014, **2***,* 27-46.
4. C. E.Thomas, A. Ehrhardt andM. A. Kay, Progress and problems with the use of viral vectors for gene therapy,*Nat. Rev. Genet.* 2003; **4,** 346-358.
5. G. U.Dachs, DG. J. Dougherty, I. J.Stratford, D. J Chaplin, Targeting gene therapy to cancer: a review,*Oncol. Res.* 1997,**9,** 313-325.
6. H.Yin, R. L.Kanasty, A. A.Eltoukhy, A. J.Vegas, J. R.Dorkin andD. G. Anderson, Non-viral vectors for gene-based therapy,*Nat. Rev. Genet.* 2014, **15,** 541–555.
7. C. W.Pouton andL. W. Seymour, Key issues in non-viral gene delivery, *Adv. Drug Deliv. Rev.*1998, **34,** 3–19.

8. M. S. Al-Dosari andX.Gao, Nonviral gene delivery: principle, limitations, and recent progress,*Am. Assoc. Pharm. Sci. J.*2009**,11,** 671-681.

9. S.Svenson andD. A. Tomalia, Dendrimers in biomedical applications – reflections on the field,*Adv. Drug Deliv. Rev*. 2005,**57,** 2106–2129.

10. C.Dufes, I. F. Uchegbu andA.G. Schatzlein, Dendrimers in gene delivery, *Adv. Drug Deliv. Rev.*2005, **57,** 2177–2202.

11. Y.Gao, G.Gao, Y.He, T.Liu andR.Qi, Recent advances of dendrimers in delivery of genes anddrugs. *Mini Rev. Med. Chem.* 2008, **8,** 889–900.

12. Q.Xu, C.H.Wang andD. W. Pack, Polymeric Carriers for Gene Delivery: Chitosan and poly(amidoamine) dendrimers. *Curr. Pharm. Des.*2010, **16***,* 2350–2368.

13. Y.Cheng, Z.Xu, M.Ma andT.Xu, Dendrimers as drug carriers: Applications in different routes of drug administration,*J. Pharm. Sci.*2008**, 97,** 123–143.

14. R.Esfand andD. A. Tomalia, Poly(amidoamine) (PAMAM) dendrimers: From biomimicry to drug delivery and biomedical applications,*Drug Discov. Today*2001**, 6,** 427–436.

15. A. U. Bielinska, J. F. Kukowska-Latallo andJ. R.Baker, Jr. The interaction of plasmid DNA with polyamidoaminedendrimers: mechanism of complex formation and analysis of alterations induced in nuclease sensitivity and transcriptional activity of the complexed DNA, *Biochim. Biophys. Acta.* 1997**, 1353,** 180–190.

16. H.Arima, K.Motoyama andT. Higashi, Potential use of poly (amidoamine) dendrimer conjugates with cyclodextrins as novel carriers for siRNA, *Pharmaceuticals* 2012, **5,** 61-78.

17. S.Biswas, andV. P. Torchilin, Dendrimers for siRNA Delivery*, Pharmaceuticals* 2013,**6,** 161-183.

18. D. G. Shcharbin, B.Klajnert andM.Bryszewska, Dendrimers in gene transfection. *Biochem. (Moscow)* 2009, **74,** 1070-1079.

19. J. F. Kukowska-Latallo, A. U.Bielinska, J.Johnson, R.Spindler, D. A.;Tomalia and J. R. Baker, Jr. Efficient transfer of genetic material into mammalian cells using Starburst polyamidoaminedendrimers,*Proc. Natl. Acad. Sci. U. S. A.*1996,**3,**4897−4902.

20. Y.Cheng, L. Zhao, Y.Li andT.Xu, Design of biocompatible dendrimers for cancer diagnosis and therapy: current status and future perspectives. *Chem. Soc. Rev.* 2011,**40,** 2673−2703.

21. J. D. Eichman, A. U.Bielinska, J. F. Kukowska-Latallo andJ. R. Baker, Jr. The use of PAMAM dendrimers in the efficient transfer of genetic material into cells. *Pharm. Sci. Technol. Today*2000, **3,** 232–245.

22. A.Naik, Y. N. Kalia andR. H. Guy, Transdermal drug delivery: overcoming skin's barrier function,*Pharm. Sci. Technol. Today*2000, **9,** 318–326.

23. K. L. Killops, L. M. Campos andC. J. Hawker, Robust, efficient, and orthogonal synthesis of dendrimers via thiolene "click" chemistry,*J. Am. Chem. Soc.*2008,**15,** 5062-5064.

24. J.Yang, Q.Zhang, H.Chang andY Cheng. Surface-Engineered Dendrimers in Gene Delivery. *Chem. Rev.***2015,** *115,* 5274−5300.

25. H. Liu, H. Wang, W. Yang, and Y. Cheng, *J. Am. Chem. Soc*. **2012**, *134*, 17680−17687.

26. M. Wang, H. Liu, L. Li and Y. Cheng, *Nat. Com*. **2014**, DOI: 10.1038/ncomms405.

27. V.Vamsi, K.Venuganti andO. Perumal, P.Poly(amidoamine) dendrimers as skin penetration enhancers: Influence of charge, generation,and concentration,*J. Pharm. Sci.*2009,**98, 2345–2356.**

28. P.Kesharwani,S.Banerjee, U.Gupta, M. C. I. M. Amin, S.Padhye, F. H. Sarkar andA. K. Iyer, PAMAM dendrimers as promising nanocarriers for RNAi therapeutics *Mater. Today*2015, **18,** 565–572.

29. C. S. Braun, J. A.Vetro, D. A. Tomalia, G. S. Koe, J. G. Koe andC. R.Middaugh,Structure/Function Relationships of Polyamidoamine/DNA Dendrimers as Gene Delivery Vehicles,*J. pharm. Sci.*2005,**94,** 423-436.

30. J.Haensler andF. C.Szoka, Jr. Polyamidoamine cascade polymers mediate efficient transfection of cells in culture,*Bioconjugate Chem*. 1993,**4,** 372–379.

31. F.Tajarobi, M.El-Sayed, B. D.Rege, J. E. Polli andH.Ghandehari, Transport of poly (amidoamine) dendrimers across Madin-Darby canine kidney cells,*Int J. Pharm.*2001, **215,** 263–267.

32. A. J. Hollins, M.Benboubetra, Y.Omidi, B. H. Zinselmeyer, A. G. Schatzlein, I. F. Uchegbu andS. Akhtar, Evaluation of generation 2 and 3 poly(propylenimine) dendrimers for the potential cellular delivery of antisense oligonucleotides targeting the epidermal growth factor receptor,*Pharm. Res.*2004, **21***,* 458-466.

33. H. K. Alajangi and D.Santhiya, Fluorescence and Förster resonance energy transfer investigations on DNA oligonucleotide and PAMAM dendrimer packing interactions in dendriplexes**.** ***Phys. Chem. Chem. Phys.,***2015,**17**, 8680-8691

34. V. V. Venuganti, P.Sahdev, M.Hildreth, X.Guan andO. Perumal, Structure-skin permeability relationship of dendrimers,*Pharm. Res.*2011,**28**, 2246–2260.

35. Y. Yang, S. Sunogrot, C. Stowell, J.Ji, C.-W.Lee, J. W.Kim, S. A. Khan andS. Hong, Effect of size, surface charge, and hydrophobicity of poly(amidoamine) dendrimers on their skin penetration,*Biomacromol.* 2012, **13,** 2154–2162.

36. W. H. Yu, M. Kashani-Sabet, D.Liggitt, D.Moore, andT. D. Heath, R. J.Debs. Topical gene delivery to murine skin,*J. Invest. Dermatol.* 1999, **112,** 370–375.

37. R. C.Mehta, K. K. Stecker, S. R. Cooper, M. V. Templin, Y. J. Tsai, T. P. Condon, C. F.Bennett andG. E. Hardee, Intercellular adhesion molecule-1 suppression in skin by topical delivery of antisense oligonucleotides,*J. Invest. Dermatol.*2000,**115,** 805–812.

38. Y.W. Chien, Transdermal therapeutic systems.In *Controlled Drug Delivery*, Robinson, J.R., Lee V.H.L.,Eds.;Marcel Dekker Inc,New York, 1987, pp 523–549.

39. E.R. Figueroa, A.Y. Lin, J. Yan, L. Luo, A. E. Foster, R. A. Drezek, *Biomaterial.* **2014**, *35*, 1725–34.

40. Y. W. WoN, M. Lee, H. A. Kim, K. Nam, D. A. Bull, S. W. Kim, *Mol. Pharma*. **2013**, *10*, 3676–3683.

41. J. Li, S. Li, S. Xia, J. Feng, X. Zhang, Y. Hao,L. Chen, X. Zhang, *oncotarget*. **2015**, *6*, 28, 26177-26191.

42. D.Santhiya, R. Dias. S.Dutta P. K.Das, M.G.Miguel, B.Lindman and S. Maiti, Kinetic studies of amino acid-based surfactant binding to DNA,*J. Phys. Chem. B*2012,**116,**5831-5837.

43. M. A.Mintzer andE. E. Simanek. Non-viral vectors for gene delivery.*Chem. Rev.*2009, 109,259−302**.**

44. DNA Interactions with Polymers and Surfactants; Dias, R. S.; Lindman, B., Eds.; John Wiley and Sons: Hoboken, N.J., 2008.

45. Wei Chen, Nicholas J. Turro and Donald A. Tomalia, *Langmuir.* **2000,** *16***,** 15-19.

46. E.; Grueso E.; Roldan andF. Sanchez, Kinetic Study of the Cetyltrimethylammonium/DNA interaction,J. Phys. Chem. B2009,113,8319−8323.

47. D.Dey, S.Kumar, S.Maiti andD.Dhara, Stopped-flow kinetic studies of poly (amidoamine) dendrimer−calf thymus DNA to form dendriplexes,J. Phys. Chem. B2013,117, 13767−1377.

48. A. M. D. L. Pena, A. E. Mansilla, J. A. Pulgarin andA. Molina, A. and P. F. Lopez, Stopped-flow determination of dipyridamolein pharmaceutical preparations by micellar-stabilized room temperature.phosphorescence, Talanta1999,48, 1061−1073.

49. E.Vuorimaa, A.Urtti, R. Seppänen ,H. Lemmetyinen andM.YliperttulaTime-resolved fluorescence spectroscopy reveals functional differences of cationic polymer−DNA complexes. J. Am. Chem. Soc., 2008, 130, 11695–11700.

50. M. L Ainalem, A. M. Carnerup, J.Janiak, V.Alfredsson, T.Nylander andK. Schillen, condensing DNA with poly(amido amine) dendrimers of different generations: means of controlling aggregate morphology,Soft Matter2009,5, 2310−2320.

51. H. M. Evans, A.; Ahmad, K.; Ewert, T.; Pfohl A.; Martin-Herranz, R. F. Bruinsma andC. R. Safinya, Structural polymorphism of DNA−dendrimer complexes,Phys. Rev. Lett.2003,91, 75501−75504.

52. R.Golan, L. I. Pietrasanta, W.Hsieh andH. G. Hansma, DNA Toroids: Stages in Condensation. Biochem.1999,38, 14069−14076.

53. O.Boussif, F.Lezoualc'h, M. A. Zanta, M. D. Mergny, D.Scherman, B.Demeniex andJ-P. Behr, A versatile vector for gene and oligonucleotide transfer into cells in culture and in vivo: Polyethylenimine, Proc. Natl. Acad. Sci. U.S.A. 1995, 92, 7297–7301.

54. A.M. Tartakoff, Perturbation of vesicular traffic with the carboxylic ionophoremonensin, Cell 1983, 32, 1026–1028.

55. S. Drose andK. Altendorf, Bafilomycins and concanamycins as inhibitors of V-ATPases and P-ATPases, J. Exp. Biol.1997,200, 1–8.

56. R.Wattiaux, N.Laurent, S.; Wattiaux-De Coninck andM. Jadot, Endosomes, lyso-somes: their implication in gene transfer,Adv. Drug Deliv. Rev.2000,41, 201–208.

57. Y.Yang, S.Sunoqrot, C.Stowell, J. Ji, C. W Lee, J. W.; Kim, S. A. Khanand andS. Hong, Effect of size, surface charge, and hydrophobicity of poly(amidoamine) dendrimers on their skin penetration. Biomacromolecules, 2012, 13, 2154−2162.

58. S. Hong, A. U. Bielinska, A. Mecke,B. Keszler, J. L. Beals, X. Shi, L. Balogh, B. G. Orr, J. R. Baker, Jr. and M. M. B. Hol, *Bioconjugate.Chem*. **2004**, *15*, 774−782.

SCOPE FOR FUTURE STUDIES

Dendrimer based nano-carriers have recently emerged as an efficient delivery vehicles in skin. The flexibility of these systems in terms of size, shape, placement and number of functional groups provides them an edge over the other known transdermal delivery systems. Therefore, the novelty of our study focuses on developing less toxic and cost effective low-generation dendrimers for successful gene transfection and holds immense potential for further development of this carrier for gene delivery to skin. In this context the dendrimer carrier might pave way for future alternatives. One of the problems of gene therapy with nanomaterials is the accessibility of target organs and the retention and stability of the nanocomplex for extended period before reaching the target organ in effective concentrations. However, gene delivery to research on more such materials for easy delivery of therapeutic nucleic acids to skin using a non-viral route is necessary. Overall we emphasize a convenient, versatile and possibly patient compliant approach to deliver large hydrophillic macromolecules like nucleic acids across skin in a non-toxic manner. Further, I would like to study in detail **Skin penetration in tissue.**

LIST OF PUBLICATIONS

1. "Bio-inspired synthesis of microporous bioactive glass-ceramic using CT-DNA as a template"

   Deenan Santhiya, **Hema kumari Alajangi**, Fara Anjum, Sevi Murugavel, Munia Ganguli,

   ***J. Mater. Chem. B*, 2013, 1, 6329-6338. (Impact Factor: 4.872)**

2. "Fluorescence and Förster resonance energy transfer investigations on DNA oligonucleotideand PAMAM dendrimer packing interactions in dendriplexes"

   Hema Kumari Alajangi and Deenan Santhiya,

   ***Phys. Chem. Chem. Phys.*, 2015, 17, 8680-8691. (Impact Factor: 4.449)**

3. "Role of Unmodified Low GenerationPAMAM Dendrimers in Efficient Non-Toxic Gene Transfection"

   Hema Kumari Alajangi, Poornemaa Natarajan, ManikaVij, MuniaGanguli, Deenan Santhiya,

   ***ChemistrySelect* 2016, *1*, 5206- 5217**. **(Impact Factor: 3.318)**

4. "Investigation on PAMMAM dendrimer and 14mer oligonucleotides packing kinetics by Stopped-Flow Fluorescence Spectroscopy"

   Hema Kumari Alajangi and Deenan Santhiya,

   Manuscript communicated.

CONFERENCE PROCEEDINGS

1. Attended and presented a poster entitled "*An investigation on PAMAM Dendrimer – oligonucleotide interaction for gene therapy applications*" in ***National Fluorescence Conference*** held in **Kolkata** Dec 3rd to 8th 2012: **Hema Kumari Alajangi** and Deenan Santhiya*.

2. Attended and presented a poster entitled "*An Investigation on PAMAM Dendrimer – Oligonucleotide Interaction for Gene Therapy Applications*" in ***International Conference on Chemical Biology*** held on Feb 6th to 8th 2014 at **IICT-Hyderabad**, **Hema Kumari Alajangi** and Deenan Santhiya***.**

3. Attended and presented a poster entitled "*Efficient targeted plasmid DNA delivery by PAMAM – DNA dendriplexes* in **International Conference on Nanostructured Materials and Nanocomposites (ICNM 2014) at IIUCNN, Mahatma Gandhi University, Kottayam, Kerala** held on Dec 19th to 21st 2014: **Hema Kumari Alajangi**, Poornemaa Natrajan and Deenan Santhiya*.